

**Synthesis, Structure and Reactivity of
Manganese Complexes Supported by
Carbon or Nitrogen Donor Ligands**

Dissertation

zur Erlangung des Doktorgrades

der Mathematisch-Naturwissenschaftlichen Fakultäten

der Georg-August-Universität zu Göttingen

vorgelegt von

Diplom-Chemiker

Jianfang Chai

aus Anyang, Henan

(CHINA)

Göttingen 2004

D7

Referent: Prof. Dr. Dr. h. c. mult. H. W. Roesky

Korreferent: Prof. Dr. F. Meyer

Tag der mündlichen Prüfung: 03. 11. 2004

*Dedicated to my parents and my wife
for their love and affection*

Acknowledgment

The work described in this doctoral dissertation has been carried out under the guidance and supervision of Professor Dr. Dr. h. c. mult. H. W. Roesky at the Institut für Anorganische Chemie der Georg-August-Universität in Göttingen between November 2001 and August 2004.

I am sincerely grateful to

Professor Dr. Dr. h. c. mult. H. W. Roesky

for his constant guidance, motivation, suggestions and discussion throughout this work. I also thank him for the personal kindness and care during my stay in Göttingen.

I thank Mr. H.-G. Schmidt, Dr. M. Noltemeyer, Dr. I. Usón, Dr. Q. Ma, Mr. V. Jancik, Mr. D. Vidovic and Prof. J. Magull for their help in the X-ray crystal structure determinations and their friendship. I thank Mr. W. Zolke, Mr. R. Schöne and Dr. G. Elter (NMR spectra), Dr. X. Ren and Mr. J. Sass (magnetic susceptibility), Dr. D. Böhler, Mr. T. Schuchardt and Mrs. A. Rehbein (mass spectra), Mrs. A. C. Stückl (EPR spectra), Mr. M. Hesse, H.-J. Feine (IR spectra), Mr. J. Schimkowiak, Mr. M. Schlote and the staff of the Analytical Laboratories for their full support during my research work.

I would like to express my thanks to Mr. H. Zhu and Dr. C. He for collaborative work and Mr. H. Fan for theoretical calculations. I thank Dr. H. Hao, Dr. G. Bai, Dr. Y. Ding, Mrs. Y. Peng for their help at the beginning of the work. I also thank Mr. T. Blunck, Mr. S. Singh, Mr. U. N. Nehete, Mr. Z. Yang, Dr. M. Gorol, Dr. J. Janssen, Dr. H. Hohmeister, Dr. P. Lobinger, Dr. J. Rong, Dr. G. Nikiforov, Dr. A. Stasch, Mr. S. K. Srisailam, Dr. K. Most and many others for providing a friendly work atmosphere. The help rendered by Dr. M. Witt during writing this thesis is gratefully acknowledged.

I thank my former graduate advisors Prof. J. Wang and Prof. L. Tang in Nankai University (Tianjin, P. R. China), from whom I learnt my early lessons of research.

The full support and encouragement from my wife Jing Zhang, my parents and other relatives made this work possible.

Abbreviations

Ar	aryl
av	average
br	broad
<i>n</i> Bu	<i>n</i> -butyl
°C	degree Celsius
Cp	cyclopentadienyl
d	day(s), doublet
dec.	decomposition
DME	1,2-dimethoxyethane
δ	chemical shift (ppm)
Δ	difference
EI	electron impact ionization
Et	ethyl
equiv (s)	equivalent(s)
g	gram(s)
h	hour(s)
Hz	Hertz
IR	infrared
<i>J</i>	coupling constant
K	Kelvin
L	HC(CMeNAr) ₂
L'	monovalent ligand
λ	wavelength
M	metal
M ⁺	molecular ion
m	multiplet
Me	methyl
mg	milligram(s)
min	minute(s)
mL	milliliter(s)
mmol	millimol(ar)

m/z	mass/charge
MS	mass spectrometry
μ	bridging
$\tilde{\nu}$	wave number
NMR	nuclear magnetic resonance
Ph	Phenyl
ppm	parts per million
<i>i</i> Pr	<i>iso</i> -propyl
q	quartet
r.t.	room temperature
s	singlet
t	triplet
<i>tert</i>	tertiary
THF	tetrahydrofuran
TMEDA	tetramethylethylenediamin
TMS	tetramethylsilane
<i>Z</i>	number of molecules in the unit cell

TABLE OF CONTENTS

1. Introduction	1
1.1. Manganese N-Heterocyclic Carbene Complexes	1
1.2. Low-aggregated Organomanganese(II) Complexes of Type L'MnR	
(L' = monovalent ligand)	2
1.3. Complexes with Low-valent and Low-coordinated Manganese	3
1.4. Dinuclear Manganese Complexes	3
1.5. Aims and Objectives of the Present Work	5
2. Results and Discussion	6
2.1. Monomeric Manganese(II) N-Heterocyclic Carbene Complexes 2 - 4	6
2.1.1. Synthesis and Spectroscopic Characterization of Complexes	
{[C(Me)N(<i>i</i> Pr)] ₂ C} ₂ MnX ₂ (X= Cl (2), I (3), MeCOO (4))	6
2.1.2. X-ray Solid-state Structural Analyses of Complexes 2 - 4	7
2.1.3. Solid-state Powder EPR Spectra of 2 - 4	12
2.2. Synthesis, Structure and Reactivity of Manganese Chlorides 7 - 10 Containing	
a Bulky β-Diketimate Ligand	12
2.2.1. Synthesis and Spectroscopic Characterization of Complexes 7 - 10	13
2.2.2. X-ray Solid-state Structural Analyses of Complexes 7 - 10	15
2.2.3. Reactivity of Compound 8 and its Organmanganese Derivatives 11 - 13	
of Type LMnR (R = Cp, Me and Ph)	19
2.2.4. Reactivity of Compound 9 and Formation of Compounds LMnC ₃ H ₅ (THF) (14)	
and [LMn(μ -CCPh)] ₂ (15)	25
2.3. Synthesis and Structure of the Dinuclear Manganese Acetate 16	29
2.3.1. Synthesis and Spectroscopic Characterization of [LMn(μ -MeCOO)] ₂ (16)	29

2.3.2. X-ray Solid-state Structural Analysis of Complex 16	29
2.4. Synthesis, Structure and Reactivity of Manganese Iodides 17 - 19 Containing the Bulky β-Diketimate Ligand	31
2.4.1. Synthesis and Spectroscopic Characterization of Complexes 17 - 19	31
2.4.2. X-ray Solid-state Structural Analyses of Complexes 17 and 18	33
2.4.3. Reactivity of Compound 19 and the Derivative LMnNHAr{C[N(<i>i</i> Pr)C(Me)] ₂ } (20)	35
2.5. Synthesis, Characterization and Reactivity of the First Compound with Three-coordinate Manganese(I) 21	37
2.5.1. Synthesis and Spectroscopic Characterization of [LMn] ₂ (21)	37
2.5.2. X-ray Solid-state Structural Analysis of Compound 21	37
2.5.3. Reactivity of Compound 21 and the Derivative [LMn(μ -O)] ₂ (22)	38
2.6. Synthesis and Structure of the Dinuclear Manganese Compound Containing a Bulky Diamide Ligand	40
2.6.1. Synthesis and Spectroscopic Characterization of [ArN(CH ₂) ₃ NAr][Li(OEt ₂)] ₂ (23) and Mn ₂ [ArN(CH ₂) ₃ NAr] ₂ (24)	40
2.6.2. X-ray Solid-state Structural Analyses of Compounds 23 and 24	41
2.6.3. Magnetic Susceptibility Measurement of Compound 24	44
3. Summary and Outlook	46
3.1. Summary	46
3.2. Outlook	52
4. Experimental Section	53
4.1. General procedures	53
4.2. Starting materials	54
4.3. Synthesis	54

4.3.1. Synthesis of $\{[C(Me)N(iPr)]_2C\}_2MnCl_2$ (2)	54
4.3.2. Synthesis of $\{[C(Me)N(iPr)]_2C\}_2MnI_2$ (3)	55
4.3.3. Synthesis of $\{[C(Me)N(iPr)]_2C\}_2Mn(MeCOO)_2$ (4)	55
4.3.4. Synthesis of LK (6)	56
4.3.5. Synthesis of $LMn(\mu-Cl)_2Li(OEt)_2$ (7)	56
4.3.6. Synthesis of $[LMn(\mu-Cl)]_2$ (8)	56
4.3.7. Synthesis of $LMn(\mu-Cl)_2Mn(THF)_2(\mu-Cl)_2MnL$ (9)	57
4.3.8. Synthesis of $[LMnCl_2][\{C(Me)N(iPr)\}_2CH]$ (10)	57
4.3.9. Synthesis of $LMnCp(THF)$ (11)	58
4.3.10. Synthesis of $[LMn(\mu-Me)]_2$ (12)	58
4.3.11. Synthesis of $LMnPh$ (13)	59
4.3.12. Synthesis of $LMnC_3H_5(THF)$ (14)	59
4.3.13. Synthesis of $[LMn(\mu-CCPh)]_2$ (15)	59
4.3.14. Synthesis of $[LMn(\mu-MeCOO)]_2$ (16)	60
4.3.15. Synthesis of $LMnI(THF)$ (17)	60
4.3.16. Synthesis of $[LMn(\mu-I)]_2$ (18)	60
4.3.17. Synthesis of $LMnI\{C[N(iPr)C(Me)]_2\}$ (19)	61
4.3.18. Synthesis of $LMnNHAr\{C[N(iPr)C(Me)]_2\}$ (20)	61
4.3.19. Synthesis of $[LMn]_2$ (21)	62
4.3.20. Synthesis of $[LMn(\mu-O)]_2$ (22)	62
4.3.21. Synthesis of $[ArN(CH_2)_3NAr][Li(OEt)_2]_2$ (23)	63
4.3.22. Synthesis of $Mn_2[ArN(CH_2)_3NAr]_2$ (24)	63
5. Handling and Disposal of Solvents and Residual Wastes	64
6. Crystal data and Refinement Details	65
7. References	85

1. Introduction

There is widespread interest in manganese complexes due to their synthetic methodology, theoretical implications and vantage of applications in organic synthesis and catalysis.¹ In addition, manganese complexes have attracted special attention regarding their important role in the material science and bioinorganic chemistry.² Development of new materials with novel magnetic properties and attempts to model the structures and functions of manganese metalloenzymes have driven this area as the most active and expansive field.² The discovery of the selective epoxidation catalysts based on the Mn(III) salen system has also attracted much effort on the manganese coordination chemistry in the search for higher selectivities and enantiospecific catalysis.^{2,3} However, synthesizing such complexes is still a challenge for the chemists along with the investigation of spectroscopic and structural characteristics of these molecules and perspective elaborating new catalysts. In this connection, design and choice of the ligands are important for these purposes.

In the following part, some of the work, which is related to the content of the present thesis, will be discussed in detail.

1.1. Manganese N-Heterocyclic Carbene Complexes

N-Heterocyclic carbenes have attracted great attention in ligand design and homogeneous catalysis as neutral and two electron donors⁴ since Arduengo et al. reported the first stable crystalline N-heterocyclic carbene in 1991.⁵ The isolation of the free stable N-heterocyclic carbenes enables the easy synthesis of a variety of carbene adducts that previously were inaccessible.⁶ So a number of N-heterocyclic carbene complexes of main group element and transition metal have been synthesized and isolated,⁴ some of which have been successfully applied as catalysts in a variety of organic reactions such as iridium-catalyzed transfer hydrogenation⁷ and ruthenium-catalyzed olefin metathesis, especially palladium-catalyzed C–C coupling reactions: the Heck, Suzuki and Kumada reactions.^{4,8} Recently, iron(II) halides bearing N-heterocyclic carbene ligand of composition $\{[\text{C}(\text{Me})\text{N}(\text{iPr})_2\text{C}]_2\text{FeX}_2$ (X = Cl, Br) were found to be remarkably active and efficient catalysts for atom transfer radical polymerization.⁹

Manganese carbene complexes are important due to their applications in organic synthesis and theoretical implications.¹⁰ In spite of the impressive results of N-heterocyclic carbene complexes, manganese complexes containing N-heterocyclic carbenes are rare and have not attracted much attention to date.^{4a} To the best of our knowledge, only few manganese N-heterocyclic carbene complexes are known including $\text{MeC}_5\text{H}_4(\text{CO})_2\text{MnC}[\text{N}(\text{Me})\text{CH}_2]_2$,¹¹ $(\text{CO})_3\text{MnBr}\{\text{C}[\text{N}(\text{Me})\text{CH}_2]_2\}_2$ ¹¹ and $(\text{CO})_5\text{MnC}[\text{N}(\text{BH}_3)\text{C}(\text{Me})\text{C}(\text{Me})\text{N}(\text{Me})]$ ¹² with a formal oxidation state of +1 at the manganese. Furthermore, no X-ray structural data of manganese N-heterocyclic carbene complexes were available. Therefore, it was of interest to synthesize and structurally characterize N-heterocyclic carbene complexes containing manganese with the most common oxidation state +2.

1.2. Low-aggregated Organomanganese(II) Complexes of Type $\text{L}'\text{MnR}$

($\text{L}' = \text{monovalent ligand}$)

There is widespread interest in organomanganese(II) complexes, since such complexes have extensive applications in organic synthesis.^{1c,1d} For instance, manganese(II) alkyl and aryl complexes have proved to be excellent reagents in C-C coupling reactions and can be compared to other organotransition metal complexes such as widely used organocopper reagents.¹³ Moreover, they show excellent thermal stability, high chemoselectivity and excellent functional group tolerance.^{13,14} In spite of the impressive results obtained thus far, major efforts are focused on carbonyl and cyclopentadienyl complexes. Organomanganese complexes having ligands without carbonyl and cyclopentadienyl groups are far less abundant although the chemistry of those species is no less interesting,^{1a} in which complexes of type $\text{L}'\text{MnR}$ ($\text{L}' = \text{monovalent ligand}$) are even more rare. Compounds of composition XMnR ($\text{X} = \text{halide}$) have only been used as intermediates without isolation.¹⁵ To the best of our knowledge, only few compounds of composition $[\text{MnR}(\text{NPET}_3)]_4$ ($\text{R} = \text{Me}, n\text{Bu}, \text{PhCC}, 4\text{-MeC}_6\text{H}_4\text{CC}, \text{Me}_3\text{SiCC}$) have been structurally characterized containing a heterocubane structure.¹⁶ Despite of the interesting perspectives of organomanganese(II) complexes, there are no structural investigations known of lower aggregated complexes (monomer or dimer). So it was of interest to prepare low-aggregated organomanganese complexes by designing suitable ligands.

1.3. Complexes with Low-valent and Low-coordinated Manganese

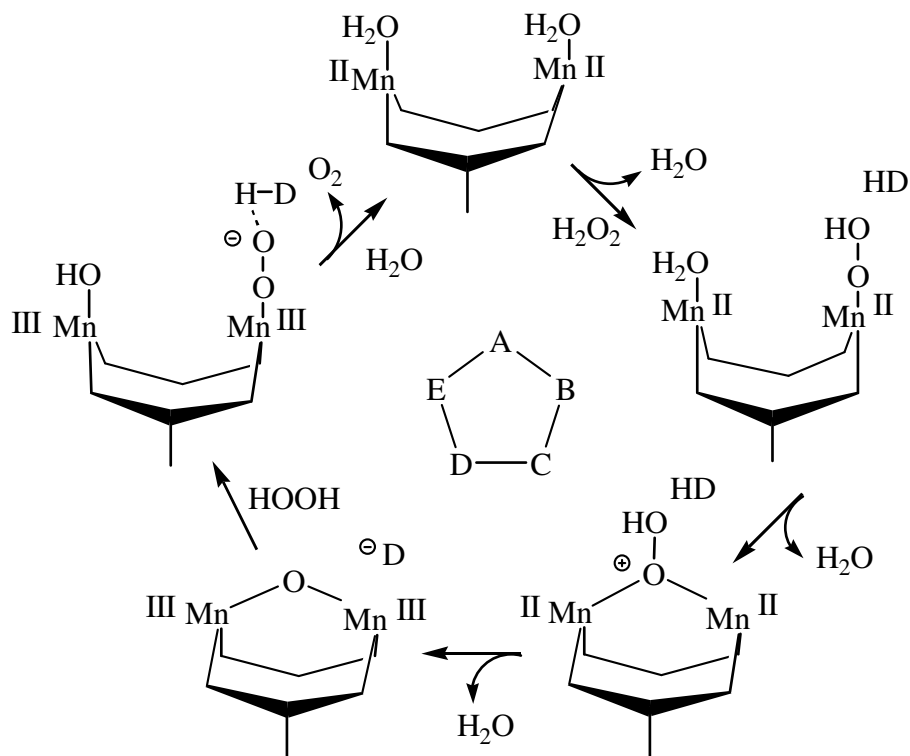
Complexes with low-valent manganese are important due to their photochemistry as well as their significance in free-radical chemistry.¹⁷ For example, the dinuclear carbonyl compound $\text{Mn}_2(\text{CO})_{10}$ has shown rich photochemistry and can catalyze the ring opening of β -propiolactones.¹⁸

Transition metal complexes containing low-coordinated metal centers are quite rare. Partly this is due to the difficulty associated for such metal sites to acquire 16 or 18 valence electrons. Low-coordination numbers often yield the metal centers of unusual orbital structure,¹⁹ which would also render its reactivity very interesting.¹⁹ Although manganese complexes with low-coordinated centers are known, these involve manganese in oxidation states of +2 or higher.²⁰ To the best of our knowledge, coordination number three are rare in complexes with low-valent manganese until now. In this view, one can realize that the ligand design combined with the corresponding synthetic methodology for complexes with low-valent and low-coordinated manganese centers is an exciting challenge. In addition, it is of interest to explore their unique reactivity.

1.4. Dinuclear Manganese Complexes

Dinuclear manganese complexes, especially those with carboxylate or oxygen bridges, are important since such molecules are involved in many natural processes.²¹ Dinuclear manganese core are often seen in biological systems, such as manganese catalase, manganese ribonucleotide, arginase and thiosulfate oxidase, which exist as the catalytic centers of these enzymes.²² Manganese catalases are the well-studied redox enzymes, which protect organisms from oxidative damage to scavenge the appreciable levels of H_2O_2 produced during O_2 metabolism in cells.²² They are capable of catalyzing the disproportionation of high level H_2O_2 to O_2 and H_2O , and each unit contains a dinuclear manganese core as the catalytic center. The dimanganese core works as a two-electron mediator between a $[\text{Mn}(\text{III})]_2$ form and a reduced $[\text{Mn}(\text{II})]_2$ form in H_2O_2 disproportionation.²³ A possible mechanism of this process is shown in Scheme 1 (DH/D represent the proton donor and acceptor).²² In recent years, several kinds of dinuclear manganese model complexes have been explored and show catalase activity.²⁴ However, only a few of these functional model systems proceed via the $[\text{Mn}(\text{II})]_2 \rightleftharpoons [\text{Mn}(\text{III})]_2$ redox

cycle similar to the enzymes.²⁴ Therefore it is still a challenge for chemists to mimic the coordination environment and functions of the manganese centers in such enzymes.

Scheme 1

1.5 Aims and Objectives of the Present Work

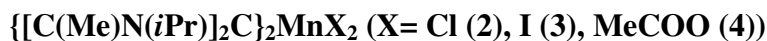
Based on the aforementioned background materials, there is clearly a vast potential to explore the chemistry of manganese by carefully selecting or designing ligands. The aims of this thesis are the following by using the appropriate ligand systems:

- To synthesize manganese(II) N-heterocyclic carbene complexes and investigate their properties;
- To synthesize low-aggregated organomanganese(II) complexes of type $L'MnR$;
- To study the synthesis, property and reactivity of complexes with low-valent and low-coordinated manganese;
- To investigate the synthesis and property of dinuclear manganese compounds.

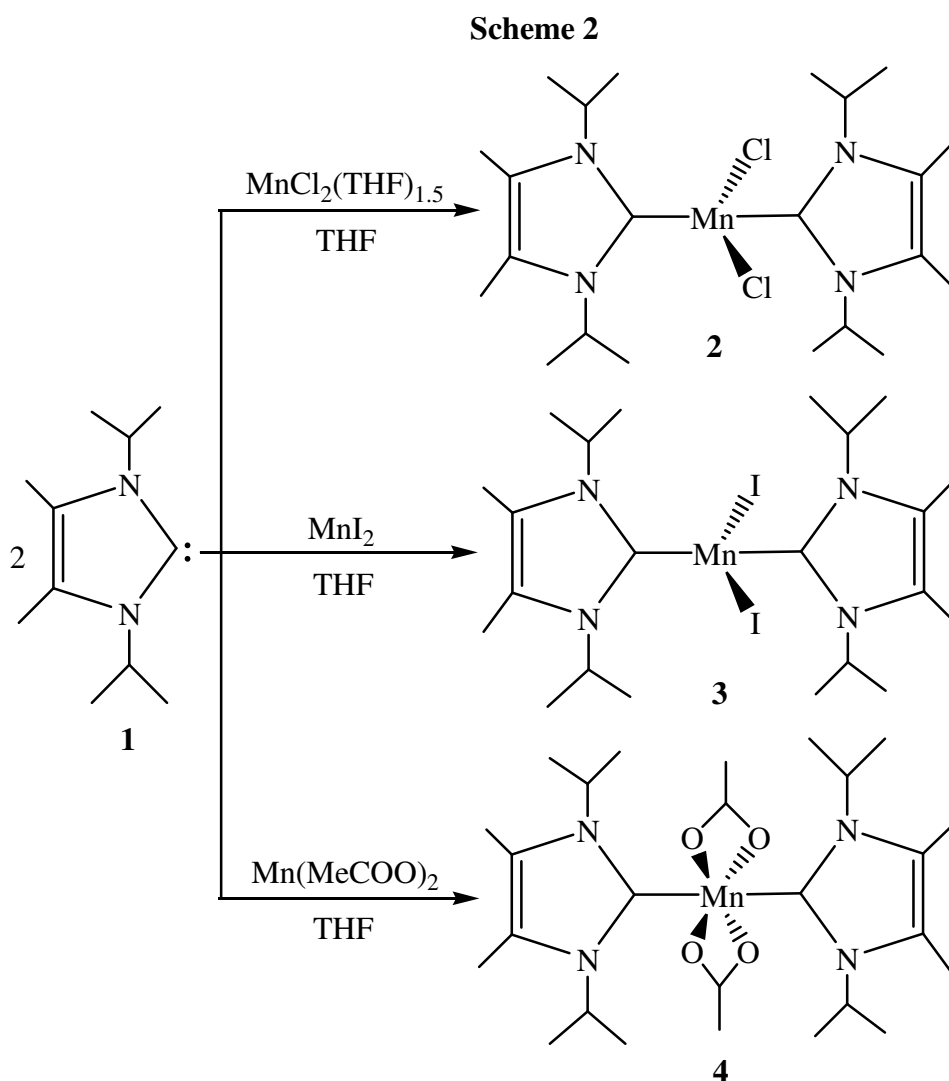
2. Results and Discussion

2.1. Monomeric Manganese(II) N-Heterocyclic Carbene Complexes **2** - **4**

2.1.1. Synthesis and Spectroscopic Characterization of Complexes



The isolation of free stable N-heterocyclic carbenes enables the easy synthesis of a variety of carbene adducts that previously were inaccessible.⁶ The reaction of $\text{MnCl}_2(\text{THF})_{1.5}$, MnI_2 and $\text{Mn}(\text{MeCOO})_2$, respectively, with 2 equiv. of the stable carbene $[C(\text{Me})N(i\text{Pr})]_2\text{C}$ (**1**) in THF at room temperature readily afforded the corresponding carbene adducts **2** - **4** in good yields (Scheme 2).



Compounds **2** and **4** are colorless solids and compound **3** is a light-orange solid. Compounds **2** and **3** are moderately air sensitive and can be exposed to air for a short period of time as solids, while compound **4** is much more sensitive. All compounds **2** - **4** are of poor solubility in nonpolar solvents, while readily soluble in solvents such as CH₂Cl₂ and MeCN. Compound **4** has also a good solubility in THF, but **2** and **3** are sparingly soluble in THF. Complexes **2** - **4** have been characterized by mass spectrometry, IR spectroscopy, X-band EPR, microanalysis and X-ray solid-state structural analyses. EI-MS spectra of these compounds are similar: the molecular ion peaks are not observed rather the free carbene fragment appears as the most intense peak at m/z 180 (100 %) indicating the cleavage of the Mn-C bond in these compounds under electron-impact mass spectrometry conditions, consistent with the results reported in the literature.²⁵ The IR spectrum of compound **4** displays two prominent vibrations for the O-C-O part of the acetate group ν_{as} (1599 cm⁻¹) and ν_s (1406 cm⁻¹).

2.1.2. X-ray Solid-state Structural Analyses of Complexes **2** - **4**

Compounds **2** and **3** are the first structurally characterized manganese halides possessing N-heterocyclic carbene ligands. Single crystals of **2** and **3** suitable for X-ray structural analyses were obtained by recrystallization in THF at 4 °C, respectively. The molecular structures of **2** and **3** are shown in Figures 1 and 2, respectively; selected bond lengths and angles are listed in Table 1.

The manganese atoms in **2** and **3** are bonded to two halides and two carbene carbons and have a distorted tetrahedral geometry. A crystallographic twofold axis passes through the metal atom bisecting the angles X-Mn-X and C-Mn-C. There is a slight difference between the two structures due to the different ion radius of Cl and I. Both the X-Mn-X (111.5°) and C-Mn-C (103.0°) angles in **2** are slightly larger than the corresponding ones in **3** (109.0° and 102.4°, respectively). The dihedral angle between the two carbene planes is 84.5° in **2** and 77.0° in **3**. These differences possibly result from the stronger repulsion between iodine and carbene in **3** than that between chlorine and carbene in **2**, which are also reflected by the EPR spectra.

The Mn-C bond lengths (av. 2.21 Å) in **2** and **3** are in the expected range of Mn-C single bonds, but significantly shorter in comparison with the Mn-P bond lengths found in MnI₂(PET₃)₂²⁶ (av. 2.53 Å) and [MnI₂(PPhMe₂)_n]²⁷ (av. 2.67 Å). The Mn-I distances (av. 2.72 Å) in **3** are a little longer than those in MnI₂(PET₃)₂²⁶ (av. 2.67 Å) due to the different

trans effect. However, the I-Mn-I (109.0°) and C-Mn-C (102.4°) angles in **3** are significantly smaller than the corresponding ones (120.1° and 115.1° , respectively) in $\text{MnI}_2(\text{PEt}_3)_2$.²⁶

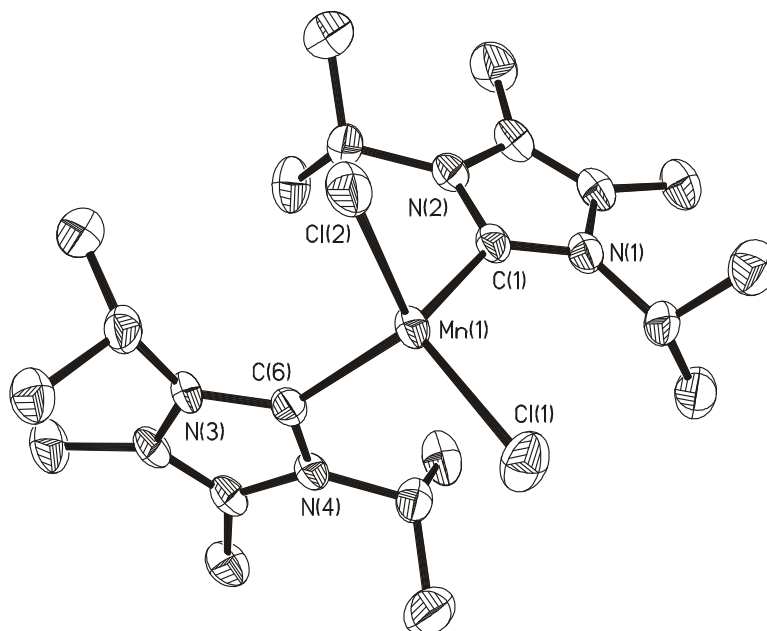


Figure 1. Molecular structure of **2** (50 % probability ellipsoids). Hydrogen atoms are omitted for clarity.

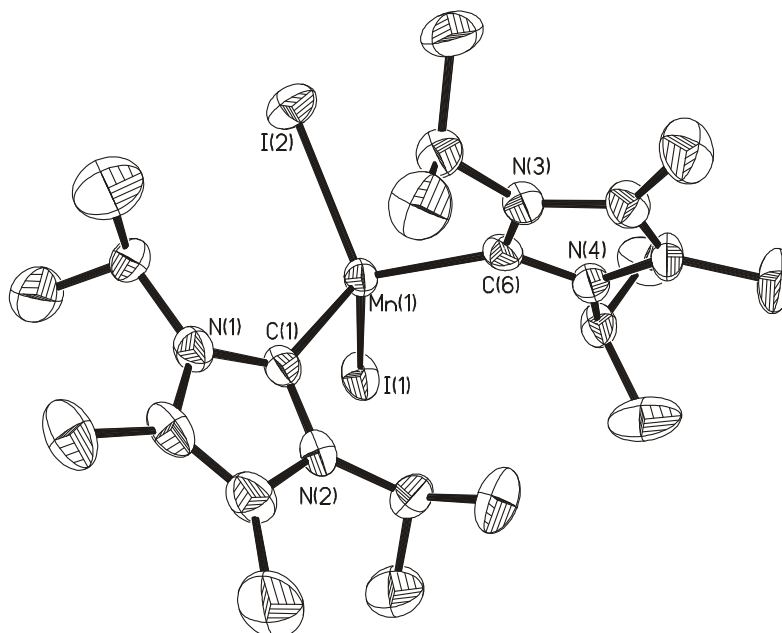


Figure 2. Molecular structure of **3** (50 % probability ellipsoids). Hydrogen atoms are omitted for clarity.

The N(1)-C(1)-Mn(1) (131.6°) and N(3)-C(6)-Mn(1) (132.3°) angles in **2** deviate significantly from their corresponding counterparts N(2)-C(1)-Mn(1) (123.9°) and N(4)-C(6)-Mn(1) (122.6°), which implies that both the N-heterocyclic carbenes are *in-plane* bending.²⁸ However, *out-of-plane* bending is only observed for one N-heterocyclic carbene ligand (C(6), N(3), C(7), C(8) and N(4)) and the Mn(1)-C(6) bond is out of the N-heterocyclic carbene plane by 6.4°. The other N-heterocyclic carbene and the central manganese atom are coplanar. In **3**, both the N-heterocyclic carbene ligands are *out-of-plane* bending as shown by the Mn-C bond angles deviating from the corresponding N-heterocyclic carbene planes by 4.7° and 4.3°, respectively. These angles are in the normal range.²⁵

Table 1. Selected bond lengths (Å) and bond angles (°) for compounds **2** and **3**

Compound 2			
Mn(1)–Cl(1)	2.3535(11)	C(6)–Mn(1)–C1(1)	108.92(9)
Mn(1)–Cl(2)	2.3575(10)	C(1)–Mn(1)–Cl(2)	105.78(8)
Mn(1)–C(1)	2.214(3)	N(1)–C(1)–Mn(1)	131.6(2)
Mn(1)–C(6)	2.219(3)	N(3)–C(1)–Mn(1)	132.3(2)
N(1)–C(1)	1.355(4)	C(6)–Mn(1)–Cl(2)	114.64(9)
N(2)–C(1)	1.355(4)	Cl(1)–Mn(1)–Cl(2)	111.47(4)
N(3)–C(6)	1.355(4)	N(1)–C(1)–N(2)	104.5(3)
N(4)–C(6)	1.359(4)	N(3)–C(6)–N(4)	104.6(3)
C(1)–Mn(1)–C(6)	103.02(12)	N(2)–C(1)–Mn(1)	123.9(2)
C(1)–Mn(1)–Cl(6)	112.77(9)	N(4)–C(1)–Mn(1)	122.6(2)
Compound 3			
Mn(1)–I(1)	2.7307(7)	C(1)–Mn(1)–I(1)	106.46(10)
Mn(1)–I(2)	2.7114(8)	C(6)–Mn(1)–I(1)	116.60(10)
Mn(1)–C(1)	2.210(4)	C(1)–Mn(1)–I(2)	116.89(11)
Mn(1)–C(6)	2.204(4)	N(1)–C(1)–Mn(1)	131.7(3)
N(1)–C(1)	1.356(5)	N(3)–C(1)–Mn(1)	124.5(3)
N(2)–C(1)	1.352(6)	C(6)–Mn(1)–I(2)	105.79(11)
N(3)–C(6)	1.354(5)	I(1)–Mn(1)–I(2)	109.04(2)
N(4)–C(6)	1.352(5)	N(1)–C(1)–N(2)	104.7(3)
C(1)–Mn(1)–C(6)	102.35(15)	N(3)–C(6)–N(4)	104.1(3)

Compound **4** is the first structurally characterized monomeric manganese complex containing two symmetric chelating acetate groups. Single crystals suitable for X-ray structural analysis were grown from THF solution at $-26\text{ }^{\circ}\text{C}$. The molecular structure is shown in Figure 3; selected bond lengths and bond angles are listed in Table 2. Complex **4** crystallizes in the monoclinic space group $C2/c$. The central manganese atom is surrounded by four oxygen atoms from the two chelating carboxyl groups and two carbene carbon atoms in a highly distorted octahedral geometry. The complex adopts a symmetric structure. A mirror plane passes through the manganese atom bisecting the two acetate groups and the two carbenes.

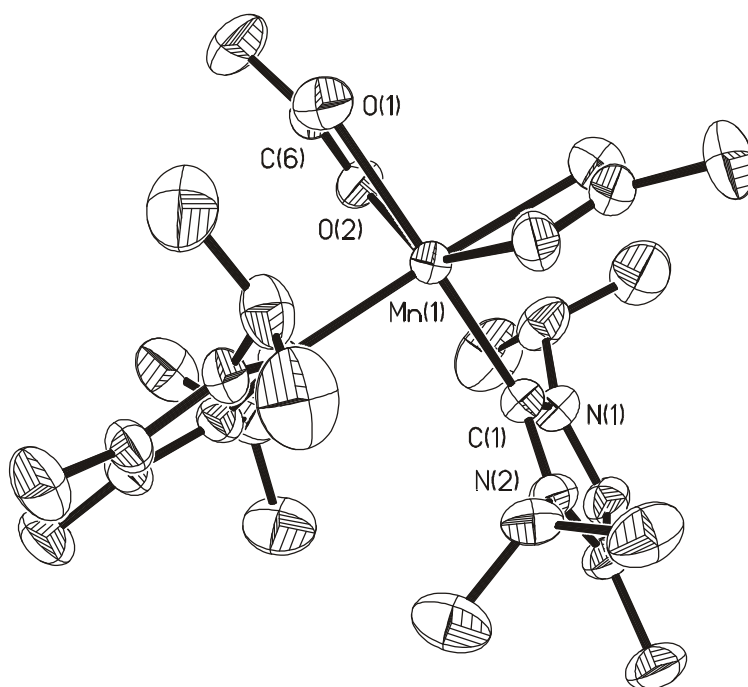


Figure 3. Molecular structure of **4** (50 % probability ellipsoids). Hydrogen atoms are omitted for clarity.

The two acetate groups are symmetrically bonded in a chelating fashion to the manganese atom resulting in the formation of two MnOCO four-membered rings. Both rings are planar and nearly orthogonal as shown by a dihedral angle of 85.8° . Manganese complexes containing chelating carboxyl groups are rare.²⁹ The Mn-O distances from the O *trans* to the N-heterocyclic carbene carbon (2.34 Å) are slightly longer than those (2.23 Å) from the O *cis* to the carbon, probably due to the strong donor property of the N-heterocyclic carbene. Accordingly, the shorter Mn-O bond is associated with a longer carboxyl C-O bond. The

average value (2.29 Å) of the Mn-O distance is significantly longer than that of the bridging carboxyl group in $[\text{Mn}_2(\mu\text{-MeCOO})_x]^{4-x}$ system (1.99-2.13 Å) and also longer than that (av. 2.07 Å) of the chelating acetate group in $(\text{MeCOO})\text{Mn}(\text{CO})_2(\text{PPh}_3)_2$.^{30,31} The distance from the manganese atom to the central carbon atom of the acetate group (2.61 Å) is in the non-bonding range.³¹

The C-Mn-C angle in **4** is 96.7°, which shows that the two N-heterocyclic carbenes are in a *cis* position. The Mn-C distance (2.25 Å) is in the range (2.20-2.27 Å) of the Mn-C(N-heterocyclic carbene) distances known and is slightly longer than those in **2** and **3**.

Interestingly, both *in-plane* bending and *out-of-plane* bending of the N-heterocyclic carbenes are not observable in **4**. The similar N(1)-C(1)-Mn(1) (129.3°) and N(2)-C(1)-Mn(1) (126.7°) angles do not support any *in-plane* bending of the N-heterocyclic carbenes.

Table 2. Selected bond lengths (Å) and bond angles (°) for compound **4**

Mn(1)–O(1)	2.343(2)	C(1)–Mn(1)–O(2A)	97.34(8)
Mn(1)–O(2)	2.233(2)	O(2)–Mn(1)–O(2A)	146.33(12)
Mn(1)–O(1A)	2.343(2)	O(2)–Mn(1)–C(1A)	97.34(8)
Mn(1)–O(2A)	2.233(2)	O(2)–Mn(1)–O(1)	56.92(8)
Mn(1)–C(1)	2.254(3)	O(2)–Mn(1)–O(1A)	98.60(8)
Mn(1)–C(6)	2.612(3)	O(1)–Mn(1)–C(1A)	87.69(9)
Mn(1)–C(1A)	2.254(3)	O(1)–Mn(1)–O(1A)	93.65(12)
Mn(1)–C(6A)	2.612(3)	O(1)–Mn(1)–O(2A)	98.60(8)
O(1)–C(6)	1.238(4)	O(1A)–Mn(1)–O(2A)	56.92(8)
O(2)–C(6)	1.258(4)	O(1A)–Mn(1)–C(1A)	161.79(9)
N(1)–C(1)	1.364(3)	O(2A)–Mn(1)–C(1A)	104.91(8)
N(2)–C(1)	1.356(3)	O(1)–C(6)–O(2)	122.0(3)
C(1)–Mn(1)–C(1A)	96.68(13)	N(1)–C(1)–N(2)	104.0(2)
C(1)–Mn(1)–O(1)	161.79(9)	N(2)–C(1)–Mn(1)	126.67(18)
C(1)–Mn(1)–O(1A)	87.69(9)	N(1)–C(1)–Mn(1)	129.32(18)
C(1)–Mn(1)–O(2)	104.91(9)		

2.1.3. Solid-state Powder EPR Spectra of **2** - **4**

Manganese(II) complexes exhibit a great variety of EPR signals related to their structures.³² The X-band EPR spectra of complexes **2** - **4** were recorded at ambient temperature with powder samples. As expected, a strong resonance in complexes **2** and **3** is observed near $g_{\text{eff}} = 4.3$ due to their tetrahedral geometry.³³ In addition, compound **2** exhibits two shoulders to lower field and several weaker bands to higher field, while the spectrum of **3** is much simpler: another strong resonance ($g_{\text{eff}} = 2$) and a very weak one at high field. The spectrum of compound **4** exhibits a very strong band ($g_{\text{eff}} = 2$) and a weaker one (near $g_{\text{eff}} = 4.3$) and has shoulders to higher and lower field of the main line. The spectrum of **4** is similar to that of complex $\text{Mn}(o\text{-phen})_2(\text{NCS})_2$, which has a very small D value (near zero) and a large λ value (near $1/3$) (D and λ are zero-field splitting parameters).³⁴ The spectrum is consistent with the symmetric structure of **4** and the *cis* arrangement of the two carbene ligands.

2.2. Synthesis, Structure and Reactivity of Manganese Chlorides **7** - **10** Containing a Bulky β -Diketimate Ligand

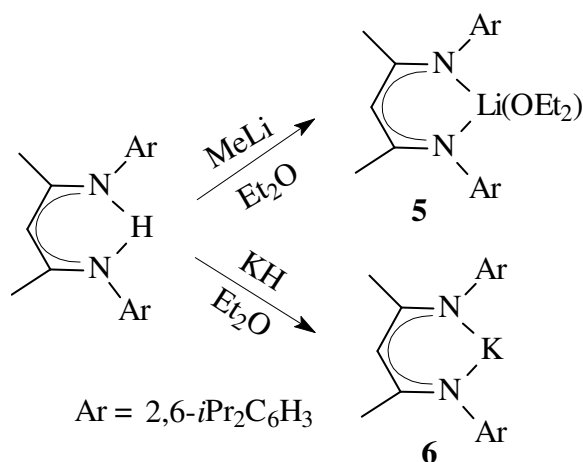
In the past few years there is increasing interest in β -diketimate ligands, especially those with bulky aryl groups at the nitrogen atoms, which have excellent steric and electronic properties to stabilize unusual metal sites.³⁵ A variety of main group element, transition metal and lanthanide complexes containing such ligands have been synthesized and characterized, some of which have novel structures and good catalytic activities.³⁵ For example, the first monomeric Al(I) compound LAl ($\text{L} = \text{HC}(\text{CMeNAr})_2$, $\text{Ar} = 2,6\text{-}i\text{Pr}_2\text{C}_6\text{H}_3$) as a stable carbene analogue was synthesized in our group.³⁶ Very recently, an aluminium dihydroxide with terminal OH groups and the first terminal hydroxide containing alumoxane were also obtained using the same bulky ligand.³⁷

In spite of the impressive results obtained by using β -diketimate ligands now known, little work has appeared on manganese β -diketimate complexes. Chlorides are normally the most common and available sources of manganese(II), however, manganese chlorides containing such ligands remain rare prior to this work.

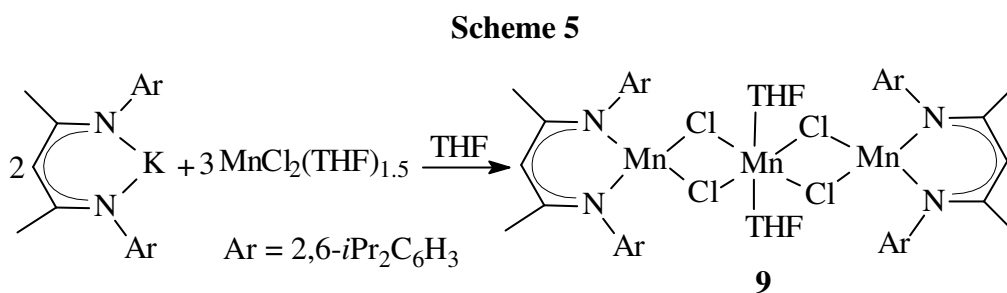
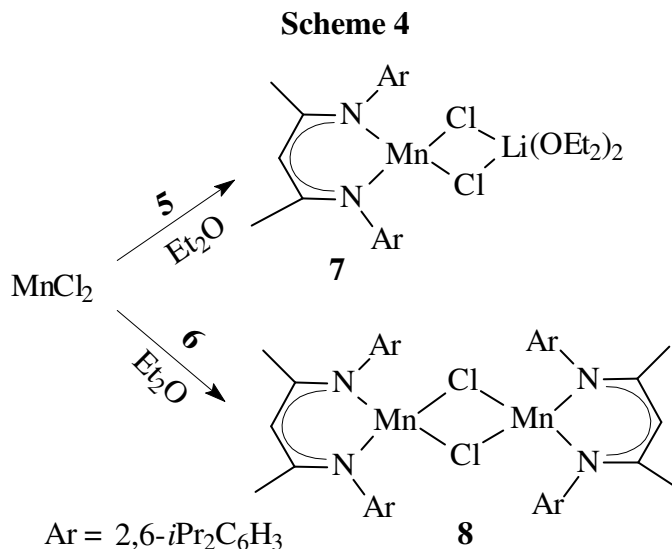
2.2.1. Synthesis and Spectroscopic Characterization of Complexes 7 - 10

The β -diketiminate lithium salt $\text{LLi}(\text{OEt}_2)$ (**5**) has been reported previously and widely used as a metathesis reagent.³⁸ The preparation of **LK** (**6**) was described resulting from the reaction of **LH** with $\text{KN}(\text{SiMe}_3)_2$ in relatively low yield (27 %).³⁹ Herein we report the convenient preparation of **5** as a crystalline solid in good yield (87 %) by the reaction of **LH** and **KH** in diethyl ether at room temperature (Scheme 3). ^1H NMR and elemental analyses are consistent with those of the literature.³⁹ Compound **6** is stable under an inert atmosphere and can be kept for a long time without decomposition.

Scheme 3

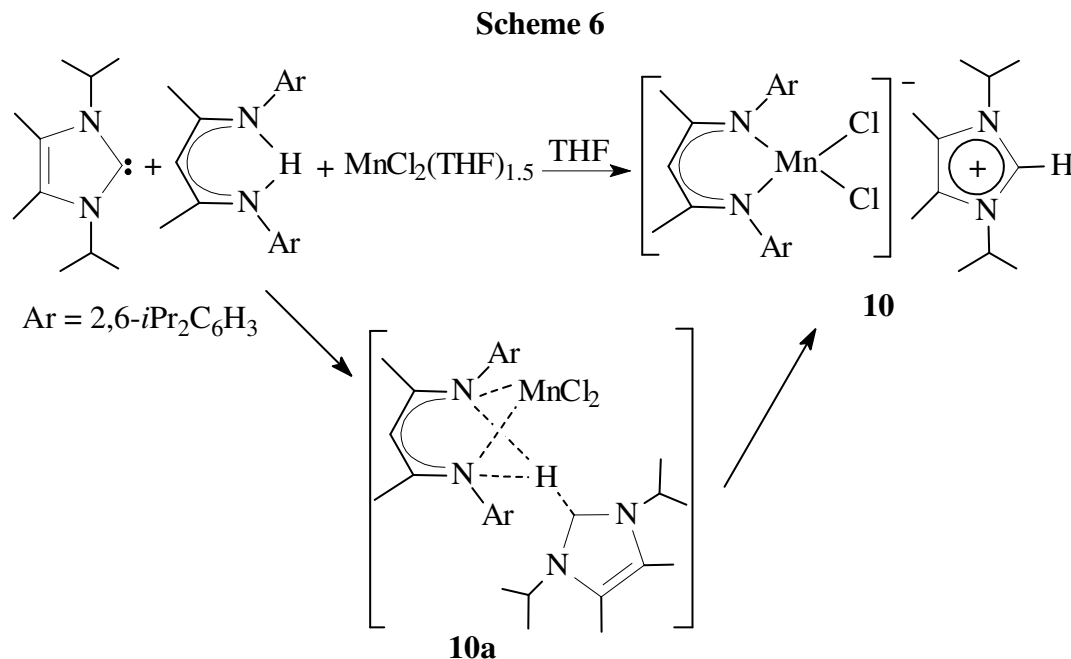


The reaction of **5** and anhydrous MnCl_2 in diethyl ether afforded the metalate complex $\text{LMn}(\mu\text{-Cl})_2\text{Li}(\text{OEt}_2)_2$ (**7**) in high yield (Scheme 4). Attempts to remove the coordinated lithium salt from the manganese center were unsuccessful. Expectedly, the reaction of MnCl_2 with one equiv. of **6** in diethyl ether readily gave the dimeric compound $[\text{LMn}(\mu\text{-Cl})_2]_2$ (**8**) in high yield. Attempts to prepare the di- β -diketiminate complex by using 2 equiv. of **5** or **6** were unsuccessful. However, the analogous reaction of **6** and $\text{MnCl}_2(\text{THF})_{1.5}$ in THF resulted in the unexpected formation of the trinuclear complex $\text{LMn}(\mu\text{-Cl})_2\text{Mn}(\text{THF})_2(\mu\text{-Cl})_2\text{MnL}$ (**9**) in good yield, although a ratio of 1:1 of the starting materials was employed (Scheme 5).



When the N-heterocyclic carbene [C(Me)N(*i*Pr)]₂C (**1**) was employed as the acceptor for the proton of LH, the novel ionic compound [LMnCl₂][{C(Me)N(*i*Pr)}₂CH] (**10**) was easily obtained as a yellow crystalline solid in high yield from the reaction of LH, MnCl₂(THF)_{1.5}, and **1** in THF at room temperature. However, no reaction occurs when in either case LH and **1** or LH and MnCl₂(THF)_{1.5} were mixed in THF at room temperature. Therefore we suppose that the process for the formation of **10** is a concerted one and may proceed through the intermediate **10a** (Scheme 6).

Complexes **7** - **10** are crystalline yellow solids soluble in THF. These complexes were characterized by elemental analyses, EI-MS and IR. The EI-MS of **7** and **9** show absence of the molecular ion peak and [LMnCl]⁺ *m/z* 507 appears as the most intense ion. The molecular ion peak of the dimer **8** in the EI mass spectrum is not observed, whereas half of the molecular mass [1/2M]⁺ appears at *m/z* 507 as the most intense peak. Interestingly, the ion [M-H]⁺ in the mass spectrum of **10** can be seen albeit with low intensity (2 %), followed by [LMnCl]⁺ *m/z* 507 (43 %) and [{C(Me)N(*i*Pr)}₂CH]⁺ 181 (52 %).



2.2.2. X-ray Solid-state Structural Analyses of Complexes 7 - 10

The X-ray solid-state structural analyses reveal that $\text{LMn}(\mu\text{-Cl})_2\text{Li}(\text{OEt}_2)_2$ (**7**) is monomeric, $[\text{LMn}(\mu\text{-Cl})_2]$ (**8**) is dimeric, and $\text{LMn}(\mu\text{-Cl})_2\text{Mn}(\text{THF})_2(\mu\text{-Cl})_2\text{MnL}$ (**9**) trinuclear in the solid state (Figures 4 - 6). $[\text{LMnCl}_2][\{\text{C}(\text{Me})\text{N}(\text{iPr})\}_2\text{CH}]$ (**10**) crystallizes as separated anion $[\text{LMnCl}_2]^-$ and cation $[\{\text{C}(\text{Me})\text{N}(\text{iPr})\}_2\text{CH}]^+$. The structure of the anion is shown in Figure 7.

In the compounds **7**, **8** and **10**, each manganese atom is bound to two nitrogen atoms of the chelating ligand and two chlorine atoms in a distorted tetrahedral geometry. The molecule of **9** consists of a linear trinuclear compound with four bridging chlorine atoms and two chelating ligands adopting a symmetric structure, which, in fact, is one $\text{MnCl}_2(\text{THF})_2$ molecule captured by the dimer $[\text{LMn}(\mu\text{-Cl})_2]$ (**8**). The central Mn(2) atom in **9** adopts a distorted octahedral coordination with two THF molecules in *trans* position, while the other two manganese atoms achieve a distorted tetrahedral geometry. The backbone of the chelating ligand is nearly planar and the manganese atoms in these compounds are out of the C_3N_2 planes (0.45 Å in **7**, 0.47 Å in **8**, 0.36 Å in **9** and 0.70 Å in **10**). The order of the N-Mn-N angles is **9** (91.3°) < **10** (91.6°) < **7** (92.2°) < **8** (92.8°), while the order of the Mn-N bond lengths is **10** (av. 2.11 Å) > **7** (av. 2.08 Å), **8** (av. 2.08 Å) and **9** (2.08 Å), which indicates that the metal center in **10** is more weakly bonded to the chelating ligand due to the two terminal Mn-Cl bonds. The terminal Mn-Cl distances (av. 2.36 Å) in **10** are comparable to

those of the bridging ones in **7** (av. 2.38 Å), **8** (av. 2.33 Å) and **9** (av. 2.40 Å) due to the anionic character of the LMnCl₂ in **10**. Accordingly, the Cl-Mn-Cl angle in **10** (112.0°) is significantly larger than those in **7** (96.2°), **8** (90.5°) and **9** (91.4°).

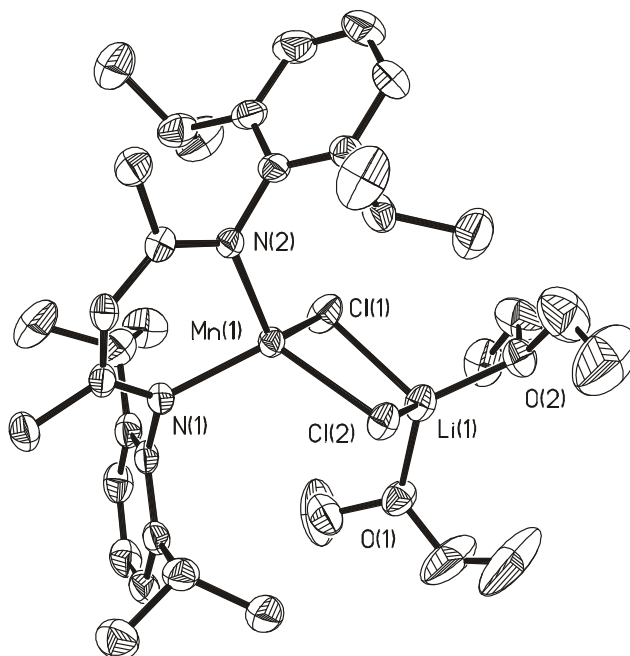


Figure 4. Molecular structure of **7** (50 % probability ellipsoids). Hydrogen atoms are omitted for clarity.

The lithium atom in **7** is connected by two bridging chlorides and two oxygen atoms of two coordinated ether molecules in a distorted tetrahedral geometry. The structure is like that of the alkali metal adducts of the β -diketiminato metal complexes of general formula LM(μ -X)₂Li(ether)₂ (X = Cl, I).^{20a,40} The Li-Cl and Li-O distances (av. 2.38 and 1.96 Å, respectively) are similar to those found in LM(μ -Cl)₂Li(THF)₂ (M = Fe(II), Co(II)).^{20a,40c}

The central core of **8** contains an ideal planar four-membered Mn₂Cl₂ ring, which bisects and is perpendicular (89.2°) to the two chelating ligands around it. The distance between two manganese atoms is 3.28 Å, which can be compared to that in [LMn(μ -I)]₂⁴¹ (**18**) (3.62 Å) and is out of the range of a Mn-Mn bond. The internal Cl(1)-Mn(2)-Cl(2) and Mn-Cl-Mn angles (84.7 and av. 92.0°, respectively) in **9** result in the Mn-Mn distances (3.56 Å), which are longer than that observed in **8**. Similar to that in **8**, the two bridging Mn₂Cl₂ rings in **9** are ideally coplanar, which bisect and are perpendicular (90.0°) to the two chelating ligands

around them. The structure of the cation $[\{C(Me)N(iPr)\}_2CH]^+$ in **10** is similar to that in $[\{C(Me)N(Me)\}_2CH][Ph_5C_5]$.⁴²

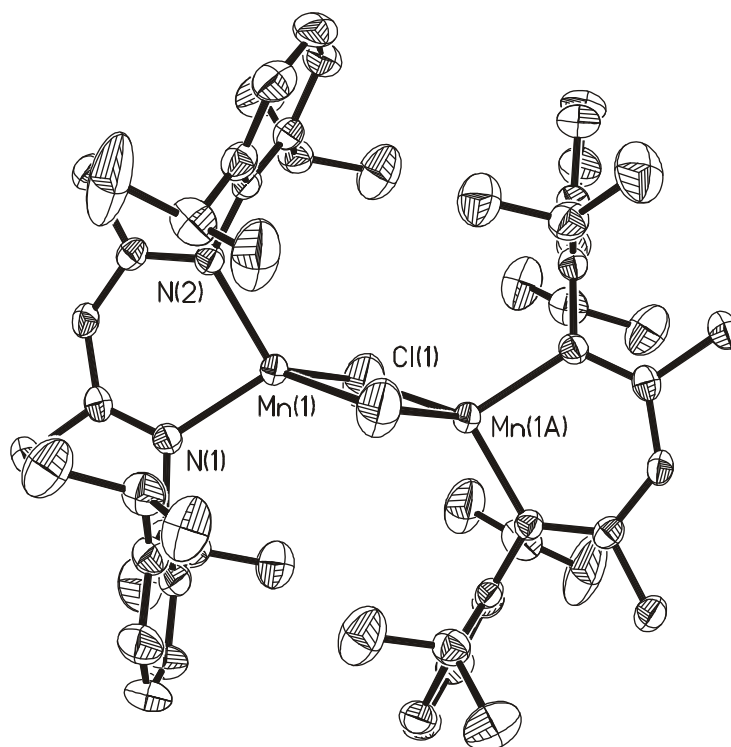


Figure 5. Molecular structure of **8** (50 % probability ellipsoids). Hydrogen atoms are omitted for clarity.

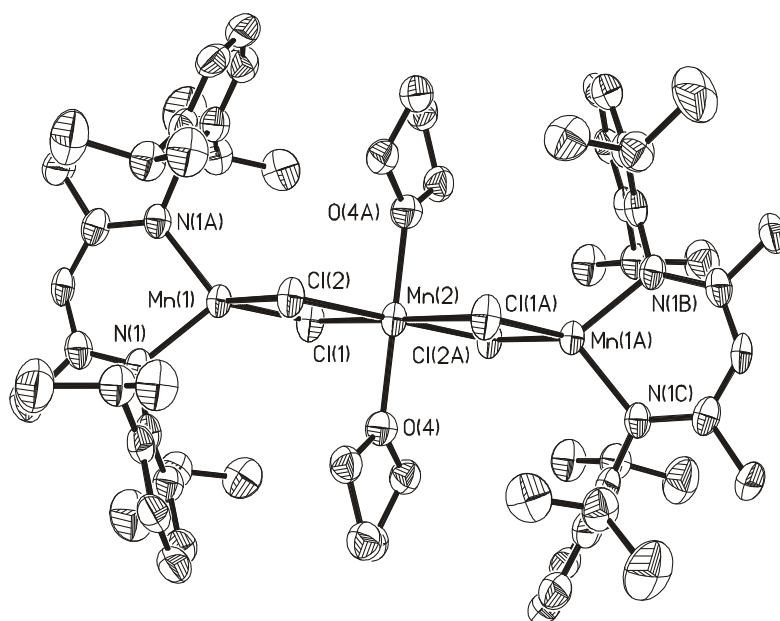


Figure 6. Molecular structure of **9** (50 % probability ellipsoids). Hydrogen atoms are omitted for clarity.

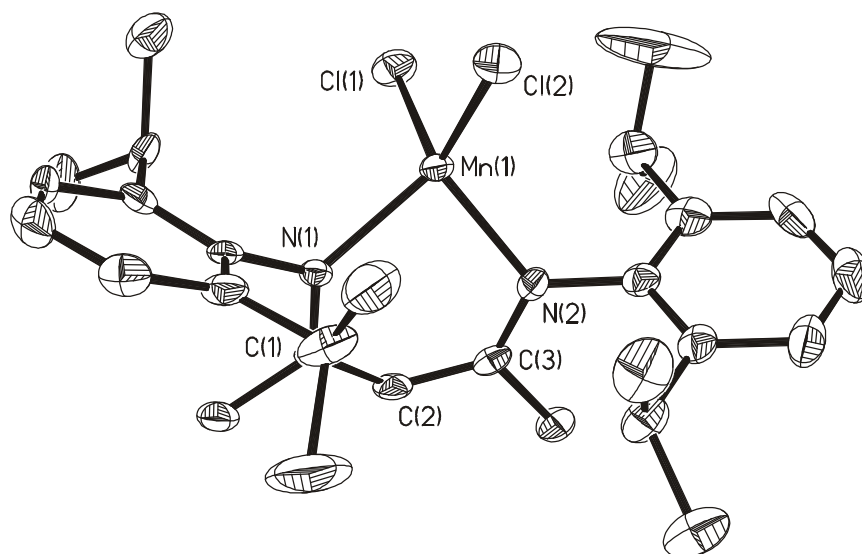


Figure 7. Crystal structure of the anion of **10** (50 % probability ellipsoids).
Hydrogen atoms are omitted for clarity.

Table 3. Selected bond lengths (Å) and bond angles (°) for compounds **7** and **8**

Compound 7			
Mn(1)–N(1)	2.083(2)	N(1)–Mn(1)–N(2)	92.21(8)
Mn(1)–N(2)	2.072(2)	N(1)–Mn(1)–Cl(1)	118.99(7)
Mn(1)–Cl(1)	2.3688(11)	N(2)–Mn(1)–Cl(1)	116.72(7)
Mn(1)–Cl(2)	2.3887(10)	Cl(1)–Mn(1)–Cl(2)	96.10(3)
Li(1)–Cl(1)	2.371(5)	N(1)–Mn(1)–Cl(2)	115.29(6)
Li(1)–Cl(2)	2.383(5)	N(2)–Mn(1)–Cl(2)	119.48(6)
Li(1)–O(1)	1.948(6)	Cl(1)–Li(1)–Cl(2)	96.20(17)
Li(1)–O(2)	1.975(6)	O(1)–Li(1)–O(2)	114.7(3)
Compound 8			
Mn(1)–N(1)	2.0830(9)	N(1)–Mn(1)–N(2)	92.80(3)
Mn(1)–N(2)	2.0819(10)	N(1)–Mn(1)–Cl(1)	117.09(3)
Mn(1)–Cl(1)	2.3422(7)	N(2)–Mn(1)–Cl(1)	118.34(3)
Mn(1)–Cl(1A)	2.3093(6)	Cl(1)–Mn(1)–Cl(1A)	90.49(2)
Mn(1A)–Cl(1)	2.3093(6)	N(1)–Mn(1)–Cl(1A)	119.74(3)
Mn(1)–Mn(1A)	3.275	N(2)–Mn(1)–Cl(1A)	120.93(3)

Table 4. Selected bond lengths (Å) and bond angles (°) for compounds **9** and **10**

Compound 9			
Mn(1)–N(1)	2.077(5)	N(1)–Mn(1)–N(1A)	91.3(2)
Mn(1)–N(1A)	2.077(4)	N(1)–Mn(1)–Cl(1)	120.65(13)
Mn(1)–Cl(1)	2.391(2)	N(1)–Mn(1)–Cl(2)	117.80(12)
Mn(1)–Cl(2)	2.412(2)	Cl(1)–Mn(1)–Cl(2)	91.36(7)
Mn(2)–Cl(1)	2.576(2)	O(4)–Mn(2)–O(4A)	180.0
Mn(2)–Cl(2)	2.5266(19)	O(4)–Mn(2)–Cl(2)	90.0
Mn(2)–O(4)	2.200(6)	O(4)–Mn(2)–Cl(1)	90.0
Mn(1)–Mn(2)	3.564	Cl(1)–Mn(2)–Cl(2)	84.65(6)
Compound 10			
Mn(1)–N(1)	2.102(2)	N(1)–Mn(1)–N(2)	91.64(8)
Mn(1)–N(2)	2.111(2)	N(1)–Mn(1)–Cl(1)	107.84(6)
Mn(1)–Cl(1)	2.3890(11)	N(2)–Mn(1)–Cl(1)	109.42(7)
Mn(1)–Cl(2)	2.3370(10)	Cl(1)–Mn(1)–Cl(2)	112.00(4)

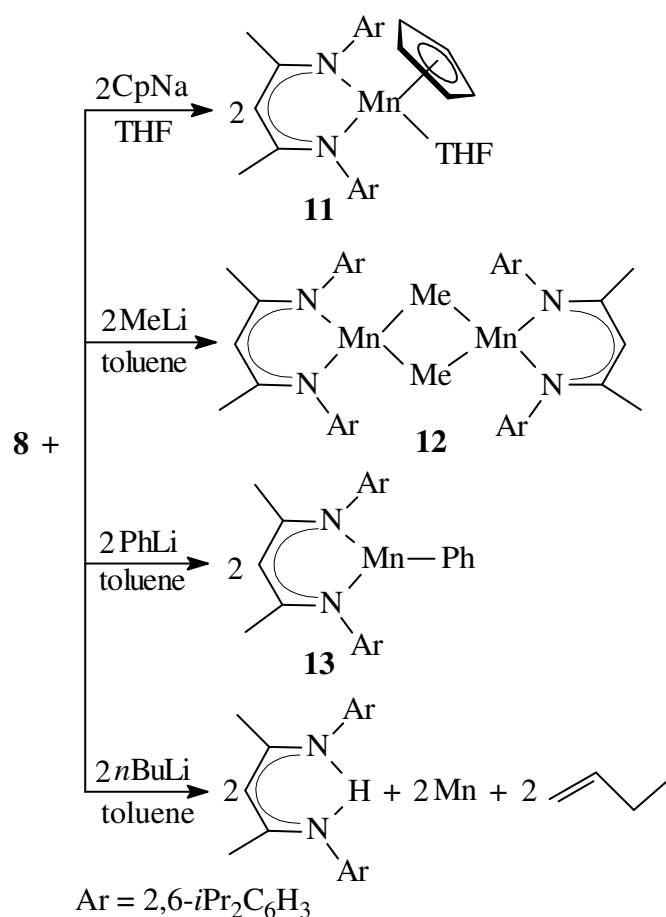
2.2.3. Reactivity of Compound **8** and its Organomanganese Derivatives **11** - **13** of Type LMnR (R = Cp, Me and Ph)

The substitution reactions of **8** with some nucleophiles were investigated in order to prepare organomanganese(II) complexes. Treatment of **8** with CpNa, MeLi and PhLi, respectively, resulted in the formation of the complexes LMnCp(THF) (**11**), [LMn(μ -Me)]₂ (**12**) and LMnPh (**13**) (Scheme 7). The monocyclopentadienyl manganese(II) compound **11** was readily obtained as yellow crystals from the reaction of **8** and 2 equiv. of CpNa in THF in high yield. Compound **11** is a rare example of a half-sandwich manganese(II) complex with the metal center of 17 valence electrons.⁴³ The addition of MeLi and PhLi, respectively, to **8** in toluene at low temperature smoothly provided the dimeric compound **12** and the monomer **13** in moderate yields. However, the successful isolation of pure **12** and **13** was not easy due to the difficult removal of small amounts of unreacted starting material **8**, so it requires several purification steps. The RLi reagents should be in some excess due to the stoichiometric amounts given in scheme 7. Recrystallization of the product from pentane has to be repeated. The reaction of **8** with *n*BuLi, however, resulted in a precipitate of a manganese mirror and LH, confirmed by EI-MS and ¹H NMR. The proposed mechanism for this reaction is obviously the direct intramolecular elimination of the alkyl group and the

chelating ligand. A similar decomposition pathway was suggested for various dialkyl Mn(II) species.⁴⁴

Complexes **11** - **13** are crystalline yellow solids, which are sensitive to air or moisture and were handled in a glove-box under purified nitrogen. Below the corresponding melting points of these compounds (210 - 212 °C for **11**, 190 - 192 °C for **12** and 230 - 232 °C for **13**), no decomposition was observed. In the EI-MS of **11**, [LMnCp]⁺ appears at *m/z* 537 as the most intense peak without the coordinated solvent, followed by *m/z* 472 [LMn]⁺ (92 %). EI-MS of **12** shows that the molecular peak M⁺ is absent, however, half of the molecular mass [LMnMe]⁺ is observed (*m/z* 487, 6 %) and the most intense peak (*m/z* 472) was assigned to [LMn]⁺. For **13**, M⁺ was observed at *m/z* 549 (3 %), followed by [M-C₆H₆]⁺ (*m/z* 471) as the most intense peak.

Scheme 7



The molecular structure of **11** is shown in Figure 8. Compound **11** is monomeric with the Cp coordinated to the manganese center and crystallizes in the orthorhombic space group *P*2₁2₁2₁. The metal center has a pseudotetrahedral geometry and is surrounded by the

cyclopentadienyl ring, the oxygen atom of the coordinated THF and two nitrogen atoms of the chelating ligand. The Mn-C distances (2.42 - 2.58 Å) are in the range of those found in $[\text{MeC}_5\text{H}_4\text{MnPEt}_3(\mu\text{-X})]_2$ (X = Cl, Br, I) (2.40 - 2.63 Å)⁴³ and $\text{CpMnTMEDA}(\eta^1\text{-Cp})$ (2.44 - 2.57 Å).⁴⁵ The Mn-N distances (av. 2.13 Å) in **11** are the longest and the N-Mn-N angle (90.3°) is the smallest among those in complexes **7** - **13**, which is in agreement with the higher coordination number of manganese. The Cp, the ligand plane and the THF plane are nearly orthogonal to each other.

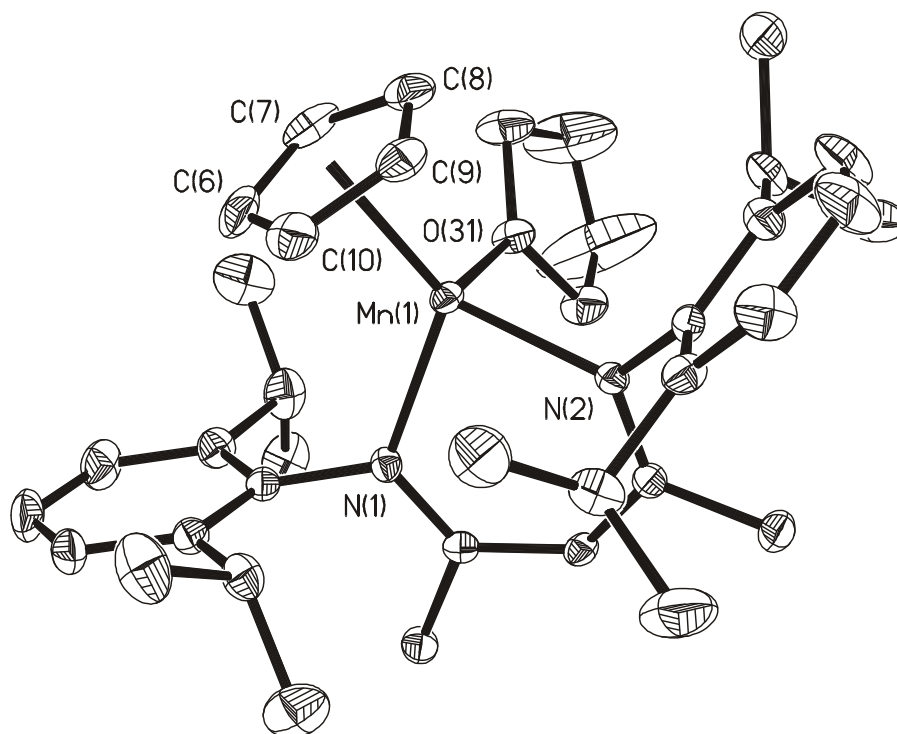


Figure 8. Molecular structure of **11** (50 % probability ellipsoids). Hydrogen atoms are omitted for clarity.

Table 5. Selected bond lengths (Å) and bond angles (°) for compound **11**

Mn(1)–N(1)	2.1242(15)	N(1)–Mn(1)–N(2)	90.26(5)
Mn(1)–N(2)	2.1306(15)	N(1)–Mn(1)–O(31)	97.69(5)
Mn(1)–O(31)	2.2787(12)	N(2)–Mn(1)–O(31)	97.60(6)
Mn(1)–C(6)	2.547(2)	N(1)–Mn(1)–C(6)	96.96(6)
Mn(1)–C(7)	2.442(2)	N(2)–Mn(1)–C(6)	144.79(7)
Mn(1)–C(8)	2.419(2)	O(31)–Mn(1)–C(6)	115.34(6)
Mn(1)–C(9)	2.5088(19)	N(1)–Mn(1)–C(7)	120.33(7)
Mn(1)–C(10)	2.5778(19)	N(2)–Mn(1)–C(7)	147.88(7)

Compound **12** is the first structurally characterized manganese alkyl complex containing bridging methyl groups. The solid-state structure of **12** (Figure 9) shows that the manganese centers have a distorted tetrahedral geometry. The backbone of the chelating ligand is nearly planar and the manganese atom is out of this plane (0.56 Å). The central core contains an ideally planar four-membered Mn_2C_2 ring, which bisects and is perpendicular (89.5°) to the two chelating ligands around it. The distance between two manganese atoms (2.81 Å) indicates a weak interaction rather than a strong Mn-Mn bond.^{13,46,47} The distance is comparable to that of the similar Mn_2C_2 core reported in the literature such as those in $\text{Mn}_2(\text{CH}_2\text{C}_6\text{H}_4\text{NMe}_2)_4$ ⁴⁷ (2.81 Å), $\text{Mn}_2(\text{CH}_2\text{SiMe}_3)_4(\text{PMe}_3)_2$ ⁴⁸ (2.77 Å) and $\text{Mn}_2(\text{CH}_2\text{CMe}_2\text{Ph})_4$ ⁴⁶ (2.72 Å). The Mn-C bond length (av. 2.27 Å) is in the range of those (2.22 - 2.28 Å) in the manganates $[\text{Li}(\text{TMEDA})]_2[\text{MnR}_4]$ (R = Me, Et, Bu, CH_2SiMe_3).^{46,49}

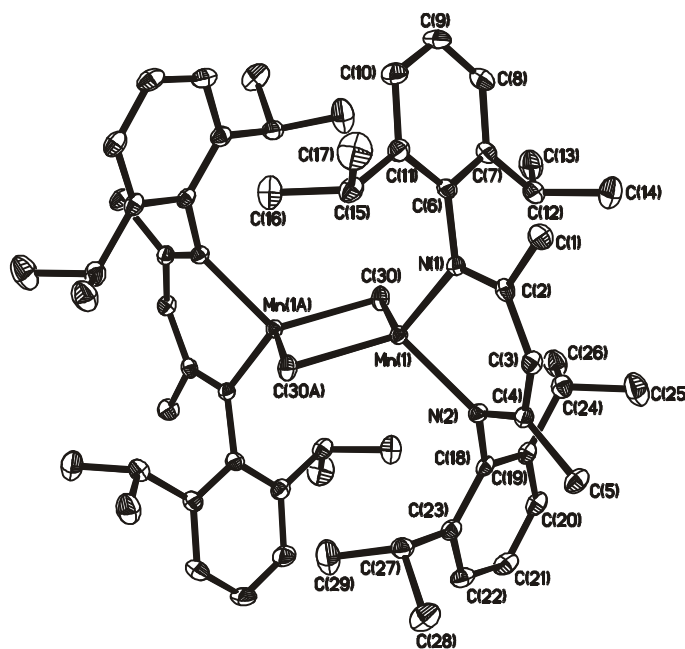


Figure 9. Molecular structure of **12** (35 % probability ellipsoids). Hydrogen atoms are omitted for clarity.

Single-crystals suitable for X-ray structural analysis of **13** were obtained by crystallization from diethyl ether. The X-ray solid-state structural analysis reveals a mononuclear three-coordinate manganese center with a terminal phenyl group. The sum of the angles at the metal center is 359.9° , which shows that the manganese center has a planar trigonal geometry. The six-membered MnN_2C_3 rings are essentially planar, co-planar with the terminal phenyl ring with a mean deviation $\Delta = 0.02$ Å. The dihedral angle between the

terminal Ph ring and the Ph rings of the aryl groups on the nitrogen is 83.9° . The Mn-C bond length in **13** is 2.08 \AA , which is particularly short compared to those reported for all other terminal Mn-Ph derivatives,⁵⁰ however, in the range of those in MnR_2 ($\text{R} = \text{C}(\text{SiMe}_3)_3$ ^{51a} and CH_2CMe_3 ^{51b}) ($2.01 - 2.10 \text{ \AA}$) possessing two-coordinate manganese(II) atoms. The Mn-N bond lengths in **13** are the shortest among those in compounds **7** - **13** probably due to the low-coordinated metal center consistent with the theoretical calculated results.

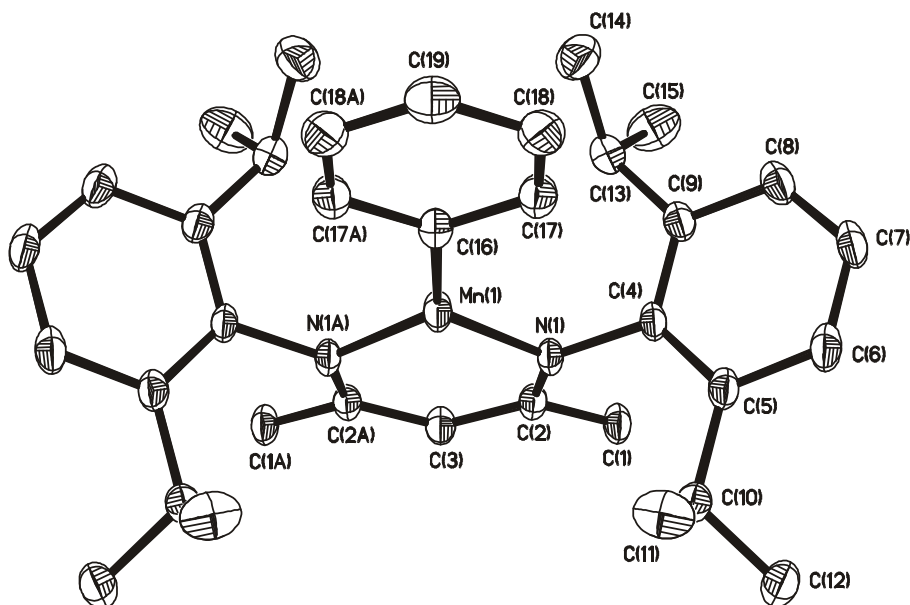


Figure 10. Molecular structure of **13** (30 % probability ellipsoids). Hydrogen atoms are omitted for clarity.

DFT calculations were carried out to get further insight into the geometry and electronic structure of compound **13**. RI-BP86 (TZVP for Mn, SV(P) for the other atoms) with the program Turbomole 5.5⁵² was used throughout the calculations except for the localized orbital shown in Figure 11, where B3LYP (6-311G(d) for Mn and 6-31G(d) for the other atoms) in Gaussian 98⁵³ was used. The reliability of RI-BP86 was tested by comparing the optimized geometry with the experimental structure of compound **13**. The maximum deviation of bond length is less than 0.03 \AA and of the bond angle is less than 4° . These results show the reliability of the RI-BP86 program compared to the X-ray data of compound **13**.

One aim of the theoretical study was to explain the co-planarity of the Ph ring with the chelating ligand. The result distinctively shows that the two rings in vertical position are less

stable than in a planar arrangement by 2.9 kcal/mol. However, if the Ar groups on the nitrogen are replaced by H atoms, the two rings in a vertical position are more stable than a co-planar arrangement by 57.4 kcal/mol, which indicates that the co-planar arrangement of the two rings results from the influence of the Ar groups, not the conjugation between the two rings. The role of the Ar groups can be attributed to two aspects: one is steric repulsion. If the two rings are forced in vertical positions, several short distances between H(Ph) and H(Ar) can be found; the other is phenyl-phenyl interaction. In **13** the terminal Ph and the Ar groups are nearly in their optimized position for this kind of interaction.⁵⁴

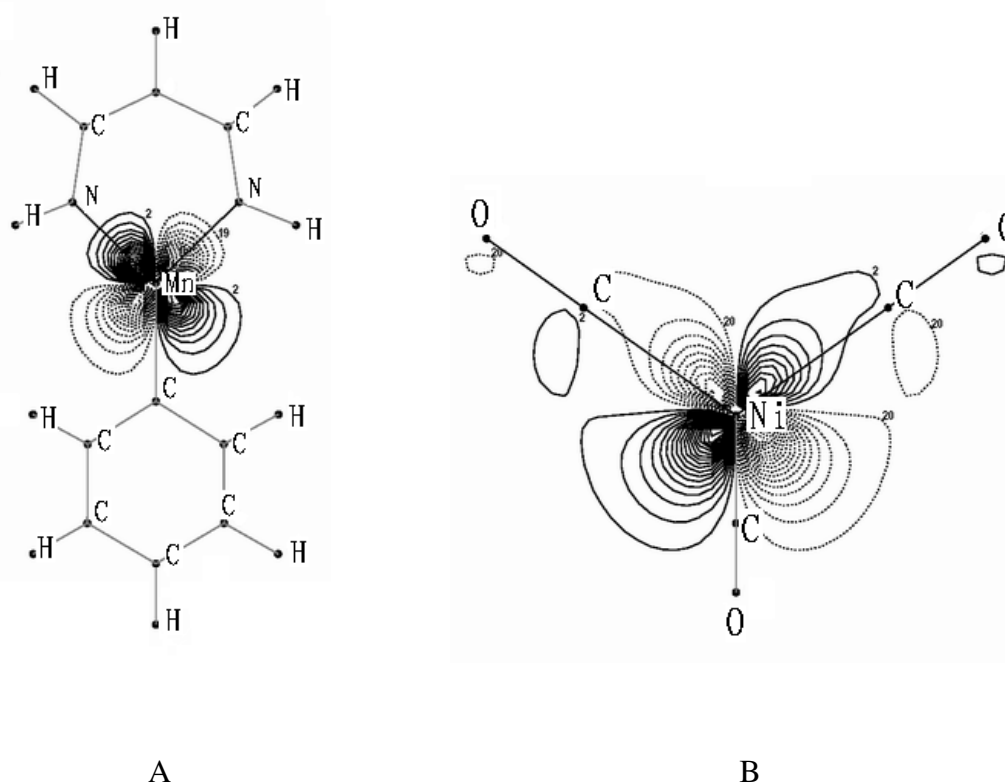


Figure 11. The most extended d orbital of the Mn in **13** (A) and of the Ni in Ni(CO)₄ (B).

The calculated results do not support the existence of significant Mn-C and Mn-N d- π conjugation in **13**. This is demonstrated by replacement of the terminal Ph group by CH₃, where the Mn-C d- π conjugation is impossible, while the Mn-C bond length almost does not change significantly (2.05 - 2.06 Å). Compound **13** was calculated by the B3LYP method (the ligand is replaced by C₃H₅N₂) and the molecular orbital was localized by Boys methods,^{55a} the most extended d orbital of Mn was drawn by MOLDEN 3.8 program^{55b} (Figure 11). However, when the most extended Ni d orbital of Ni(CO)₄ is compared with that of Mn in **13**, the latter d orbital is well localized around Mn, while in Ni(CO)₄ the d

orbitals are reformed and overlap with other atoms. These results indicate that the Mn-C and Mn-N bonds have pure σ character and the rather short Mn-C and Mn-N distances are attributed to the low coordination number of the central metal.

Table 6. Selected bond lengths (\AA) and bond angles ($^\circ$) for compounds **12** and **13**

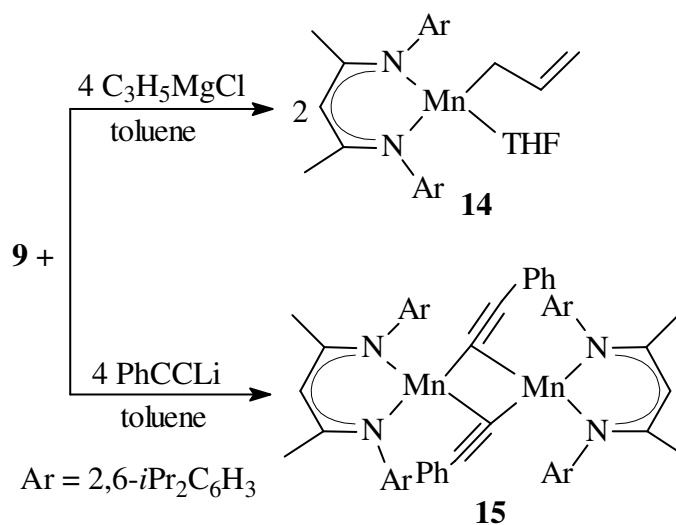
Compound 12			
Mn(1)-N(1)	2.125(2)	N(1)-Mn(1)-N(2)	89.68(6)
Mn(1)-N(2)	2.129(2)	N(1)-Mn(1)-C(30)	117.53(8)
Mn(1)-C(30)	2.241(2)	N(2)-Mn(1)-C(30)	117.18(8)
Mn(1)-C(30A)	2.306(2)	N(1)-Mn(1)-C(30A)	114.41(7)
Mn(1)-Mn(1A)	2.809(1)	N(2)-Mn(1)-C(30A)	114.72(8)
Compound 13			
Mn(1)-N(1)	2.041(3)	N(1)-Mn(1)-N(1A)	91.31(16)
Mn(1)-N(1A)	2.041(3)	N(1)-Mn(1)-C(16)	134.27(8)
Mn(1)-C(16)	2.077(6)	N(1A)-Mn(1)-C(16)	134.28(8)

2.2.4. Reactivity of Compound **9** and Formation of Compounds $\text{LMnC}_3\text{H}_5(\text{THF})$ (**14**) and $[\text{LMn}(\mu\text{-CCPh})]_2$ (**15**)

Addition of $\text{C}_3\text{H}_5\text{MgCl}$ and PhCClLi to **9** in toluene, respectively, at low temperature smoothly provided the monomeric compound $\text{LMnC}_3\text{H}_5(\text{THF})$ (**14**) and the dimeric compound $[\text{LMn}(\mu\text{-CCPh})]_2$ (**15**) in moderate yields (Scheme 8). The efforts to identify other species were unsuccessful. Compared to the substitution reactions of the dimer **8** with MeLi and PhLi , the reactions of **9** with $\text{C}_3\text{H}_5\text{MgCl}$ and PhCClLi resulted in easily accessible products **14** and **15**, which can be purified by recrystallization from hexane.

Complexes **14** and **15** are yellow crystalline solids soluble in THF. They are highly sensitive to air and moisture. In the EI-MS of **14**, $[\text{LMnC}_3\text{H}_5]^+$ is observed at m/z 537 (8%) without the coordinated THF, followed by m/z 472 $[\text{LMn}]^+$ as the most intense peak. Interestingly, the molecular ion M^+ at m/z 1146 in the mass spectrum of **15** can be seen albeit with very low intensity (1%), followed by $[1/2\text{M}]^+$ m/z 573 (40%) and $[\text{LMn-H}]^+$ m/z 471 (100%). The vibration for the bridging $\text{-C}\equiv\text{C-}$ group in the IR spectrum of **15** appears at 2034 cm^{-1} , which is consistent with the decrease of the bond strength of the $\text{C}\equiv\text{C}$ unit due to the π -interaction with the metal center.⁵⁶

Scheme 8



Complexes **14** and **15** were characterized by single-crystal X-ray diffraction. The structures are shown in Figures 12 and 13, respectively. Selected bond lengths and angles are given in Table 7.

Compound **14** is a monomeric species with the allyl ligand bound to the four-coordinate manganese center in an η^1 arrangement. To the best of our knowledge, **2** is the first structurally characterized allyl-manganese complex with η^1 bonding of the ligand. The metal center is of distorted tetrahedral geometry surrounded by the allyl group, a THF molecule and the chelating ligand. The backbone of the chelating ligand is nearly planar with the manganese atom out of this plane (0.53 Å), which is nearly in orthogonal position with the plane formed by Mn(1), C(6) and O(1). The Mn-C bond length (2.13 Å) is in the range of Mn-C single bonds and a little shorter than those in manganese complexes with allyl groups in an η^3 mode.⁵⁷ The large difference between the distances of C(7)-C(8) (1.31 Å) and C(6)-C(7) (1.44 Å) shows there is no significant delocalization of π -electrons in the allyl group. The distance between Mn(1) and C(8) (3.88 Å) do not support any bonding interaction. Interestingly, both the N-Mn-N angle (92.2°) and the Mn-N bond lengths (av. 2.09 Å) in **14** are larger than the corresponding ones in **9** (91.3° and 2.08 Å, respectively) due to the different *trans* effect.

The solid-state structure of **15** reveals a dimer formed by two bridging phenylethynyl groups, which is best described by assuming that Mn(1)-C(30) is a σ -bond, and that the two monomer units are linked together through π -bonding by donation of π -electron density of one C \equiv C bond to the empty orbital of the other metal center. To the best of our knowledge,

compound **15** is the first structurally characterized dinuclear manganese complex containing bridging alkynyl groups. Similar to complexes **9** and **14**, the manganese atom is out of the chelating ligand plane (0.47 Å). The central core contains an ideal planar four-membered Mn_2C_2 ring, which bisects and is perpendicular (90.8°) to the two chelating ligands around it. The distance between the two manganese atoms (3.12 Å) is beyond a Mn-Mn bonding range and significantly longer than those in dimeric manganese alkyl complexes $[\text{LMn}(\mu\text{-Me})]_2$ (**12**) (2.81 Å) and $\text{Mn}_2(\text{CH}_2\text{SiMe}_3)_4(\text{PMe}_3)_2$ ⁴⁸ (2.77 Å). This indicates that the bridge bonding in **15** is different from those in other dimeric species.⁴⁸ The carbon-carbon triple bond length (1.23 Å) is longer than the accepted average value of 1.21 Å,⁵⁸ reflecting the π -interaction between the triple bond and the metal center. Similar bond lengths are observed in $[\text{CuCl}(\eta^2\text{-PhCCMn}(\text{CO})_3(\text{dppe}))]$ ^{59a} (1.23 Å) and $\{\text{Cu}[\eta^2\text{-}i\text{BuCCMn}(\text{CO})_3(\text{dppe})]_2\}\text{PF}_6$ ^{59b} (1.24 Å) having alkynyl-manganese groups π -bonded to the copper. Despite the π -interaction between the triple bond and the metal center in **15**, the Mn(1A)-C(30)-C(31) unit remains almost linear (177.0°). The Mn-C bond lengths (av. 2.22 Å) are significantly longer than those (1.90 - 2.08 Å) in manganese complexes with terminal alkynyl groups.^{16a}

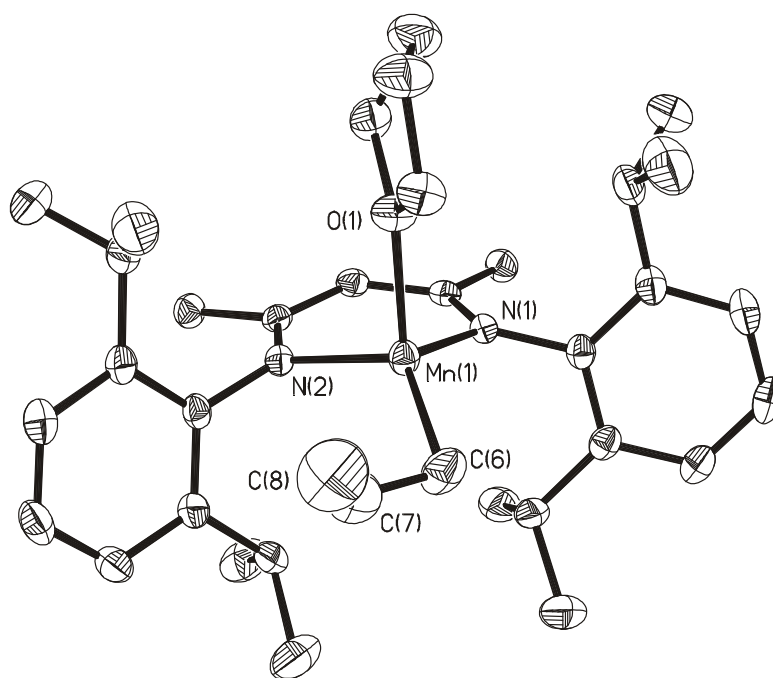


Figure 12. Molecular structure of **14** (50 % probability ellipsoids). Hydrogen atoms are omitted for clarity.

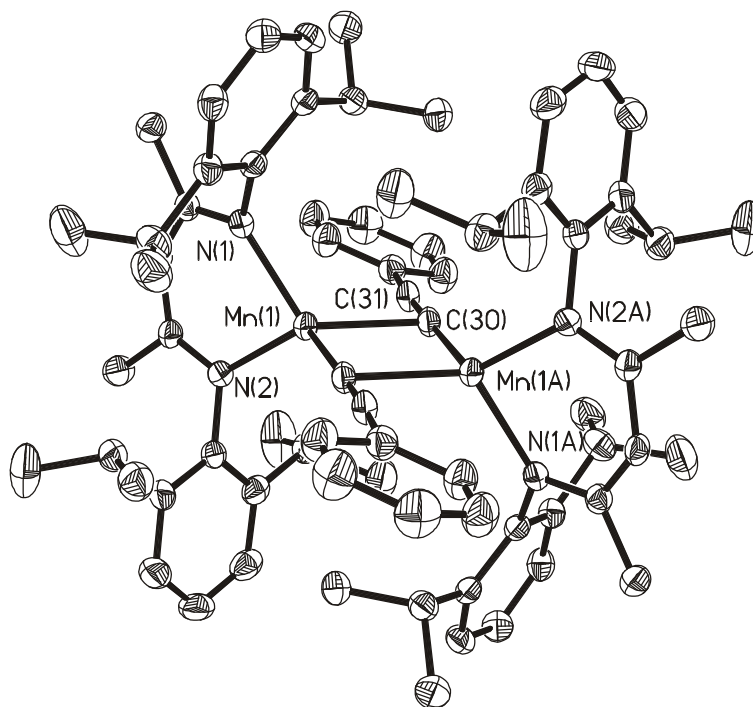


Figure 13. Molecular structure of **15** (50 % probability ellipsoids). Hydrogen atoms are omitted for clarity.

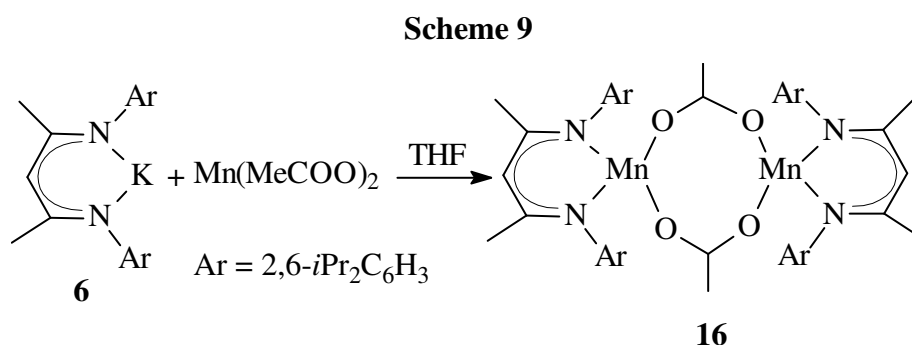
Table 7. Selected bond lengths (Å) and bond angles (°) for compounds **14** and **15**

Compound 14			
Mn(1)–N(1)	2.0915(16)	N(1)–Mn(1)–N(2)	92.19(6)
Mn(1)–N(2)	2.0948(15)	N(1)–Mn(1)–C(6)	123.58(7)
Mn(1)–C(6)	2.132(2)	N(2)–Mn(1)–C(6)	123.35(8)
Mn(1)–O(1)	2.1632(14)	N(1)–Mn(1)–O(1)	102.62(6)
C(7)–C(8)	1.305(4)	N(2)–Mn(1)–O(1)	101.77(6)
C(6)–C(7)	1.444(3)	C(6)–Mn(1)–O(1)	109.60(8)
Compound 15			
Mn(1)–N(1)	2.0907(18)	N(1)–Mn(1)–N(2)	89.60(7)
Mn(1)–N(2)	2.1045(18)	N(1)–Mn(1)–C(30)	119.51(8)
Mn(1)–C(30)	2.298(2)	N(2)–Mn(1)–C(30)	120.78(7)
Mn(1)–C(30A)	2.133(2)	C(30)–Mn(1)–C(30A)	90.55(8)
Mn(1A)–C(30)	2.133(2)	N(1)–Mn(1)–C(30A)	116.68(8)
Mn(1)–Mn(1A)	3.1202(7)	N(2)–Mn(1)–C(30A)	122.72(8)
C(30)–C(31)	1.226(3)	Mn(1A)–C(30)–C(31)	177.17(19)

2.3. Synthesis and Structure of the Dinuclear Manganese Acetate **16**

2.3.1. Synthesis and Spectroscopic Characterization of [LMn(μ -MeCOO)]₂ (**16**)

Dinuclear manganese complexes bridged by carboxylate groups have attracted great attention since such systems are known to exist at the active centers of some manganese-containing enzymes.⁶⁰ It was of interest to model the structures and functions of the manganese centers in such enzymes. The doubly carboxylate-bridged complex [LMn(μ -MeCOO)]₂ (**16**) was prepared from **6** and Mn(MeCOO)₂ in THF in good yield (Scheme 9). However, compound **16** could not be obtained when **5** was used instead of **6**.



The molecular ion peak of the dimeric complex **16** in the mass spectrum is not observed, whereas half of the molecular mass $[1/2M]^+$ is found at m/z 531 as the most intense peak. The IR spectrum of **16** displays the prominent vibrations for the O-C-O part of the bridging acetate groups ν_{as} (1602 cm⁻¹) and ν_s (1437 cm⁻¹).

2.3.2. X-ray Solid-state Structural Analysis of Complex **16**

Compound **16** crystallizes in the monoclinic space group $P2_1/n$ with four molecules per unit cell. The structure of **16** is shown in Figure 14. The central manganese atoms are bonded to two nitrogen atoms each from the chelating ligands and two oxygen atoms from the two bridging acetates in a distorted tetrahedral fashion. To the best of our knowledge, compound **16** is the first example of a doubly carboxylate-bridged complex with four-coordinate manganese(II). Similar to complexes **7** - **15**, the manganese atoms in **16** are out of the chelating ligand planes (av. 0.64 Å). Complex **16** contains two peripheral six-membered C₃N₂Mn rings and one central eight-membered C₂Mn₂O₄ macrocycle. The six- and eight-membered rings are nearly orthogonal to each other as shown by a dihedral angle of 85.8°.

The two acetates are in the bidentate $\mu_{1,3}$ syn-syn bridging mode, which is rare in the doubly carboxylate-bridged manganese(II) complexes.⁶⁰ The Mn-O distances (av. 2.01 Å) for the acetate bridges in **16** compare well with those (2.00 - 2.24 Å) observed in the manganese complexes adopting the same $\mu_{1,3}$ mode.²⁴ The non-bonding Mn-Mn distance (4.32 Å) is in the range (4.15 - 4.79 Å) of those found in comparable manganese(II) complexes.⁶⁰

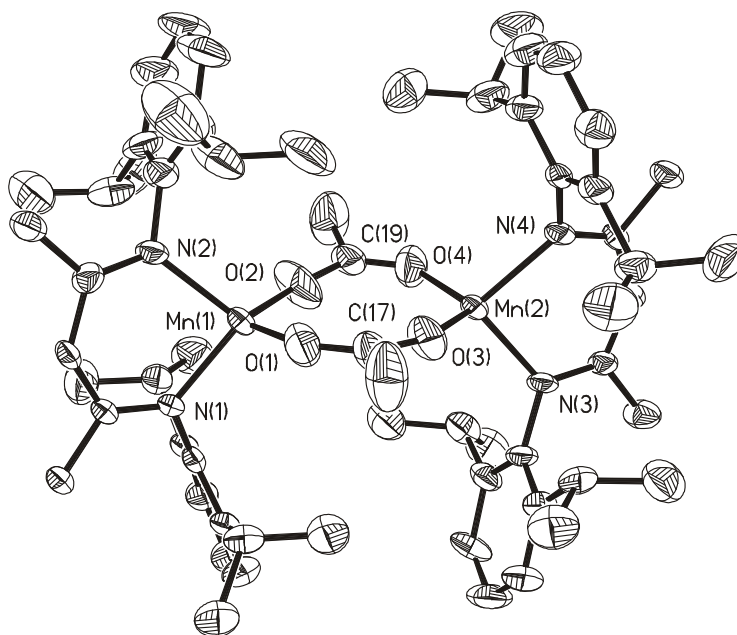


Figure 14. Molecular structure of **16** (50 % probability ellipsoids). Hydrogen atoms are omitted for clarity.

Table 8. Selected bond lengths (Å) and bond angles (°) for compound **16**

Mn(1)–N(1)	2.075(6)	N(1)–Mn(1)–N(2)	90.9 (2)
Mn(1)–N(2)	2.077(6)	N(1)–Mn(1)–O(1)	110.9(3)
Mn(1)–O(1)	2.014(7)	N(1)–Mn(1)–O(2)	115.6(3)
Mn(1)–O(2)	1.991(7)	N(2)–Mn(1)–O(1)	110.9(3)
Mn(2)–N(3)	2.082(6)	N(2)–Mn(1)–O(2)	112.3(3)
Mn(2)–N(4)	2.086(6)	O(1)–Mn(1)–O(2)	114.1(3)
Mn(2)–O(3)	2.012(7)	O(3)–Mn(2)–O(4)	117.8(3)
Mn(2)–O(4)	2.031(7)	N(3)–Mn(2)–N(4)	92.0 (2)
Mn(1)–Mn(2)	4.319(7)		

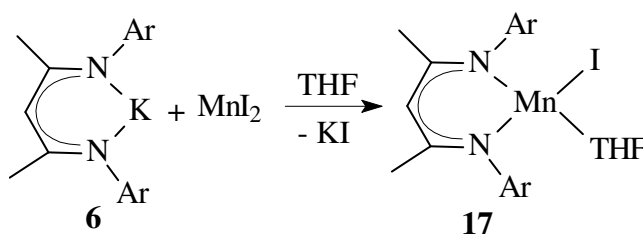
2.4. Synthesis, Structure and Reactivity of Manganese Iodides **17** - **19** Containing the Bulky β -Diketiminato Ligand

Organometallic iodide complexes have unique chemical properties due to the labile M-I bond compared to their M-Cl congeners.⁶¹ Recent results in our group proved that aluminum iodide LAlI_2 bearing the β -diketiminato ligand is a good starting material for some interesting reactions such as reduction and hydrolysis. For instance, we reported the monomeric LAl as a stable carbene analogue by reduction of LAlI_2 with potassium.³⁶ Furthermore, the aluminum dihydroxide $\text{LAl}(\text{OH})_2$ with terminal OH groups was obtained by hydrolysis of LAlI_2 using a liquid NH_3 /toluene two-phase system.³⁷ Consequently we became interested in transition metals and investigated the behavior of Mn iodides bearing β -diketiminato ligands. However, the efforts to reduce $\text{LMn}(\mu\text{-I})_2\text{Li}(\text{OEt}_2)_2$ were unsuccessful with sodium or potassium, maybe due to the stability of the lithium salt.^{40a} Therefore it was of interest to synthesize manganese iodides free of lithium salt and explore their reactivity.

2.4.1. Synthesis and Spectroscopic Characterization of Complexes **17** - **19**

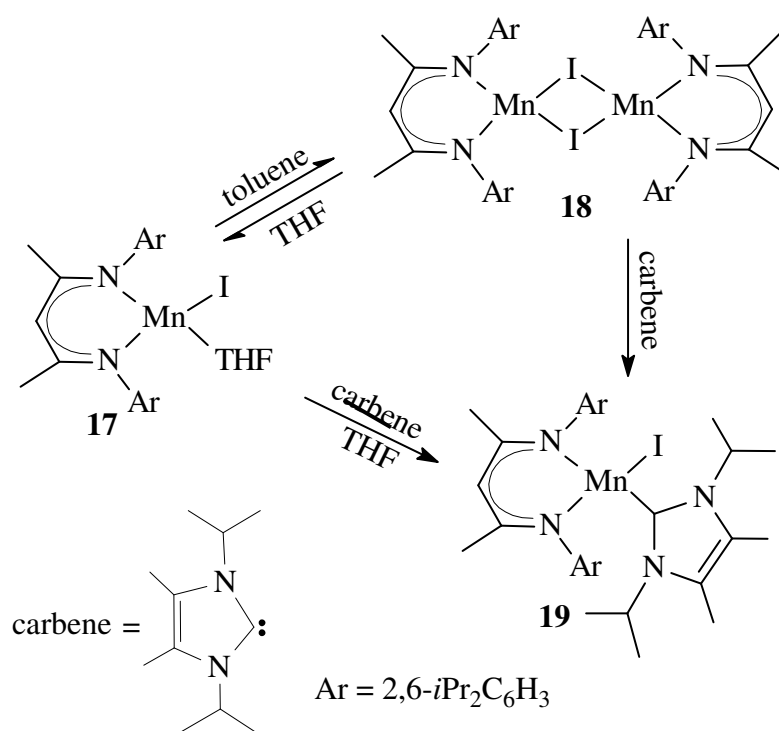
The reaction of MnI_2 with one equiv. of $\text{LLi}(\text{OEt}_2)$ (**5**) in diethyl ether afforded the heterobimetallic complex $\text{LMn}(\mu\text{-I})_2\text{Li}(\text{OEt}_2)_2$.^{40a} Attempts to remove the coordinated lithium salt from the manganese center were unsuccessful. However, the reaction of MnI_2 with one equiv. of LK (**6**) in THF easily gave the monomeric compound $\text{LMnI}(\text{THF})$ (**17**) in high yield (87 %) with a coordinated THF at the metal center. The EI-MS of **17** exhibits $[\text{LMnI}]^+$ (m/z 599) as the most intense peak without the coordinated THF. The formula of **17** was confirmed by the crystal structure (Figure 15). Attempts to prepare the di- β -diketiminato complex by using 2 equiv. of **5** or **6** were unsuccessful.

Scheme 10



Refluxing **17** in toluene for 0.5 h and removing all the volatiles in vacuum afforded the dimeric compound $[\text{LMn}(\mu\text{-I})_2]$ (**18**). Crystals suitable for X-ray analysis were obtained by recrystallization from toluene. The EI-MS of **18** does not exhibit the molecular ion peak M^+ whereas half of the molecular mass $[\text{LMnI}]^+$ is observed at m/z 599 (100 %), which shows that **18** is monomeric in the gas phase and no indication of fragments containing Mn-Mn species, which is consistent with the X-ray solid-state structural analysis. Compound **17** can also be obtained by dissolving **18** in THF (Scheme 11).

Scheme 11



Compound **17** can be considered as an adduct of a Lewis acid LMnI and a weak Lewis base THF. On the one hand, displacement the THF by a strong Lewis base $\text{C}[\text{N}(\text{iPr})\text{C}(\text{Me})_2]$ (**1**) readily afforded the carbene adduct $\text{LMnI}\{\text{C}[\text{N}(\text{iPr})\text{C}(\text{Me})_2]\}$ (**19**), which can also be obtained by adding **1** to the solution of **18** in toluene. On the other hand we were not able to prepare **18** by removing the carbene in **19**, which shows that the N-heterocyclic carbene is a much stronger σ -donor ligand. Compounds **17-19** are all soluble in polar solvents such as THF and toluene and have a poor solubility in hydrocarbon solvents.

2.4.2. X-ray Solid-state Structural Analyses of Complexes **17** and **18**

The X-ray solid-state structural analyses reveal that LMnI(THF) (**17**) is monomeric and [LMn(μ -I)]₂ (**18**) dimeric in the solid state (Figures 15 and 16). In both compounds the manganese centers are four-coordinate and display a distorted tetrahedral geometry. The backbone of the chelating ligand is nearly planar and the manganese atom is in both compounds out of the C₃N₂ plane (0.62 Å in **17** and 0.43 Å in **18**).

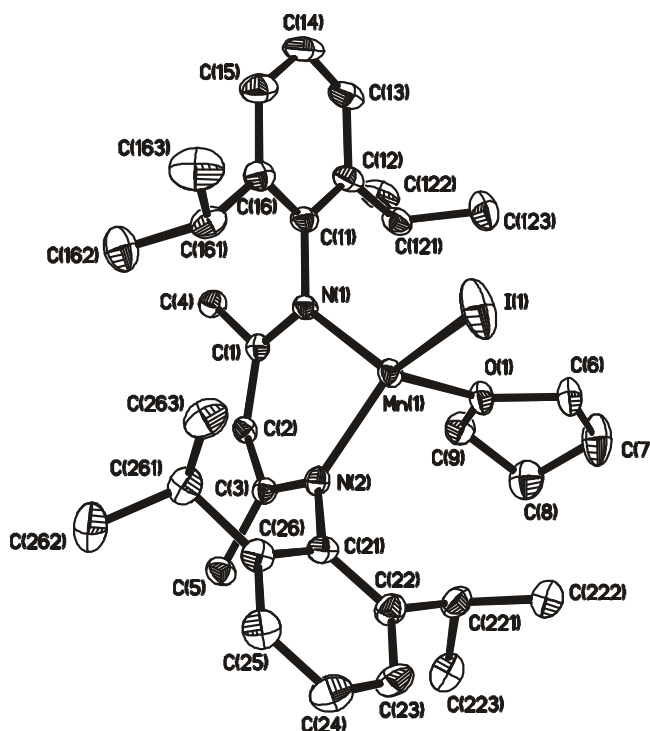


Figure 15. Molecular structure of **17** (30 % probability ellipsoids). Hydrogen atoms are omitted for clarity.

The terminal Mn-I distance (2.63 Å) in **17** is comparable to the reported values for terminal Mn-I bonds such as those in (sima)₂MnI⁶² (2.62 Å) (sima = NSiMe₃CPhNSiMe₃) and MnI₂(PEt₃)₂²⁶ (av. 2.67) Å), significantly shorter than the bridging Mn-I bonds in **18** (2.77 and 2.75 Å) and LMn(μ -I)₂Li(OEt)₂^{40a} (2.72 and 2.73 Å). The two manganese atoms are bridged by two iodine atoms in **18** and the distance between them is 3.62 Å, which is out of the range of a Mn-Mn bond. The Mn₂I₂ four-membered ring is exactly planar, bisecting and perpendicular to the two chelating ligands around it.

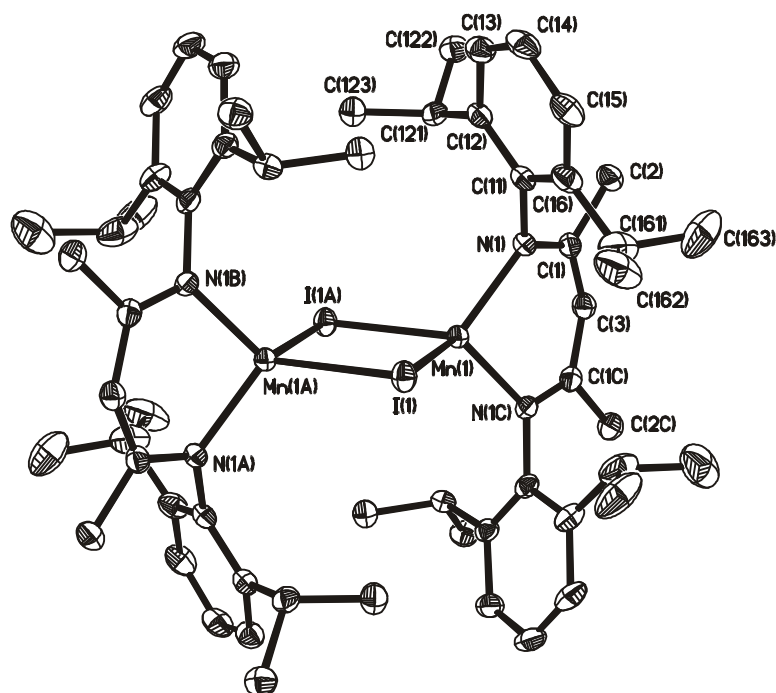


Figure 16. Molecular structure of **18** (30 % probability ellipsoids). Hydrogen atoms are omitted for clarity.

Table 9. Selected bond lengths (Å) and bond angles (°) for compounds **17** and **18**

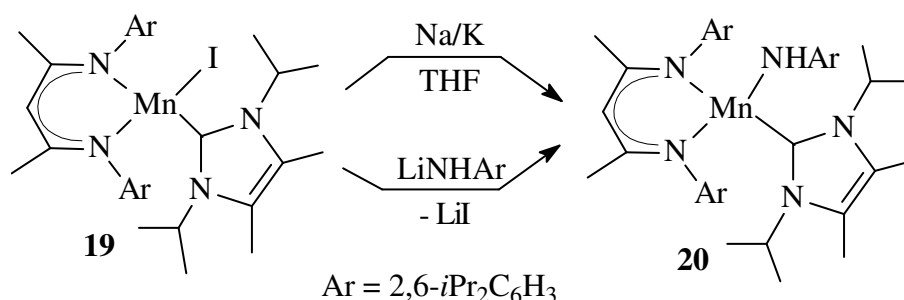
Compound 17			
Mn(1)–N(1)	2.079(3)	N(2)–Mn(1)–O(1)	104.28(12)
Mn(1)–N(2)	2.070(3)	N(1)–Mn(1)–O(1)	101.90(1)
Mn(1)–O(1)	2.155(3)	N(2)–Mn(1)–I(1)	124.79(9)
Mn(1)–I(1)	2.6272(8)	N(1)–Mn(1)–I(1)	124.12(9)
N(2)–Mn(1)–N(1)	93.56(13)	I(1)–Mn(1)–O(1)	104.96(8)
Compound 18			
Mn(1)–N(1)	2.067(2)	N(1)–Mn(1)–I(1)	119.04(7)
Mn(1)–N(1C)	2.067(2)	N(1C)–Mn(1)–I(1)	119.04(7)
Mn(1)–I(1)	2.7484(8)	N(1)–Mn(1)–I(1A)	113.02(7)
Mn(1)–I(1A)	2.7688(7)	I(1)–Mn(1)–I(1A)	98.14(2)
Mn(1A)–I(1)	2.7688(7)	Mn(1)–I(1)–Mn(1A)	81.86(2)
N(1)–Mn(1)–N(1C)	95.57(14)		

2.4.3. Reactivity of Compound **19** and the Derivative

LMnNHAr{C[N(*i*Pr)C(Me)]₂} (**20**)

Reduction of **19** by Na/K alloy at room temperature unexpectedly resulted in the formation of the monomeric compound **20** in low yield. Efforts to identify other species were unsuccessful. Assuming that Mn(II) complexes are used as radical initiators for radical polymerization processes,⁶³ it was tempting to propose that the formation of compound **20** is due to the partially decomposition of the intermediate radical [LMnC{N(*i*Pr)C(Me)}₂][•], which can not aggregate due to the presence of the bulky N-heterocyclic carbene. In the mass spectrum [LMnNHAr]⁺ was observed at *m/z* 648 (52 %), followed by [LMn]⁺ (472, 100 %). The elemental analyses are consistent with the solid-state structure. Compound **20** can also be prepared in good yield (76 %) by the reaction of **19** with LiNHAr (Scheme 12).

Scheme 12



Compound **20** crystallizes in the monoclinic space group *P*2₁/*c* with four molecules per unit cell. The structure of **20** is shown in Figure 17. The central manganese atom is bonded to three nitrogen atoms and one carbene carbon in a distorted tetrahedral fashion. The Mn-C distance (2.27 Å) in **20** is in the normal range of those in the manganates [Li(TMEDA)]₂[MnR₄]⁶⁴ (2.22 - 2.28 Å) (R = Me, Et, Bu and CH₂SiMe₃). However it is significantly longer than the Mn-C(carbene) distance in extensively studied manganese carbonyl carbene complexes CpMn(CO)₂CXY (X = Y = Me,⁶⁵ 1.87 Å; X = Y = Ph,⁶⁶ 1.89 Å; X = F, Y = Ph,⁶⁷ 1.83 Å; X = OEt, Y = Ph,⁶⁸ 1.87 Å). This may result from two reasons: one is the steric repulsion among the bulky substituents; the other is the very weak Mn→C back bonding in **20** due to the relatively high energy of the formal empty p(π) orbital of the N-heterocyclic carbene carbon, which is increased by the N→C bond.^{4a,69} In this respect, N-heterocyclic carbenes are different from the usual carbenes, which exhibit rather strong

M→C back bonding.^{68,70} The manganese atom in **20** is out of the carbene plane (0.41 Å) and the dihedral angle between the carbene plane and the chelating ligand plane is 108.8°. The Mn(1)-N(3) bond length in **20** is 2.06 Å close to those reported in Mn(II) amides.⁷¹

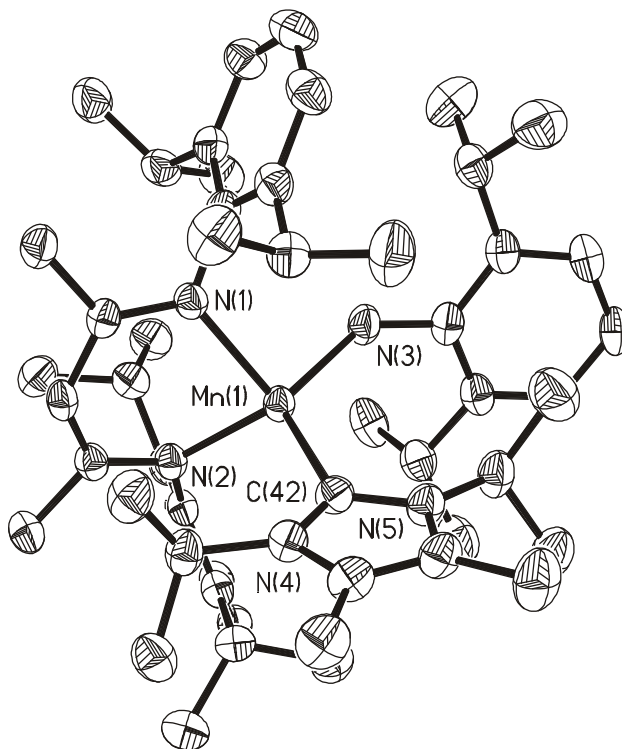


Figure 17. Molecular structure of **20** (50 % probability ellipsoids). Hydrogen atoms are omitted for clarity.

Table 10. Selected bond lengths (Å) and bond angles (°) for compound **20**

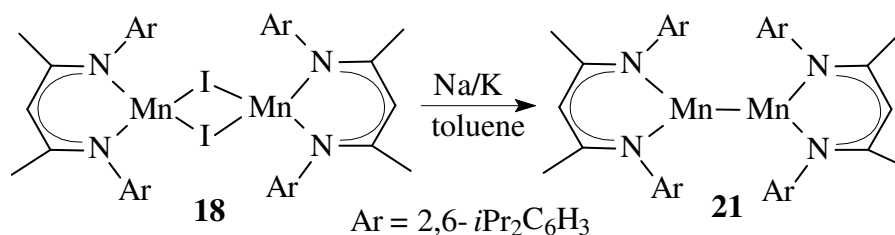
Mn(1)–N(1)	2.166(2)	N(3)–Mn(1)–N(1)	99.25(7)
Mn(1)–N(2)	2.133(2)	N(2)–Mn(1)–N(1)	88.94(7)
Mn(1)–N(3)	2.055(2)	N(3)–Mn(1)–C(42)	117.46(8)
Mn(1)–C(42)	2.270(2)	N(2)–Mn(1)–C(42)	111.68(8)
N(3)–Mn(1)–N(2)	123.25(7)	N(1)–Mn(1)–C(42)	109.83(7)

2.5. Synthesis, Characterization and Reactivity of the First Complex with Three-coordinate Manganese(I) **21**

2.5.1. Synthesis and Spectroscopic Characterization of [LMn]₂ (**21**)

The reduction of the complex [LMn(μ -I)]₂ (**18**) with Na/K alloy in toluene at room temperature affords [LMn]₂ (**21**) with three-coordinate manganese(I) as dark red crystals in about 15 % yield (Scheme 13). Compound **21** is thermally stable and melts without decomposition at 154 - 156 °C. Interestingly, the molecular ion peak of **21** at m/z 944 can be seen, albeit in low intensity (5 %) in the EI mass spectrum. The most intense peak at m/z 472 corresponds to the monomeric unit.

Scheme 13



2.5.2 X-ray Solid-state Structural Analysis of Compound **21**

Single crystals of **21** suitable for X-ray structural analysis were obtained from toluene at 4 °C. The X-ray single-crystal structural analysis of **21** reveals its dimeric nature with a central Mn₂²⁺ core (Figure 18). Each manganese is three-coordinated. The coordination environment around each manganese center consists of two nitrogen atoms of the chelating ligand and the other manganese atom in a perfectly trigonal planar environment and the sum of the bond angles around each manganese averages to 359.4°. Compound **21** contains two C₃N₂Mn six-membered rings, where the C₃N₂ portions of the rings are planar, the manganese atoms are significantly out of the planes (av. 0.53 Å). The two six-membered rings are nearly orthogonal to each other as shown by a dihedral angle of 80.6°. The Mn-N bonds (av. 2.10 Å) are slightly longer than that observed in **18** (av. 2.07 Å). Interestingly, the angle N-Mn-N (89.82°) in **21** is more acute than that observed in **18** (av. 94.59°). The Mn-Mn distance in **21** (2.72 Å) is significantly shorter than that in Mn₂(CO)₁₀¹⁸ (2.90 Å) with a formal oxidation state of 0, a little longer than that in Mn₂(CO)₇(μ -S₂)⁷² (2.67 Å) with a formal oxidation state

of +1, which compares well to that observed in $\text{Mn}_2(\text{CH}_2\text{CMe}_2\text{Ph})_4^{46}$ (2.72 Å) with a formal oxidation state of +2. This indicates that the Mn-Mn bond in **21** is weak and considered to be highly reactive.

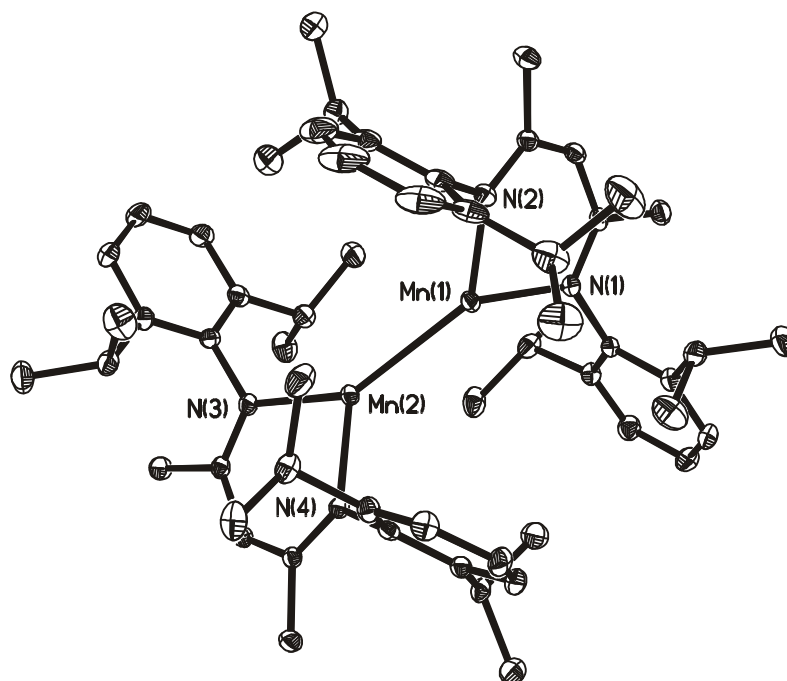


Figure 18. Molecular structure of **21** (30 % probability ellipsoids). Hydrogen atoms are omitted for clarity.

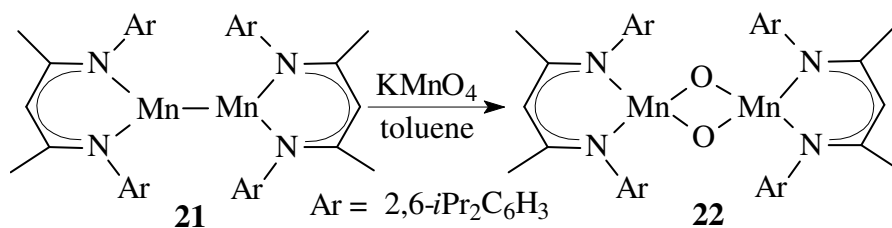
Table 11. Selected bond lengths (Å) and bond angles (°) for compound **21**

Mn(1)–N(1)	2.097(2)	N(1)–Mn(1)–N(2)	89.72(9)
Mn(1)–N(2)	2.101(2)	N(1)–Mn(1)–Mn(2)	139.96(6)
Mn(1)–Mn(2)	2.721(1)	N(2)–Mn(1)–Mn(2)	129.67(6)
Mn(2)–N(3)	2.116(2)	N(3)–Mn(2)–N(4)	89.92(8)
Mn(2)–N(4)	2.094(2)	N(3)–Mn(2)–Mn(1)	141.26(6)

2.5.3. Reactivity of Compound **21** and the Derivative $[\text{LMn}(\mu\text{-O})_2]$ (**22**)

Stirring a mixture of **21** and excess KMnO_4 in toluene at room temperature for 2 d smoothly afforded the dimeric oxide $[\text{LMn}(\mu\text{-O})_2]$ (**22**) as red crystals. Interestingly, the molecular ion peak of **22** in the EI-MS appears as the most intense peak at m/z 976.

Scheme 14



The molecular structure of **22** is shown in Figure 19. This compound contains two peripheral six-membered $\text{C}_3\text{N}_2\text{Mn}$ rings and one central four-membered Mn_2O_2 ring. Each manganese center is tetrahedrally coordinated. The dihedral angle between the six- and the four-membered rings is 39.9° . Compound **22** is the first example of bis(μ -O) complexes with four-coordinate Mn(III) centers. The Mn-O distances in **22** average to 1.82 \AA and are in the normal range ($1.79 - 1.86 \text{ \AA}$) for Mn-O bond lengths observed in other compounds.⁷³ The Mn-Mn distance in **22** is 2.66 \AA , which is the shortest separation observed in bis(μ -O) dimanganese(III) complexes.⁷³

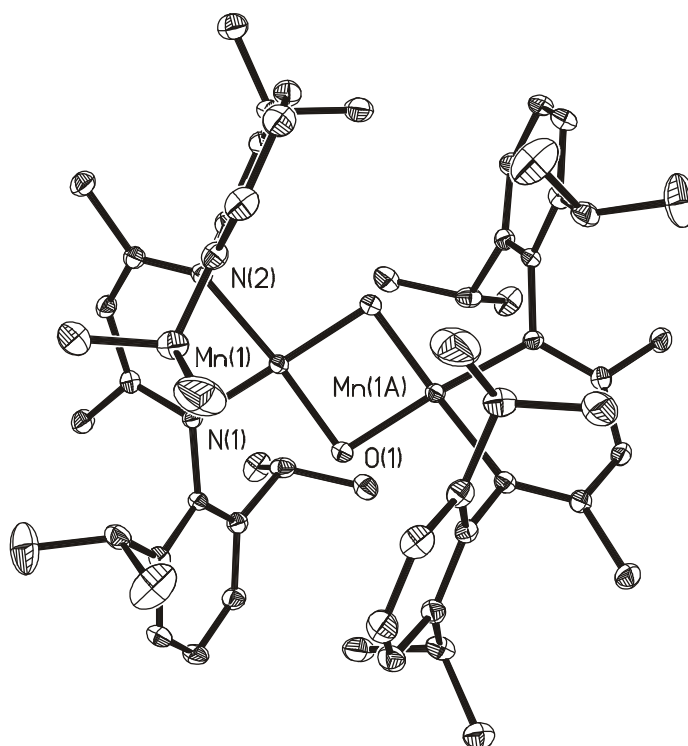


Figure 19. Molecular structure of **22** (30 % probability ellipsoids). Hydrogen atoms are omitted for clarity.

Table 12. Selected bond lengths (Å) and bond angles (°) for compound **22**

Mn(1)–N(1)	2.013(2)	N(1)–Mn(1)–N(2)	90.28(8)
Mn(1)–N(2)	2.013(2)	N(1)–Mn(1)–O(1)	96.64(8)
Mn(1)–O(1)	1.809(2)	N(2)–Mn(1)–O(1)	157.90(9)
Mn(1)–O(1A)	1.827(2)	O(1)–Mn(1)–O(1A)	85.99(7)
Mn(1)–Mn(1A)	2.659(1)	N(1)–Mn(1)–O(1A)	156.26(8)

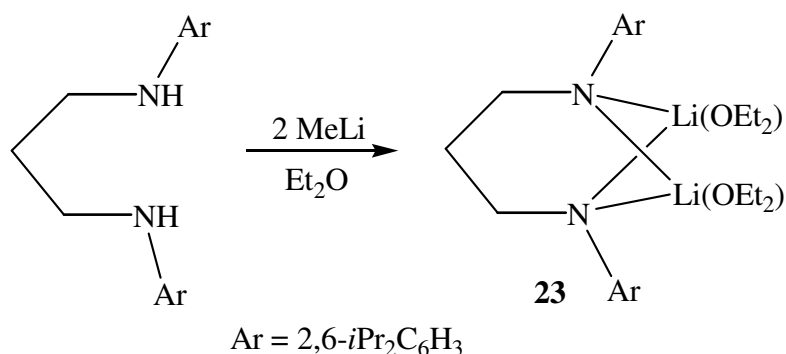
2.6. Synthesis and Structure of the Dinuclear Manganese Compound Containing a Bulky Diamide Ligand

Considering the recent success in the synthesis of complexes of main-group elements, transition metals and lanthanides with unusual properties with the bulky β -diketimate ligand [HC(CMeNAr)₂] (Ar = 2,6-*i*Pr₂C₆H₃),³⁵ we were interested in investigating the behavior of the bulky chelating diamide ligand [ArN(CH₂)₃NAr]²⁻, comparable in steric properties with the β -diketimate ligand and expected to result in interesting new organometallic chemistry. The bulky chelating diamide ligand [ArN(CH₂)₃NAr]²⁻ was previously used by McConville and co-workers as a non-Cp ligand to prepare group 4 complexes, which can catalyze olefin polymerization under ‘living’ conditions.⁷⁴ Cloke and Roesky et al. reported on lanthanide complexes bearing this ligand.⁷⁵ Recently we isolated the aluminum hydride [ArN(CH₂)₃NAr]LAlH(NMe₃) and its derivatives {[ArNH(CH₂)₃NAr]Al}₂(μ -E)₂ (E = S, Se and Te) by hydrogen transfer from chalcogen to nitrogen.⁷⁶

2.6.1. Synthesis and Spectroscopic Characterization of [ArN(CH₂)₃NAr][Li(OEt)₂]₂ (**23**) and Mn₂[ArN(CH₂)₃NAr]₂ (**24**)

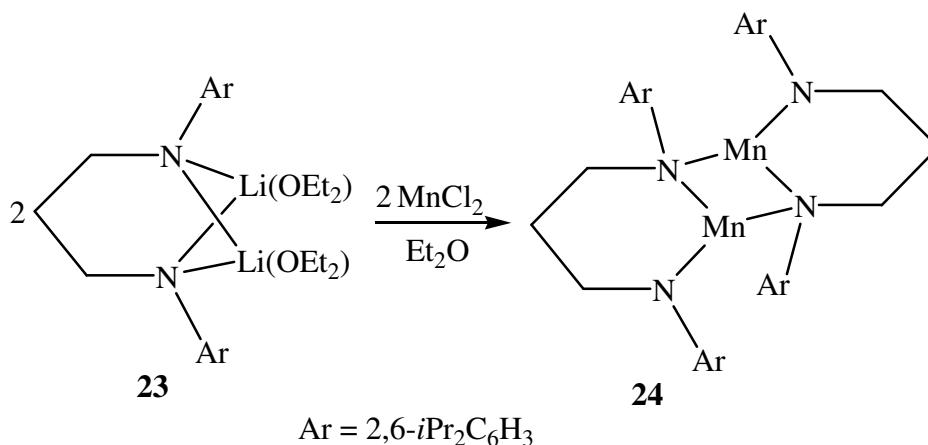
The lithiation of ArNH(CH₂)₃NHAr with 2 equiv. of MeLi in diethyl ether smoothly proceeded to afford [ArN(CH₂)₃NAr][Li(OEt)₂]₂ (**23**) as colorless crystals in high yield (Scheme 15). The existence of the coordinated diethyl ether molecules has been confirmed by ¹H NMR, elemental analysis, and X-ray solid-state structural analysis. The dilithium salt **23** is soluble in diethyl ether and stable under an inert atmosphere and is a useful reagent for metathesis reactions with metal halides.

Scheme 15



The reaction of **23** with one equiv. of anhydrous MnCl₂ in diethyl ether at low temperature smoothly provided the dimeric compound Mn₂[ArN(CH₂)₃NAr]₂ (**24**) in good yield (Scheme 16). The same compound was obtained even when 2 equiv. of MnCl₂ were employed. Complex **24** is soluble in CH₂Cl₂ and THF and has a moderate solubility in diethyl ether and toluene. Compound **23** is a colorless solid while **24** is a yellow-green crystalline solid. Complexes **23** and **24** have been characterized by EI-MS, ¹H NMR, IR and X-ray solid-state structural analysis. The molecular ion peak of **24** in the EI mass spectrum is observed at *m/z* 894 (49 %), followed by the most intense peak at *m/z* 705 [M-CH₂NAr]⁺.

Scheme 16



2.6.2. X-ray Solid-state Structural Analyses of Compounds **23** and **24**

The X-ray solid-state structural analysis of **23** (Figure 20) reveals a monomer with two three-coordinated lithium atoms. Each of the lithium atoms is bonded to two nitrogen atoms of the chelating ligand and one oxygen atom of the coordinated ether. It is better to describe the coordination sphere of the Li atoms as trigonal planar rather than trigonal pyramidal.

Two C_3N_2Li six-membered rings are formed, one displays a boat conformation while the other is in a chair conformation. The interplanar angle between the central two LiN_2 planes is 43.8° . The Li-N distances are in the normal range 1.94-2.15 Å.⁷¹ In addition, there are some very close contacts between Li(1), Li(2) and various carbon and hydrogen atoms from the chelating ligand: Li(1)-H(26a) 2.29(4) Å, Li(2)-C(2) 2.36(2) Å, and Li(2)-H(2a) 2.02(4) Å. Similar contacts have been observed in $[LiArN(CH_2)_2NArLi]_2$.⁷¹

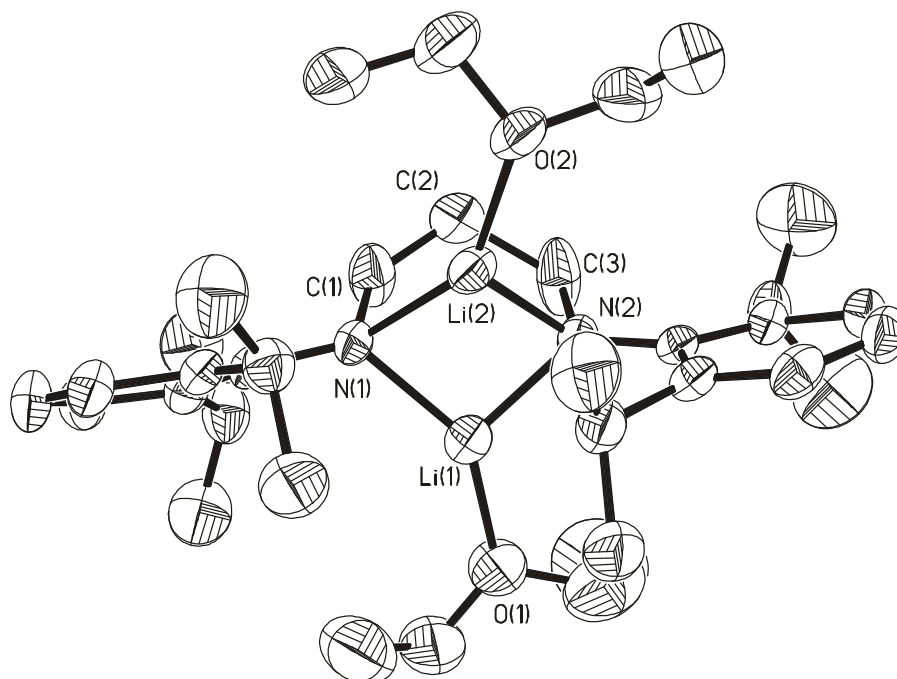


Figure 20. Molecular structure of **23** (50 % probability ellipsoids). Hydrogen atoms are omitted for clarity.

$Mn_2[ArN(CH_2)_3NAr]_2$ (**24**) crystallizes in the triclinic space group $P-1$. The dimer is formed through two bridging nitrogen atoms. The central core contains a nonplanar Mn_2N_2 four-membered ring, which is in a butterfly configuration with the dihedral angle of 28.6° . This arrangement is caused by the strain of the bulky aryl groups. Each metal atom is surrounded by three nitrogen atoms and out of this plane formed by them about 0.33 Å, so that both metal atoms are in a trigonal pyramidal geometry. The two ligands chelate two metal atoms to fuse two six-membered MnN_2C_3 rings, which display a boat conformation with the two metal atoms at the stern and the corresponding opposite carbon atoms at the bow. The manganese atom is about 0.17 Å out of the plane formed by the two carbon and two nitrogen atoms. The opposite carbon atom is about 0.72 Å out of the plane.

The ligand in complex **24** is both chelating and bridging, so that one of the nitrogen atoms is three-coordinate and the other four-coordinate. To the best of our knowledge, complex **24** is the first example with the diamide ligand in such a bonding mode. The terminal Mn-N distances (av. 1.93 Å) are significantly shorter than those of the corresponding bridging ones (av. Mn-N 2.10 Å). The terminal and bridging Mn-N distances in **24** are about 0.06 Å shorter than the corresponding distances in the dimeric silylamide $\text{Mn}_2[\text{N}(\text{SiMe}_3)_2]_4$.⁷⁷ The terminal Mn-N bond lengths are even shorter than those found in amides with two coordinate metal centers $\text{Mn}[\text{N}(\text{SiMePh}_2)_2]_2$ (1.99 Å).⁷⁸ This possibly results from the strong N→Si interaction in the silylamide.⁷⁹

The Mn-Mn distance in complex **24** is 2.69 Å, which indicates that there is some bonding interaction between the metal centers. The distance is significantly shorter than those in the commonly planar Mn_2N_2 four-membered rings.^{77,79}

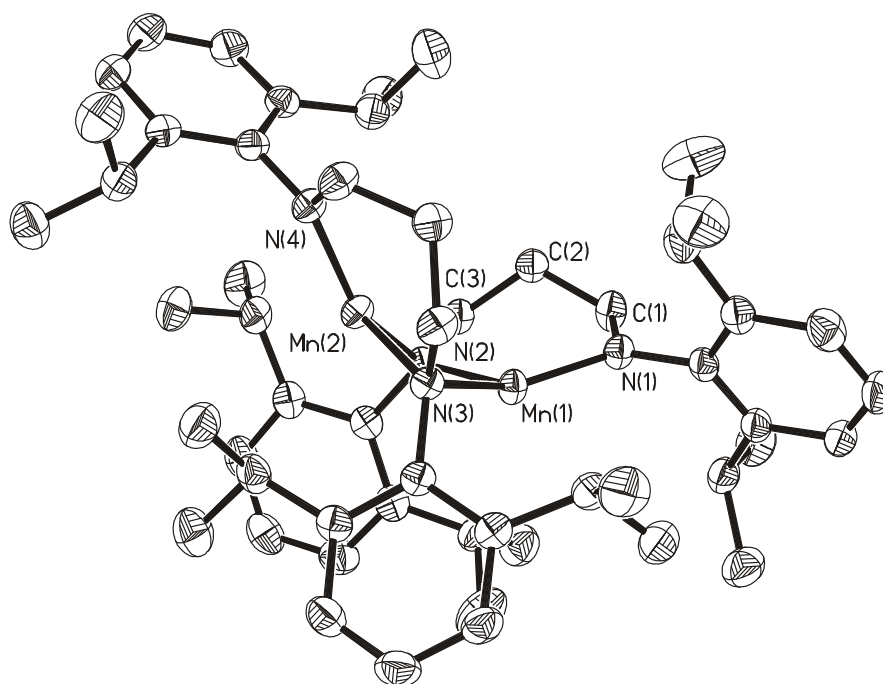


Figure 21. Molecular structure of **24** (50 % probability ellipsoids). Hydrogen atoms are omitted for clarity.

2.6.3. Magnetic Susceptibility Measurement of Compound **24**

The temperature dependence of the molar magnetic susceptibility χ_m and $\chi_m T$ for compound **24** is displayed in Figure 22. The plots of $\chi_m T(T)$ -T for the compound indicate the magnetic behavior with antiferromagnetic exchange interaction between the nearest neighboring spins. The value of $\chi_m T$ at 300 K is estimated to $6.82 \text{ emu}\cdot\text{K}\cdot\text{mol}^{-1}$, which is lower than those of the spin-only value ($s = 5/2 \text{ Mn(II)}_2$ dimer). This reveals that there exists antiferromagnetic exchange interaction between the two metal atoms.

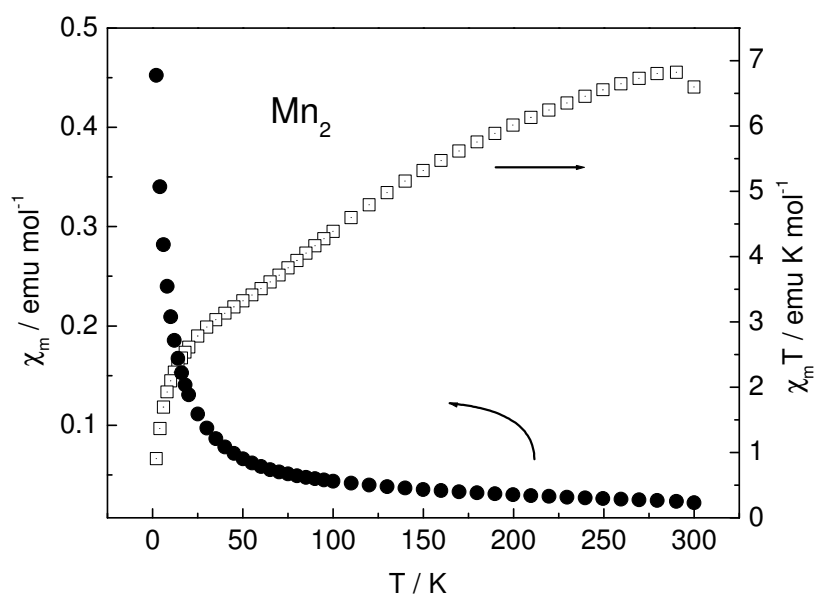


Figure 22. The plots of $\chi_m(T)$ -T and $\chi_m T(T)$ -T for compound **24**.

Table 13. Selected bond lengths [\AA] and bond angles [$^\circ$] for compounds **23** and **24**

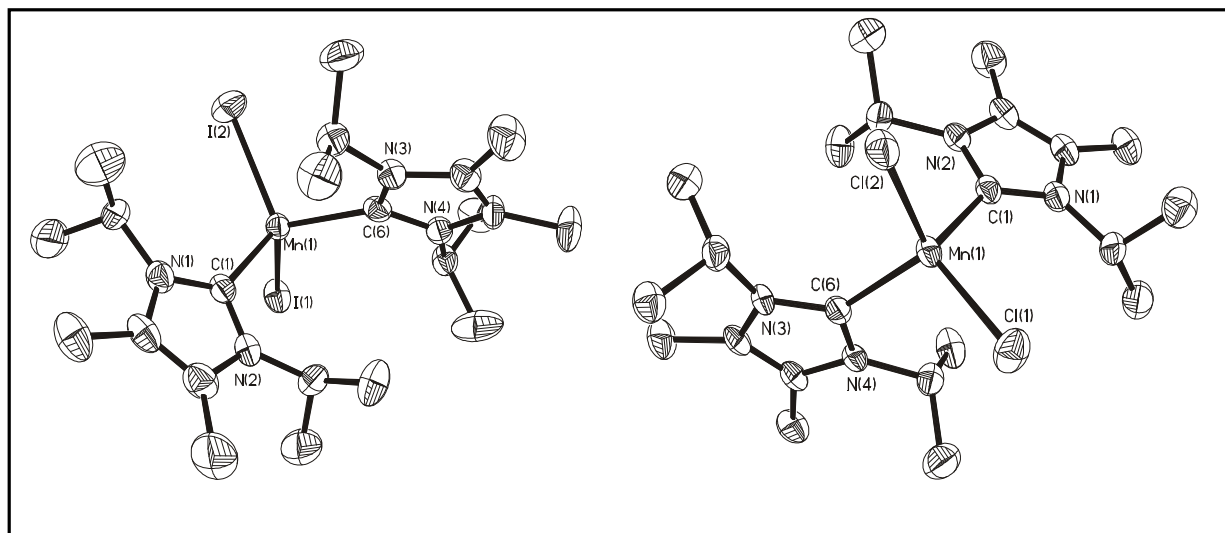
Compound 23			
Li(1)-O(1)	1.894(11)	O(1)-Li(1)-N(2)	118.3(5)
Li(1)-N(1)	1.999(10)	N(1)-Li(1)-N(2)	96.8(5)
Li(1)-N(2)	1.971(10)	O(1)-Li(1)-Li(2)	163.6(6)
Li(1)-Li(2)	2.514(13)	N(1)-Li(1)-Li(2)	51.9(3)
Li(2)-N(1)	2.028(10)	N(2)-Li(1)-Li(2)	52.4(3)
Li(2)-N(2)	2.039(10)	O(2)-Li(2)-N(1)	144.0(5)
Li(2)-O(2)	1.949(10)	O(2)-Li(2)-N(2)	114.2(5)
O(1)-Li(1)-N(1)	142.8(6)	N(1)-Li(2)-N(2)	93.7(4)
Compound 24			
Mn(1)-N(1)	1.932(2)	N(1)-Mn(1)-N(2)	106.79(10)
Mn(1)-N(2)	2.126(3)	N(1)-Mn(1)-N(3)	146.55(9)
Mn(1)-N(3)	2.078(3)	N(2)-Mn(1)-N(3)	96.72(10)
Mn(1)-Mn(2)	2.690(2)	N(1)-Mn(1)-Mn(2)	133.93(8)
Mn(2)-N(2)	2.093(3)	N(2)-Mn(1)-Mn(2)	49.86(8)
Mn(2)-N(3)	2.128(3)	N(3)-Mn(1)-Mn(2)	51.07(8)
Mn(2)-N(4)	1.935(2)	Mn(1)-N(2)-Mn(2)	79.20(9)

3. Summary and Outlook

3.1. Summary

In this thesis, N-heterocyclic carbenes, β -diketiminates and diamide ligands have been employed as supporting moieties for manganese compounds. The experimental results demonstrate that steric bulk and additional intramolecular coordination of these ligands can stabilize some unusual and unique compounds, which otherwise are inaccessible. In addition, these compounds may be useful as starting materials for further reactions.

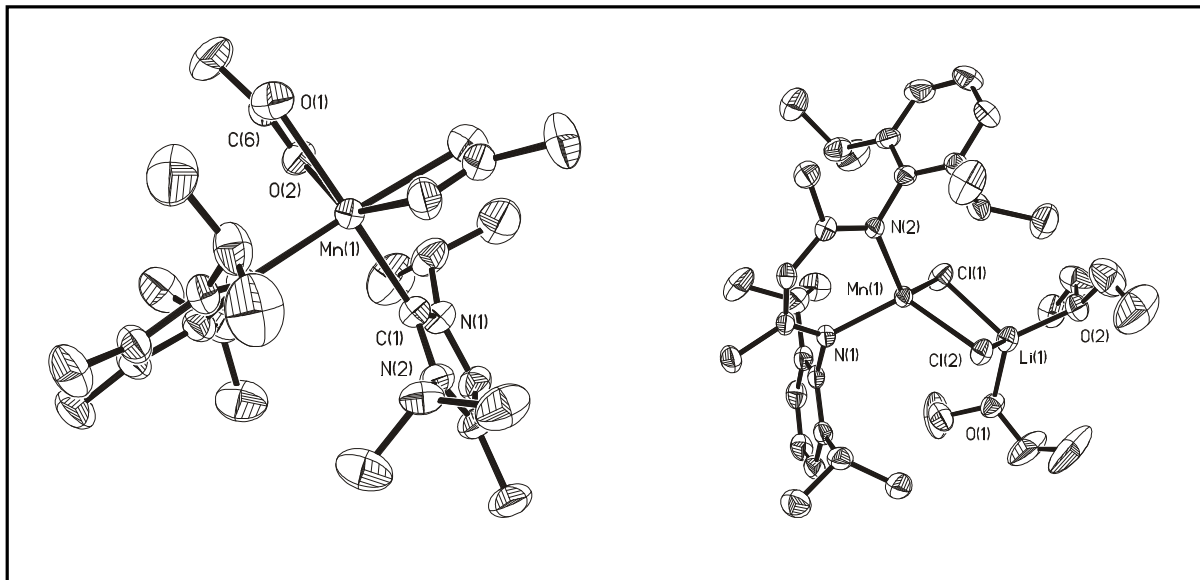
The stable N-heterocyclic carbene adducts $\{[C(Me)N(iPr)]_2C\}_2MnX_2$ ($X = Cl$ (**2**), I (**3**), MeCOO (**4**)) were obtained from the reactions of the N-heterocyclic carbene $[C(Me)N(iPr)]_2C$ (**1**) and the corresponding manganese(II) reagents in THF, respectively. The X-ray solid-state structural analyses show that all complexes **2** - **4** are monomeric and the N-heterocyclic carbene ligands in these complexes are differently arranged around the central metal atoms.



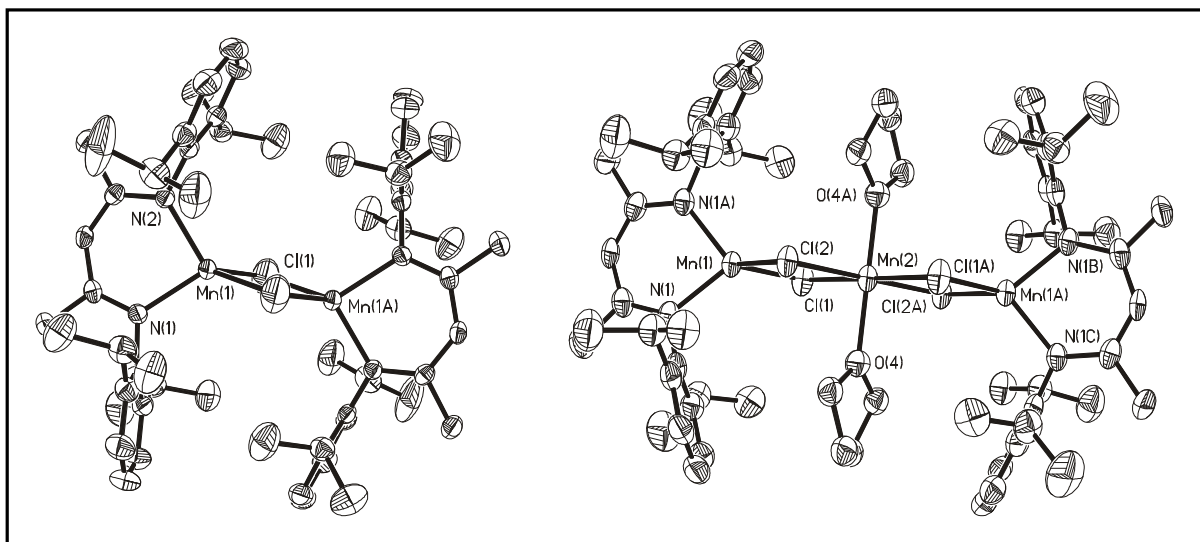
Structures of **2** and **3**

The metalate compound $LMn(\mu-Cl)_2Li(OEt)_2$ (**7**) ($L = HC(CMeNAr)_2$, $Ar = 2,6-iPrC_6H_3$) and dimeric compound $[LMn(\mu-Cl)]_2$ (**8**) were synthesized from the reaction of $MnCl_2$ with $LLi(OEt)_2$ (**5**) and LK (**6**) in diethyl ether, respectively. However, the reaction of $MnCl_2(THF)_{1.5}$ and LK (**6**) afforded the trinuclear complex $LMn(\mu-Cl)_2Mn(THF)_2(\mu-Cl)_2MnL$ (**9**) in THF. This obviously indicates the reaction is solvent dependent. Attempts to prepare the di- β -diketiminato complex by using 2 equiv. of **5** or **6** were unsuccessful. The

molecular structures of compounds **7** - **9** have been determined by X-ray solid-state structural analyses.



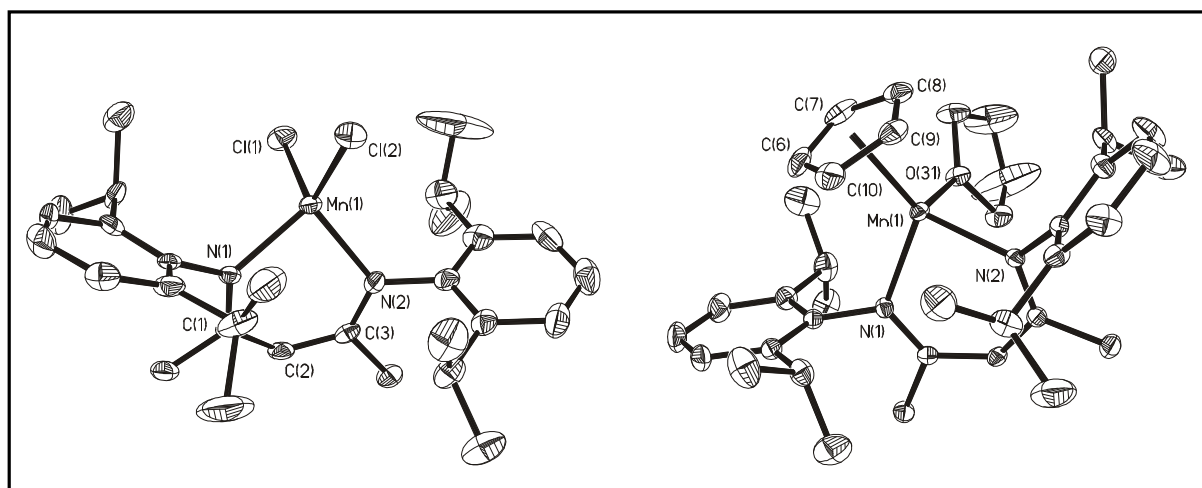
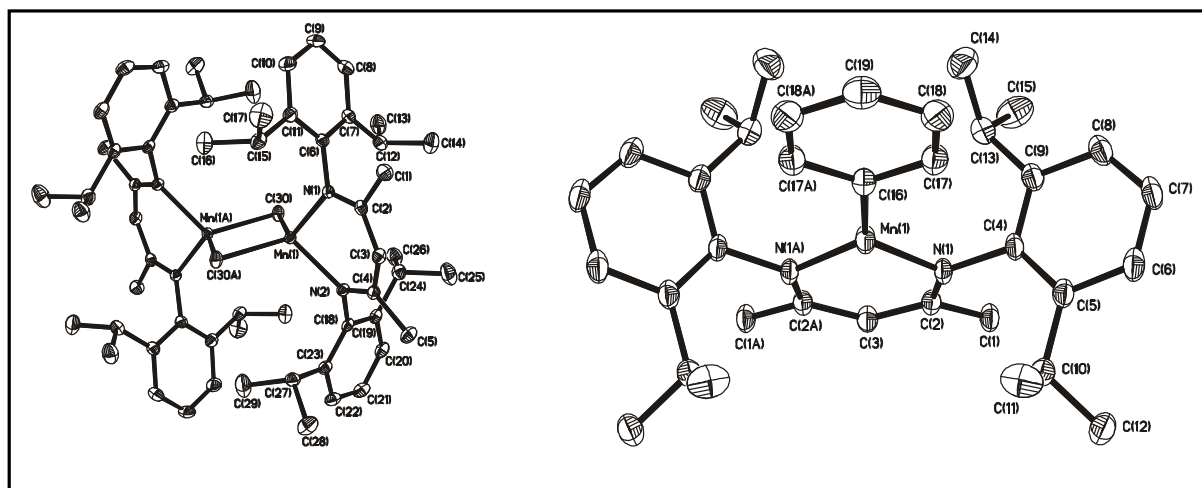
Structures of **4** and **7**



Structures of **8** and **9**

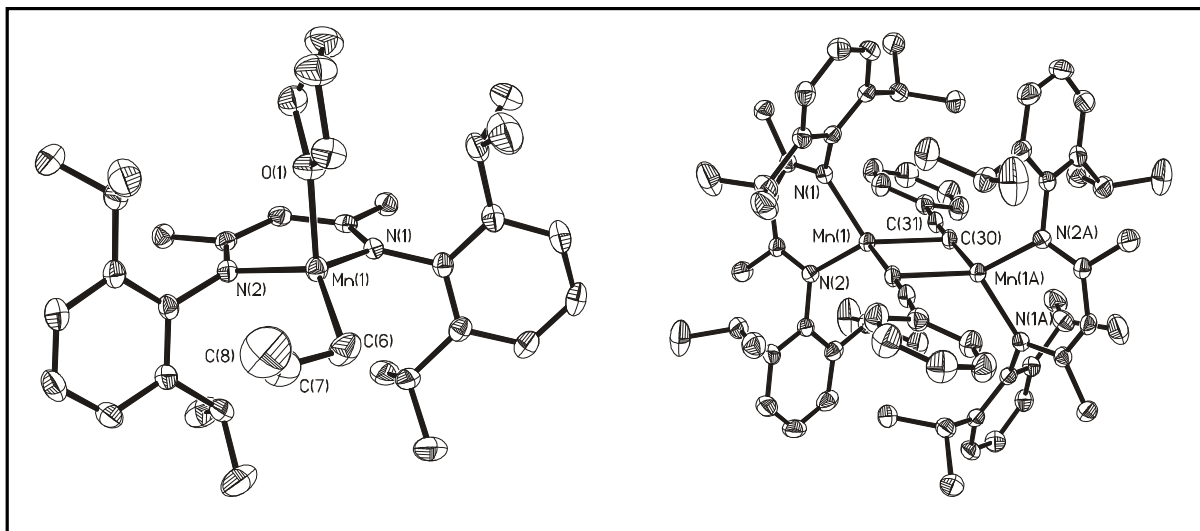
When the N-heterocyclic carbene $[\text{C}(\text{Me})\text{N}(\text{iPr})_2]\text{C}$ (**1**) was employed as the acceptor for the proton of LH, the novel ionic compound $[\text{LMnCl}_2][\{\text{C}(\text{Me})\text{N}(\text{iPr})_2\text{CH}\}]$ (**10**) was easily obtained in high yield from the reaction of LH, $\text{MnCl}_2(\text{THF})_{1.5}$ and **1** in THF.

Treatment of **8** with CpNa, MeLi and PhLi resulted in the formation of the organomanganese(II) complexes LMnCp(THF) (**11**), [LMn(μ -Me)]₂ (**12**) and LMnPh (**13**), respectively. Compound **11** is a rare example of a half-sandwich manganese(II) complex with the metal center of 17 valence electrons. Compound **12** is the first structurally characterized manganese alkyl complex containing bridging methyl groups. The structure of **13** shows a coplanar arrangement of the phenyl group and the chelating ligand around the three-coordinate metal center.

Structure of the anion of **10**Structure of **11**Structures of **12** and **13**

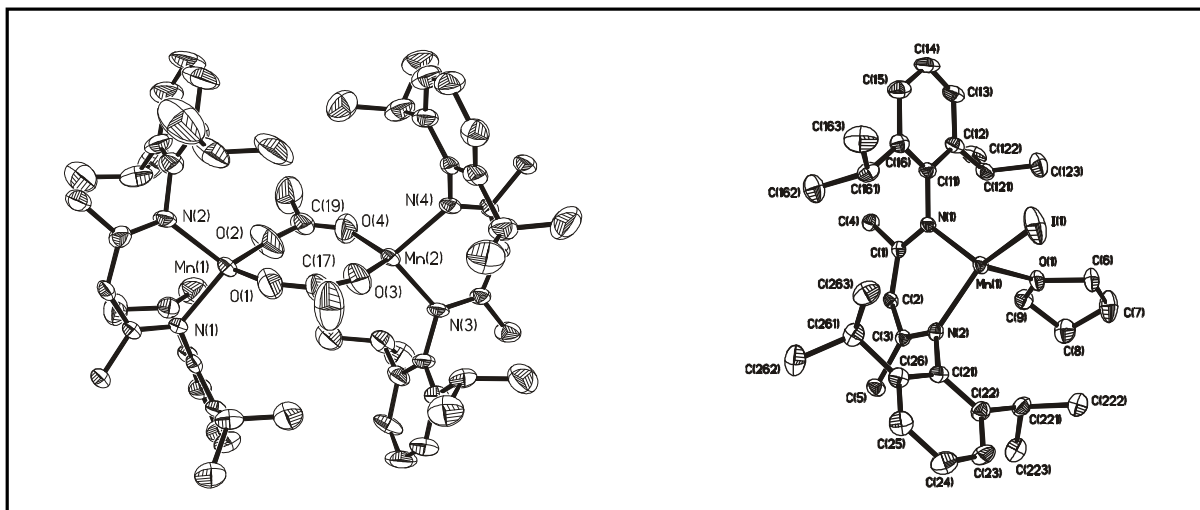
The reactivity of **9** was examined. Addition of C₃H₅MgCl and PhCClLi to **9** in toluene, respectively, readily provided the monomeric compound LMnC₃H₅(THF) (**14**) and the dimer [LMn(μ -CCPh)]₂ (**15**). Attempts to identify other species were unsuccessful. Compound **14**

is the first structurally characterized manganese complex with an η^1 bonding allyl group. The structure of **15** reveals a dimer formed by two bridging phenylethynyl groups, which is the first structurally characterized dinuclear manganese complex containing bridging alkynyl groups.



Structures of **14** and **15**

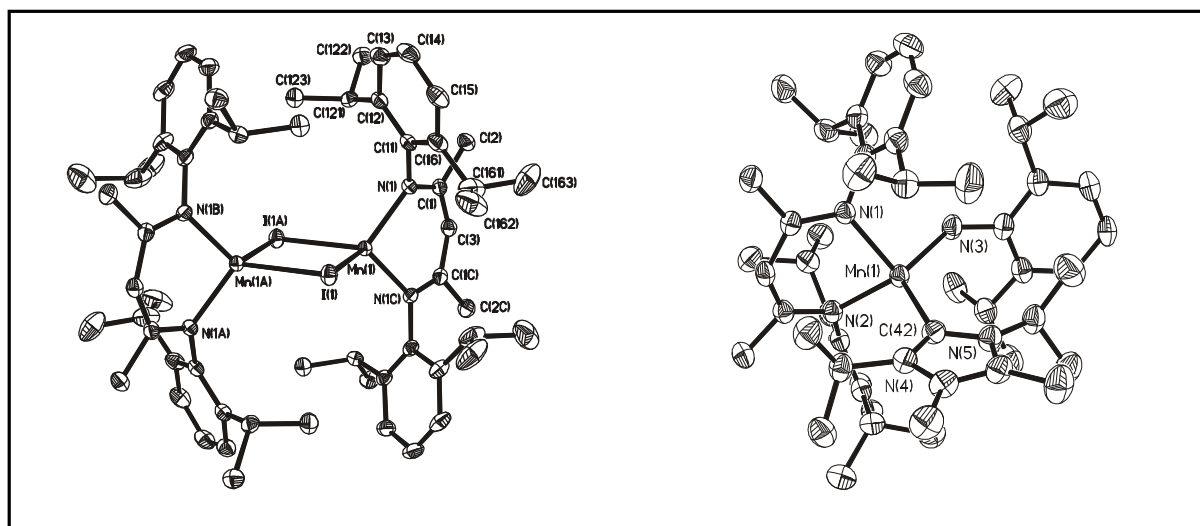
$[\text{LMn}(\mu\text{-MeCOO})_2]$ (**16**), the first example of a doubly carboxylate-bridged complex with four-coordinate manganese(II), was prepared from the reaction of **6** and $\text{Mn}(\text{MeCOO})_2$ in THF. The structure of **16** is shown below.



Structures of **16** and **17**

The monomeric compound LMnI(THF) (**17**) was isolated from the reaction of LK (**6**) and MnI₂ in THF. Refluxing **17** in toluene and removal of the volatiles in vacuum afforded the dimer [LMn(μ-I)]₂ (**18**). Compound **17** can also be obtained by dissolving **18** in THF. Displacement of the THF by the strong Lewis base [C(Me)N(*i*Pr)]₂C (**1**) readily afforded the carbene adduct LMnI{C[N(*i*Pr)C(Me)]₂} (**19**), which can also be obtained by adding **1** to the solution of **18** in toluene. Complexes **17** and **18** have been characterized by X-ray solid-state structural analyses.

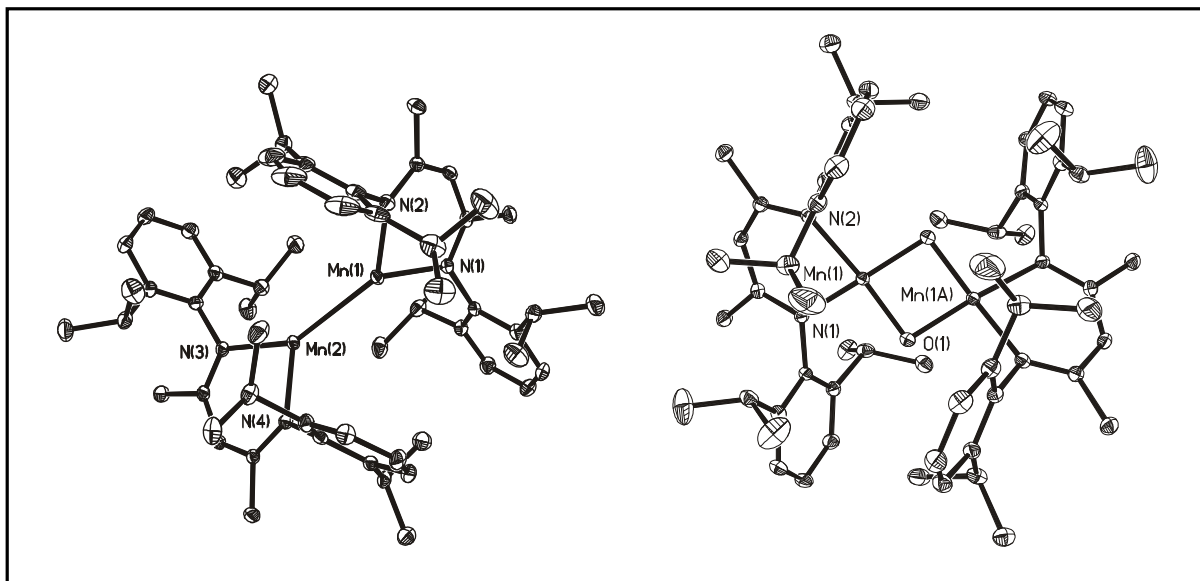
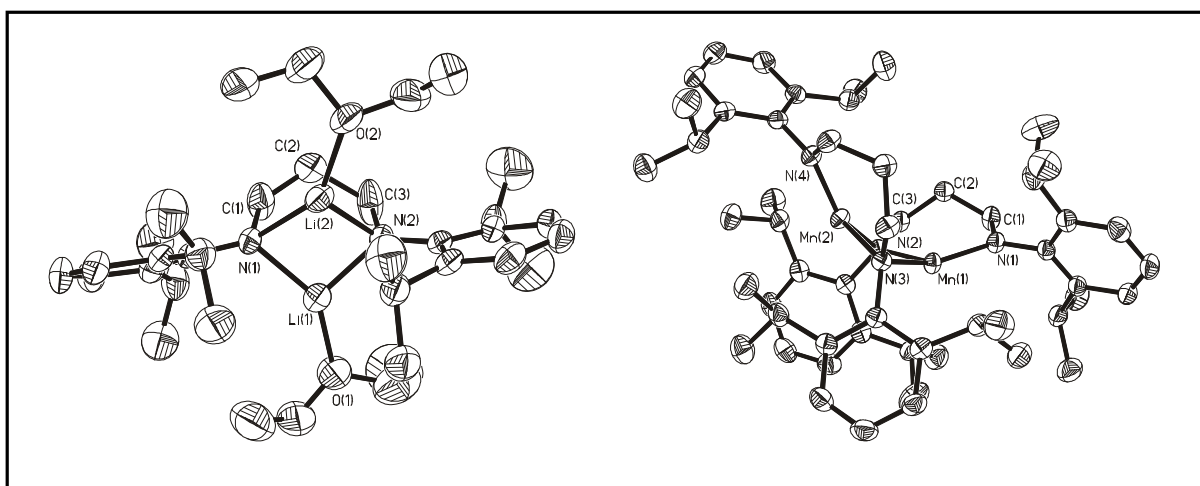
Reduction of **19** by Na/K alloy, unexpectedly, resulted in the formation of the monomer LMnNHAr{C[(N(*i*Pr)C(Me)]₂} (**20**), which can also be prepared by the reaction of **19** with LiNHAr. The Mn-C distance is comparable to those in complexes **2** - **4**.



Structures of **18** and **20**

Reduction of the dimeric iodide [LMn(μ-I)]₂ (**18**) with Na/K alloy in toluene, as anticipated, afforded the first compound with three-coordinate manganese(I) [LMn]₂ (**21**) containing a Mn-Mn bond. A mixture of **21** and excess KMnO₄ in toluene afforded the dimeric oxide [LMn(μ-O)]₂ (**22**), which is the first example of a doubly oxo-bridged complex with four-coordinate Mn(III) centers.

The reaction of ArNH(CH₂)₃NHAr with 2 equiv. of MeLi in diethyl ether resulted in the formation of the monomeric dilithium salt [ArN(CH₂)₃NAr][Li(OEt₂)₂] (**23**) in high yield. Further reaction of **23** with MnCl₂ affords the complex Mn₂[ArN(CH₂)₃NAr]₂ (**24**) with three-coordinate metal centers. Both compounds **23** and **24** were characterized by X-ray solid-state structural analyses. The two complexes contain nonplanar M₂N₂ central cores.

Structures of **21** and **22**Structures of **23** and **24**

3.2. Outlook

The focus of the work reported here has been on the synthesis, structure and reactivity of manganese compounds bearing N-heterocyclic carbenes, bulky diketiminates and diamide ligands. Some important compounds, for instance, the N-heterocyclic carbene adducts, the organomanganese complexes, and the first compound with three-coordinate manganese(I), were synthesized and structurally characterized for the first time. The reactivities of such compounds were checked preliminarily.

A continuation of this work would be:

- Further reactions of the manganese N-heterocyclic carbene complexes;
- Exploration of possible applications of the organomanganese complexes in organic synthesis and catalysis;
- Synthesis of compounds involving $[\text{Mn}(\mu\text{-E})_2]$ cores (E = S, Se, Te).

4. Experimental Section

4.1. General procedures

All experimental manipulations, unless otherwise stated, were carried out in an oxygen-free dry dinitrogen atmosphere using Schlenk glassware and techniques.⁸⁰ The handling of solid samples and the preparation of samples for spectral measurements were carried out inside a MBraun MB150-GI glove-box where the O₂ and H₂O levels were normally kept below 1 ppm. The glassware used in all the manipulations was oven-dried at 150 °C for a minimum of 5 h before use, cooled to ambient temperature *in vacuo*, and flushed with nitrogen.

Melting points were determined in sealed capillaries on a Bühler SPA-1 apparatus.

Elemental analyses were carried out by the Analytical Laboratory of the Institute of Inorganic Chemistry at the Universität Göttingen.

¹H, ⁷Li, and ¹³C *NMR spectra* (CDCl₃ or C₆D₆ solutions) were recorded on Bruker AM-250, AM-300 and AM-500 instruments. ⁷Li NMR spectra were recorded ¹H decoupled. The chemical shifts were reported in ppm with reference to external standards, more explicitly, SiMe₄ for ¹H and ¹³C nucleus and LiCl/D₂O for ⁷Li nucleus. All NMR grade solvents were dried prior to use and the samples for measurements were freshly prepared in the glove-box.

EI-mass spectra were obtained on Finnigan MAT 8230 and Varian MAT CH5 spectrometers. Only the highest peak of the respective isotopic distribution is given.

IR spectra were recorded on a Bio-Rad Digilab FTS-7 spectrometer as Nujol mulls on KBr plates. Intensities were abbreviated as follows: vs (very strong), s (strong), m (medium), w (weak).

EPR spectra were recorded on a Bruker Elexsys E 500 X-band spectrometer. All samples were measured as crystalline powders in an argon atmosphere at room temperature using a modulation frequency of 100 KHz, 3 - 5 G modulation amplitude, about 9.42 GHz microwave frequency and microwave power in the range between 2 and 10 mW as spectrometer settings.

The magnetic susceptibility measurements were carried out with a Quantum-Design-MPMS-5S-SQUID-Magnetometer in the range from 300 K to 2 K. The powdered sample was placed in a gel bucket and fixed in a non-magnetic sample holder.

X-ray structure determinations: Crystals were mounted on glass fibers in a rapidly cooled perfluoropolyether. Diffraction data of structures **2**, **3**, **4**, **7**, **8**, **10**, **16**, **17**, **18**, **23** and **24** were collected on a Stoe-Siemens-Huber four-circle diffractometer coupled to a Siemens CCD area detector and data of structures **9**, **11**, **12**, **13**, **14**, **20**, **21** and **22** were collected on a Stoe IPDS II-array detector system using Mo-K α radiation ($\lambda = 0.71073 \text{ \AA}$). Data of structure **15** were collected on a Bruker three-circle diffractometer equipped with a SMART 6000 CCD detector using Cu-K α radiation ($\lambda = 1.54178 \text{ \AA}$). The structures were solved by direct methods using the program SHELXS-97⁸¹ and refined using F^2 on all data by full-matrix-least-squares with SHELXL-97.⁸² All non-hydrogen atoms were refined anisotropically. All hydrogen atoms were included in the model at geometrically calculated positions and refined using a riding model. Crystal data for all the compounds related to the data collection, structure solution, and refinement are summarized in the tables of Section 6.

4.2. Starting materials

The starting materials, [C(Me)N(*i*Pr)]₂C⁸³ (**1**), LH,⁸⁴ LLi(OEt)₂³⁸ (**5**) (L = {HC(CMeNAr)₂}, Ar = 2,6-*i*PrC₆H₃), ArNH(CH₂)₃NHAr^{74c} and MnCl₂(THF)_{1.5}⁸⁵ were synthesized as described in the literature. Anhydrous MnCl₂ was obtained by dehydration of MnCl₂(H₂O)₄.⁸⁶ Other chemicals used in this work were purchased from Aldrich Chemical Co, ACROS, and Fluka Co and used without further purification. The NMR spectra of the manganese complexes are not available due to the paramagnetic property of manganese(II).

4.3. Synthesis

4.3.1. Synthesis of {[C(Me)N(*i*Pr)]₂C}₂MnCl₂ (**2**)

THF (40 mL) was added to a mixture of **1** (0.72 g, 4 mmol) and MnCl₂(THF)_{1.5} (0.47 g, 2 mmol) at room temperature. The suspension was stirred for 13 h. The solvent was concentrated to ca. 3 mL and the colorless precipitate was collected by filtration.

2: Yield: 0.88 g (91 %). Mp: 268 - 270 °C. C₂₂H₄₀Cl₂MnN₄ (486.42): calcd. C 54.27, H 8.22, N, 11.51; found C 54.3, H 8.2, N 11.5. IR (Nujol mull, cm⁻¹): $\tilde{\nu}$ = 1629 (m), 1552 (w), 1401 (m), 1376 (s), 1360 (s), 1262 (w), 1218 (m), 1168 (w), 1136 (m), 1107 (w), 1070 (m), 1023 (w), 968 (w), 931 (w), 905 (w), 885 (w), 803 (w), 751 (m), 722 (m), 674 (w), 544 (m), 412 (w).

4.3.2. Synthesis of {[C(Me)N(*i*Pr)]₂C}₂MnI₂ (**3**)

The procedure is the same as that described for **2** with MnI₂ (0.62 g, 2 mmol) instead of the MnCl₂(THF)_{1.5}.

3: Yield: 1.03 g (77 %). Mp: 273 - 283 °C. C₂₂H₄₀I₂MnN₄ (669.32): calcd. C 39.46, H 5.98, N 8.37; found C 39.5, H 6.0, N 8.3. IR (Nujol mull, cm⁻¹): $\tilde{\nu}$ = 1629 (m), 1552 (w), 1398 (m), 1377 (s), 1364 (s), 1291 (w), 1262 (w), 1219 (m), 1191 (w), 1168 (w), 1136 (m), 1109 (w), 1071 (m), 1023 (w), 968 (w), 931 (w), 905 (w), 886 (w), 848 (w), 803 (w), 750 (m), 722 (m).

4.3.3. Synthesis of {[C(Me)N(*i*Pr)]₂C}₂Mn(MeCOO)₂ (**4**)

THF (40 mL) was added to a mixture of **1** (0.72 g, 4 mmol) and Mn(MeCOO)₂ (0.34 g, 2 mmol) at room temperature. A clear solution was obtained immediately and stirred for 6 h. The solution was concentrated to ca. 5 mL and kept at -26 °C for 3 d to give colorless crystals of **4**.

4: Yield: 0.86 g (81 %). Mp: 156 - 158 °C. C₂₆H₄₆MnN₄O₄ (532.96): calcd. C 58.54, H 8.63, N 10.51; found C 58.6, H 8.7, N 10.1. IR (Nujol mull, cm⁻¹): $\tilde{\nu}$ = 1750 (w), 1695 (w), 1628 (s), 1599 (vs), 1573 (s), 1406 (s), 1323 (m), 1260 (m), 1238 (w), 1222 (m), 1195 (w), 1167 (w), 1138 (m), 1112 (m), 1073 (w), 1048 (w), 10231 (w), 917 (w), 908 (w), 888 (w), 804 (s), 751 (m), 722 (m), 658 (s), 648 (w), 616 (m), 544 (m), 483 (w), 457 (w), 411 (w).

4.3.4. Synthesis of LK (6)

A suspension of KH (0.18 g, 4.5 mmol) and LH (1.67 g, 4 mmol) in diethyl ether (50 mL) was stirred at room temperature for 1 d. After filtration, the light yellow filtrate was concentrated to ca. 5 mL and kept at -26 °C for 24 h to afford a crystalline solid.

6: Yield: 1.59 g (87 %). ¹H NMR and elemental analyses are consistent with those in the literature.³⁹

4.3.5. Synthesis of LMn(μ -Cl)₂Li(OEt)₂ (7)

LLi(OEt)₂ (**5**) (1.0 g, 2 mmol) in diethyl ether (15 mL) was added to a suspension of MnCl₂ (0.25 g, 2 mmol) in diethyl ether (40 mL) at -78 °C. The mixture was warmed to room temperature and stirred for 14 h. The resulting precipitate was removed by filtration. The solution was concentrated to a volume of 10 mL. Yellow crystals of **7** were obtained at -26 °C after 2 d.

7: Yield: 1.13 g (81 %). Mp: > 270 °C (dec.). C₃₇H₆₁Cl₂LiMnN₂O₂ (698.66): calcd. C 63.55, H 8.73, N 4.01; found C 63.1, H 8.5, N 4.5. EI-MS: *m/z* (%) 507 (100) [M-LiCl(OEt)₂]⁺. IR (Nujol mull, cm⁻¹): $\tilde{\nu}$ = 1624 (w), 1539 (w), 1523 (m), 1398 (m), 1366 (w), 1316 (m), 1262 (m), 1231 (w), 1176 (w), 1099 (m), 1056 (w), 1022 (m), 934 (w), 873 (w), 853 (w), 795 (m), 759 (w), 722 (w), 636 (w), 600 (w), 527 (w), 452 (w).

4.3.6. Synthesis of [LMn(μ -Cl)]₂ (8)

LK (**6**) (0.91 g, 2 mmol) in diethyl ether (15 mL) was added to a suspension of MnCl₂ (0.25 g, 2 mmol) in diethyl ether (40 mL) at -78 °C. The mixture was warmed to room temperature and stirred for 14 h. The resulting precipitate was removed by filtration. The solution was concentrated to a volume of 10 mL. Yellow crystals of **8** were obtained after 1 d at -26 °C.

8: Yield: 0.88 g (87 %). Mp: > 400 °C. C₅₈H₈₂Cl₂Mn₂N₄ (1016.06): calcd. C 68.54, H 8.13, N 5.52; found C 68.8, H 8.2, N 5.2. EI-MS: *m/z* (%) 507 (100) [1/2M]⁺. IR (Nujol mull, cm⁻¹

¹): $\tilde{\nu}$ = 1656 (w), 1623 (w), 1592 (w), 1553 (w), 1528 (w), 1326 (w), 1292 (w), 1261 (m), 1175 (m), 1098 (m), 1025 (m), 936 (w), 801 (m), 758 (w), 722 (w), 664 (w), 618 (w), 541 (w), 466 (w).

4.3.7. Synthesis of $\text{LMn}(\mu\text{-Cl})_2\text{Mn}(\text{THF})_2(\mu\text{-Cl})_2\text{MnL}$ (**9**)

LK (**6**) (0.91 g, 2 mmol) in THF (15 mL) was added to a suspension of $\text{MnCl}_2(\text{THF})_{1.5}$ (0.70 g, 3 mmol) in THF (40 mL) at -78 °C. The mixture was warmed to room temperature and stirred for 14 h. The precipitate was removed by filtration. The solution was concentrated to ca. 10 mL and kept at 4 °C for 24 h to give yellow crystals. The crystals were collected by filtration and the mother liquor was concentrated to ca. 5 mL and kept at -26 °C for 24 h to give additional crystals.

9: Yield: 1.28 g (81 %). Mp: > 400 °C. $\text{C}_{66}\text{H}_{98}\text{Cl}_4\text{Mn}_3\text{N}_4\text{O}_2$ (1286.51): calcd. C 61.56, H 7.62, N 4.35; found C 61.6, H 7.5, N 4.2. EI-MS: m/z (%) 507 (100) $[\text{LMnCl}]^+$. IR (Nujol mull, cm^{-1}): $\tilde{\nu}$ = 1525 (m), 1400 (w), 1316 (s), 1292 (w), 1263 (s), 1230 (w), 1176 (w), 1100 (s), 1098 (m), 1075 (m), 1056 (m), 1022 (s), 934 (w), 852 (w), 794 (s), 758 (m), 721 (w), 636 (w), 527 (w), 468 (w), 452 (w).

4.3.8. Synthesis of $[\text{LMnCl}_2][\{\text{C}(\text{Me})\text{N}(i\text{Pr})\}_2\text{CH}]$ (**10**)

THF (40 mL) was added to a mixture of $\text{MnCl}_2(\text{THF})_{1.5}$ (0.47 g, 2 mmol), LH (0.83 g, 2 mmol) and $[\text{C}(\text{Me})\text{N}(i\text{Pr})]_2\text{C}$ (0.36 g, 2 mmol) at room temperature. The resulting suspension was stirred for 12 h and a clear yellow solution was obtained. The solution was concentrated to ca. 10 mL and kept at 4 °C. Yellow crystals were obtained after 3 d.

10: Yield: 1.23 g (85 %). Mp: > 210 °C (dec.). $\text{C}_{40}\text{H}_{62}\text{Cl}_2\text{MnN}_4$ (724.78): calcd. C 66.23, H 8.55, N 7.73; found C 65.9, H 8.8, N 7.5. EI-MS: m/z (%) 723 (2) $[\text{M-H}]^+$, 507 (43) $[\text{LMnCl}]^+$, 202 (100) $[\text{ArNCCH}_3]^+$, 181 (52) $[\{\text{C}(\text{Me})\text{N}(i\text{Pr})\}_2\text{CH}]^+$. IR (Nujol mull, cm^{-1}): $\tilde{\nu}$ = 3126 (w), 3058 (w), 1663 (w), 1628 (w), 1551 (m), 1542 (m), 1516 (m), 1438 (s), 1400 (s), 1321 (s), 1263 (s), 1232 (m), 1193 (w), 1177 (m), 1143 (w), 1101 (s), 1056 (w), 1023 (s), 962 (w), 936 (m), 868 (w), 849 (w), 799 (s), 792 (s), 764 (m), 758 (m), 721 (w), 652 (w), 630 (w).

4.3.9. Synthesis of LMnCp(THF) (11)

CpNa (0.6 mL, 2.0 M in THF, 1.2 mmol) was added to a solution of **8** (0.51 g, 0.5 mmol) in THF (20 mL) at -78 °C. The mixture was allowed to warm to room temperature and stirred for 14 h. All volatiles were removed in vacuum and the residue was extracted with toluene (15 mL). The yellow solution was concentrated to ca. 10 mL and kept at room temperature for 2 d to give yellow crystals. The crystals were collected by filtration and the filtrate was concentrated and kept at 4 °C for 7 d to give additional crystals.

11: Total yield: 0.52 g (86 %). Mp: 210 - 212 °C. C₃₈H₅₄MnN₂O (609.77): calcd. C 74.88, H 8.87, N 4.60; found C 74.5, H 8.8, N 4.6. EI-MS: *m/z* (%) 537 (100) [M]⁺, 472 (92) [LMn]⁺. IR (Nujol mull, cm⁻¹): $\tilde{\nu}$ = 1653 (w), 1542 (w), 1521 (m), 1401 (m), 1315 (m), 1262 (s), 1231 (w), 1172 (w), 1098 (s), 1056 (m), 1028 (s), 933 (w), 872 (w), 846 (w), 793 (s), 765 (w), 751 (m), 721 (m), 667 (w), 601 (w), 466 (w).

4.3.10. Synthesis of [LMn(μ -Me)]₂ (12)

MeLi (1.5 mL, 1.6 M in diethyl ether, 2.4 mmol) was added to a suspension of **8** (1.01 g, 1 mmol) in toluene (40 mL) at -78 °C. The mixture was allowed to warm to room temperature and stirred for 14 h. All the volatiles were removed in vacuum and the residue was extracted with hexane (2 × 20 mL). The yellow solution was concentrated to ca. 20 mL and kept at room temperature for 24 h to give yellow solids of **12** containing a small amount of **8**. Recrystallization of the solid from pentane was repeated two times and crystals were obtained. The crystals were collected by filtration and the filtrate was concentrated and kept at 4 °C for one week to give additional crystals.

12: Total yield: 0.51 g (52 %). Mp: 190 - 192 °C. C₆₀H₈₈Mn₂N₄ (975.22): calcd. C 73.83, H 9.02, N 5.74; found C 73.3, H 8.8, N 5.6. EI-MS: *m/z* (%) 487 (6) [LMnMe]⁺, 472 (100) [LMn]⁺. IR (Nujol mull, cm⁻¹): $\tilde{\nu}$ = 1658 (w), 1624 (w), 1589 (w), 1552 (w), 1525 (w), 1314 (w), 1261 (m), 1174 (w), 1098 (w), 1040 (w), 1021 (w), 936 (w), 798 (m), 759 (w), 721 (w), 662 (w), 563 (w).

4.3.11. Synthesis of LMnPh (13)

The procedure is the same as that described for **12** with PhLi (2.4 mL, 1.0 M in diethyl and cyclohexane, 2.4 mmol) instead of MeLi.

13: Yield: 0.71 g (65 %). Mp: 230 - 232 °C. C₃₅H₄₆MnN₂ (549.68): calcd. C 76.41, H 8.37, N 5.09; found C 75.7, H 8.1, N 4.9. EI-MS: *m/z* (%) 549 (3) [M]⁺, 471 (100) [M-C₆H₆]⁺. IR (Nujol mull, cm⁻¹): $\tilde{\nu}$ = 1660 (w), 1640 (w), 1625 (w), 1590 (w), 1553 (w), 1531 (w), 1312 (w), 1261 (m), 1170 (w), 1095 (m), 1021 (m), 937 (w), 873 (w), 799 (m), 761 (w), 724 (w), 674 (w), 643 (w), 613 (w), 604 (w), 583 (w), 525 (w), 463 (w).

4.3.12. Synthesis of LMnC₃H₅(THF) (14)

C₃H₅MgCl (1.1 mL, 2.0 M in THF, 2.2 mmol) was added to a suspension of **9** (0.64 g, 0.5 mmol) in toluene (20 mL) at -78 °C. The mixture was allowed to warm to room temperature and stirred for 14 h. All volatiles were removed in vacuum and the residue was extracted with hexane (2 × 15 mL). The yellow solution was concentrated to ca. 15 mL and kept at 4 °C for 48 h to give yellow crystals. The crystals were collected by filtration and the filtrate was concentrated and kept at -26 °C for 7 d to give additional crystals of **14**.

14: Total yield: 0.25 g (43 %). Mp: > 173 °C (dec.). C₃₆H₅₄MnN₂O (585.75): calcd. C 73.75, H 9.22, N 4.78; found C 74.1, H 9.0, N 4.6. EI-MS: *m/z* (%) 513 (8) [M-THF]⁺, 472 (100) [LMn]⁺. IR (Nujol mull, cm⁻¹): $\tilde{\nu}$ = 1653 (w), 1521 (m), 1401 (m), 1317 (m), 1262 (s), 1175 (w), 1098 (s), 1021 (m), 933 (w), 847 (w), 794 (m), 760 (w), 738 (w), 722 (m), 693 (w), 663 (w).

4.3.13. Synthesis of [LMn(μ-CCPh)]₂ (15)

PhCCLi (2.2 mL, 1.0 M in THF, 2.2 mmol) was added to a suspension of **9** (0.64 g, 0.5 mmol) in toluene (20 mL) at -78 °C. The mixture was allowed to warm to room temperature and stirred for 14 h. All volatiles were removed in vacuum and the residue was extracted with hexane (2 × 15 mL). The yellow solution was concentrated to ca. 15 mL and kept at 4 °C for 48 h to give yellow crystals. The crystals were collected by filtration and the filtrate was concentrated and kept at -26 °C for 4 d to give additional crystals of **15**.

15: Total yield: 0.32 g (56 %). Mp: > 170 °C (dec.). C₇₄H₉₂Mn₂N₄ (1147.4): calcd. C 77.39, H 8.02, N 4.88; found C 77.1, H 8.5, N 4.7. EI-MS: *m/z* (%) 1146 (1) [M]⁺, 573 (40) [1/2M]⁺, 471 (100) [LMn-H]⁺. IR (Nujol mull, cm⁻¹): $\tilde{\nu}$ = 2034 (w), 1524 (m), 1317 (m), 1260 (s), 1177 (w), 1098 (s), 1056 (m), 1021 (s), 931 (w), 865 (w), 756 (w), 721 (m).

4.3.14. Synthesis of [LMn(μ -MeCOO)]₂ (16)

LK (**6**) (0.91 g, 2 mmol) in THF (10 mL) was added to a suspension of Mn(MeCOO)₂ (0.35 g, 2 mmol) in THF (30 mL) at -78 °C. The mixture was warmed to room temperature and stirred for 12 h. The resulting precipitate was removed by filtration. The solution was concentrated to a volume of 5 mL. Yellow crystals were obtained at -26 °C after 7 d.

16: Yield: 0.80 g (75 %). Mp: > 330 °C (dec.). C₆₂H₈₈Mn₂N₄O₄ (1063.24): calcd. C 70.00, H 8.28, N 5.27; found C 69.7, H 8.2, N 5.0. EI-MS: *m/z* (%) 531 (100) [1/2M]⁺. IR (Nujol mull, cm⁻¹): $\tilde{\nu}$ = 1602 (s), 1544 (m), 1519 (m), 1437 (s), 1380 (m), 1317(m), 1262 (w), 1177 (w), 1099 (w), 1021 (w), 933 (w), 851 (w), 793 (w), 759 (w), 643 (w).

4.3.15. Synthesis of LMnI(THF) (17)

A solution of **6** (0.91 g, 2 mmol) in THF (10 mL) was added to a suspension of MnI₂ (0.62 g, 2 mmol) in THF (35 mL) at -78 °C. The mixture was allowed to warm to room temperature and stirred for 14 h. The precipitate was removed by filtration. The filtrate was concentrated to ca. 5 mL and kept at -26 °C for 24 h to give yellow crystals of **17**.

17: Yield: 1.17 g (87 %). Mp: 379 - 381 °C. C₃₃H₄₉IMnN₂O (670.84): calcd. C 59.03, H 7.30, N 4.17; found C 59.0, H 7.2, N 4.2. EI-MS: *m/z* (%) 599 (100) [LMnI]⁺. IR (Nujol mull, cm⁻¹): $\tilde{\nu}$ = 1624 (w), 1552 (w), 1520.62 (m), 1314 (m), 1262 (m), 1174 (w), 1100 (w), 1024 (m), 935 (w), 870 (w), 852 (w), 794 (m), 757 (w), 721 (w), 600 (w), 524 (w), 468 (w).

4.3.16. Synthesis of [LMn(μ -I)]₂ (18)

A solution of **17** (1.34 g, 2 mmol) in toluene (40 mL) was refluxed for 0.5 h. All volatiles were removed in vacuum and bright yellow microcrystals of **18** were obtained.

18: Yield: 1.15 g (96 %). Mp: 271 - 273 °C (dec.). C₅₈H₈₂I₂Mn₂N₄ (1197.68): calcd. C 58.11, H 6.84, N 4.67; found C 58.3, H 6.9, N 4.9. EI-MS: *m/z* (%) 599 (100) [LMnI]⁺. IR (Nujol mull, cm⁻¹): $\tilde{\nu}$ = 1657 (w), 1625 (w), 1552 (w), 1262 (m), 1097 (m), 1023 (m), 875 (w), 800 (m), 722 (w), 659 (w), 536 (w), 468 (w).

4.3.17. Synthesis of LMnI{C[N(*i*Pr)C(Me)]₂} (19)

A solution of C[N(*i*Pr)C(Me)]₂ (0.18 g, 1 mmol) in THF (10 mL) was added to a THF (20 mL) solution of **17** (0.67 g, 1 mmol) at room temperature. The resulting solution was stirred for 1 h. After removal of all volatiles in vacuum a yellow solid was obtained.

19: Yield: 0.76 g (98 %). Mp: > 271 °C (dec.). C₄₀H₆₁IMnN₄ (778.8): calcd. C 61.63, H 7.83, N 7.19; found C 61.8, H 8.0, N 7.2. EI-MS: *m/z* (%) 599 (100) [LMnI]⁺. IR (Nujol mull, cm⁻¹): $\tilde{\nu}$ = 1625 (m), 1552 (s), 1505 (m), 1318 (m), 1261 (s), 1232 (w), 1218 (w), 1190 (w), 1171 (m), 1105 (m), 1071 (w), 1020 (m), 936 (w), 929 (w), 793 (s), 763 (m), 758 (m), 722 (m).

4.3.18. Synthesis of LMnNHAr{C[N(*i*Pr)C(Me)]₂} (20)

Route a: A solution of **19** (0.78 g, 1 mmol) in THF (20 mL) was added to a suspension of Na/K alloy (Na 0.01 g, 0.5 mmol; K 0.04 g, 1 mmol) in THF (10 mL). The mixture was stirred for 6 d at room temperature. All volatiles were removed in vacuum and the residue was extracted with *n*-hexane (10 mL). Yellow crystals of **20** were obtained after cooling for one week at 4 °C. The crystals were collected by filtration and the mother liquor was concentrated to ca. 4 mL and kept at 4 °C for 3 d to give yellow crystals.

20: Total yield: 0.19 g (23 %). Mp: 170 - 172 °C. C₅₂H₇₉MnN₅ (829.14): calcd. C 75.26, H 9.53, N 8.44; found C 74.8, H 9.9, N 8.8. EI-MS: *m/z* (%) 472 (100) [LMn]⁺, 648 (52) [LMnNHAr]⁺. IR (Nujol mull, cm⁻¹): $\tilde{\nu}$ = 3173 (w), 1633 (w), 1588 (w), 1543 (w), 1512 (m), 1420 (s), 1406 (m), 1316 (m), 1261 (m), 1169 (m), 1102 (w), 1019 (w), 929 (w), 886 (w), 841 (w), 794 (m), 758 (w), 737 (m), 722 (m), 600 (w), 565 (w), 543(w).

Route b: A THF (10 mL) solution of LiNHAr (0.18 g, 1 mmol) was added to a THF (20 mL) solution of **19** (0.78 g, 1 mmol) at -78 °C. The mixture was allowed to warm to room temperature and stirred for 14 h. After removal of all volatiles in vacuum the residue was extracted with diethyl ether (10 mL). After filtration, the yellow filtrate was concentrated to ca. 5 mL and stored at -26 °C for 3 d to give yellow crystals. Yield: 0.63 g (76 %). The spectroscopical characterization of the compound corresponds to that of the compound prepared by route a.

4.3.19. Synthesis of [LMn]₂ (**21**)

At room temperature, a suspension of **18** (0.60 g, 0.5 mmol) in toluene (30 mL) was added to a Na/K alloy (Na 0.01 g, 0.5 mmol; K 0.04 g, 1 mmol). The mixture was stirred at room temperature for 4 d and a red solution was obtained. After filtration, the solution was concentrated to ca. 10 mL. Dark red crystals were obtained at 4 °C after 7 d.

21: Yield: 0.07 g (15 %). Mp: 154 - 156 °C. C₅₈H₈₂Mn₂N₄ (945.16): calcd. C 73.65, H 8.68, N 5.93; found C 73.6, H 8.7, N 5.7. EI-MS: *m/z* (%) 944 (5) [M]⁺, 472 (100) [1/2M]⁺. IR (Nujol mull, cm⁻¹): $\tilde{\nu}$ = 1698 (w), 1654 (w), 1624 (w), 1577 (w), 1555 (w), 1261 (s), 1092 (s), 1019 (s), 937 (w), 866 (w), 799 (s), 762 (w), 722 (w), 667 (w), 614 (w), 568 (w).

4.3.20. Synthesis of [LMn(μ -O)]₂ (**22**)

KMnO₄ (0.5 g, 3.2 mmol) was added to a solution of **21** (0.2 g, 0.2 mmol) in toluene (20 mL) at room temperature. The mixture was stirred at room temperature for 2 d. Unreacted KMnO₄ was removed by filtration. The solvent was removed and the residue was extracted with diethyl ether. Red crystals were obtained at 4 °C after 4 d.

22: Yield: 0.14 g (72 %). Mp: 213 - 215 °C. C₅₈H₈₂Mn₂N₄O₂ (977.16): calcd. C 71.23, H 5.94, N 5.73; found C 70.9, H 5.7, N 5.5. EI-MS: *m/z* (%) 976 (100) [M]⁺. IR (Nujol mull, cm⁻¹): $\tilde{\nu}$ = 1659 (w), 1623 (w), 1592 (w), 1552 (w), 1528 (w), 1261 (s), 1094 (s), 1025 (s), 936 (w), 919 (w), 842 (w), 801 (s), 761 (w), 720 (w), 699 (w), 668 (w), 607 (w), 514 (w), 467 (w).

4.3.21. Synthesis of [ArN(CH₂)₃NAr][Li(OEt)₂]₂ (23)

To a diethyl ether (35 mL) solution of ArNH(CH₂)₃NHAr (1.58 g, 4 mmol) MeLi (5.5 mL, 1.6 M in diethyl ether, 8.8 mmol) was added at -78 °C. The mixture was warmed to room temperature and stirred for additional 14 h. The precipitate was removed by filtration. The filtrate was concentrated to ca. 10 mL and kept at -26 °C for 24 h to give colorless crystals. The crystals were collected by filtration and the mother liquor was concentrated to ca. 4 mL and kept at -26 °C for 24 h to give colorless crystals.

23: Total yield: 2.04 g (92 %). Mp: > 110 °C (dec.). C₃₅H₆₀Li₂N₂O₂ (554.75): calcd. C 75.78, H 10.90, N 5.05; found C 75.9, H 11.0, N 4.9. ¹H NMR (250 MHz, C₆D₆, ppm): δ = 6.91-7.22 (m, C₆H₃, 6 H), 3.38 (sept, CHMe₂, 4 H), 3.12 (t, MeCH₂O, 8 H), 3.00-3.25 (m, NCH₂CH₂, 4 H), 1.79 (b, NCH₂CH₂, 2 H) 1.34 (d, Me₂CH, 12 H), 1.23 (d, Me₂CH, 12 H) 0.95 (t, MeCH₂O, 12 H). ⁷Li NMR (300 MHz, C₆D₆, ppm): 1.90.

4.3.22. Synthesis of Mn₂[ArN(CH₂)₃NAr]₂ (24)

A solution of **23** (1.1 g, 2 mmol) in diethyl ether (10 mL) was added to a suspension of MnCl₂ (0.25 g, 2 mmol) in diethyl ether (30 mL) at -78 °C. The mixture was warmed to room temperature and stirred for additional 14 h. The precipitate was removed by filtration and extracted by dichloromethane (10 mL). A yellow-green solid was obtained by removing the solvent in vacuum. The mother liquor was concentrated to ca. 10 mL and yellow-green crystals were obtained at room temperature after 5 d.

24: Total yield: 0.64 g (72 %). Mp: > 220 °C (dec.). C₅₄H₈₀Mn₂N₄ (895.10): calcd. C 72.39, H 8.94, N 6.26; found C 72.2, H 8.9, N 6.2. EI-MS: *m/z* (%) = 894 (49) [M]⁺, 705 (100) [M-CH₂NAr]⁺, 447 (68) [1/2 M]⁺. IR (Nujol mull, cm⁻¹): $\tilde{\nu}$ = 1426 (w), 1308 (w), 1260 (w), 1243 (w), 1169 (w), 1092 (w), 1073 (w), 1041(w), 1019 (w), 857 (w), 800 (w), 786 (w), 722 (w).

5. Handling and Disposal of Solvents and Residual Wastes

- ◆ The recovered solvents were distilled or condensed into cold traps under vacuum, collected in halogen-free or halogen-containing solvent containers, and stored for disposal.
- ◆ Deuterated solvents for NMR were classified into halogen-free and halogen-containing solvents and were disposed as heavy metal wastes and halogen-containing wastes, respectively.
- ◆ The heavy metal residues were dissolved in nitric acid and were stored after neutralization in the containers for heavy metal wastes.
- ◆ Drying agents such as KOH, CaCl₂, and P₄O₁₀ were hydrolyzed and deposited as acid or base wastes.
- ◆ Whenever possible, sodium metal used for drying solvents was collected for recycling.^{87,88} The non-reusable sodium metal was carefully hydrolyzed in cold ethanol and poured into the base-bath used for cleaning glassware.
- ◆ Ethanol and acetone used for solid CO₂ cold-baths were subsequently used for cleaning glassware.
- ◆ The acid-bath used for cleaning glassware was neutralized with Na₂CO₃ and the resulting NaCl solution was washed-off into the water drainage.
- ◆ The residue of the base bath used for glassware cleaning was poured into the container for base wastes.

Amount of various types of disposable wastes generated during this work:

Metal containing wastes	10 L
Halogen-containing solvent wastes	12 L
Halogen-free solvent wastes	35 L
Acid wastes	12 L
Base wastes	20 L

6. Crystal Data and Refinement Details

Compound	2
Empirical formula	C ₂₂ H ₄₀ Cl ₂ MnN ₄
Formula weight	486.42
Temperature	200(2) K
Wavelength	0.71073 Å
Crystal system	monoclinic
Space group	<i>P</i> 2(1)/ <i>n</i>
Unit cell dimensions	$a = 11.2852(17)$ Å $b = 14.867(3)$ Å $\beta = 90.24(2)^\circ$ $c = 15.321(3)$ Å
Volume	2570.6(9) Å ³
<i>Z</i>	4
Density (calculated)	1.257 Mgm ⁻³
Absorption coefficient	0.736 mm ⁻¹
<i>F</i> (000)	1036
Crystal size	1.00 × 0.30 × 0.20 mm ³
θ range for data collection	3.54 - 22.53°
Index ranges	-12 ≤ <i>h</i> ≤ 12, -16 ≤ <i>k</i> ≤ 10, -12 ≤ <i>l</i> ≤ 16
Reflections collected	3570
Independent reflections	3348 (<i>R</i> (int) = 0.0671)
Refinement method	Full-matrix least-squares on <i>F</i> ²
Data / restraints / parameters	3348 / 0 / 274
Goodness-of-fit on <i>F</i> ²	1.081
Final <i>R</i> indices [<i>I</i> > 2σ(<i>I</i>)]	<i>R</i> 1 = 0.0460, <i>wR</i> 2 = 0.1150
<i>R</i> (all data)	<i>R</i> 1 = 0.0544, <i>wR</i> 2 = 0.1233
Largest diff. peak and hole	0.673 and -0.854 e·Å ⁻³

Compound	3
Empirical formula	C ₂₂ H ₄₀ I ₂ MnN ₄
Formula weight	669.32
Temperature	200(2) K
Wavelength	0.71073
Crystal system	monoclinic
Space group	<i>P</i> 2(1)/ <i>n</i>
Unit cell dimensions	$a = 11.2771(13) \text{ \AA}$ $b = 16.054(3) \text{ \AA}$ $\beta = 90.399(14)^\circ$ $c = 15.705(3) \text{ \AA}$
Volume	2843.1(8) \AA^3
Z	4
Density (calculated)	1.564 Mgm^{-3}
Absorption coefficient	2.650 mm^{-1}
<i>F</i> (000)	1324
Crystal size	0.80 × 0.60 × 0.30 mm^3
θ range for data collection	3.61 - 25.01°
Index ranges	-13 ≤ <i>h</i> ≤ 13, -3 ≤ <i>k</i> ≤ 19, -18 ≤ <i>l</i> ≤ 18
Reflections collected	6010
Independent reflections	4994 (<i>R</i> (int) = 0.0660)
Refinement method	Full-matrix least-squares on <i>F</i> ²
Data / restraints / parameters	4994 / 0 / 274
Goodness-of-fit on <i>F</i> ²	1.065
Final <i>R</i> indices [<i>I</i> > 2σ(<i>I</i>)]	<i>R</i> 1 = 0.0411, <i>wR</i> 2 = 0.1077
<i>R</i> (all data)	<i>R</i> 1 = 0.0440, <i>wR</i> 2 = 0.1111
Largest diff. peak and hole	1.161 and -1.433 $\text{e} \cdot \text{\AA}^{-3}$

Compound	4 incl. THF
Empirical formula	C ₃₀ H ₅₄ MnN ₄ O ₅
Formula weight	605.71
Temperature	203(2) K
Wavelength	0.71073
Crystal system	monoclinic
Space group	C2/c
Unit cell dimensions	$a = 12.970(2) \text{ \AA}$ $b = 14.374(3) \text{ \AA}$ $\beta = 106.070(10)^\circ$ $c = 19.322(2) \text{ \AA}$
Volume	3461.5(10) \AA^3
Z	4
Density (calculated)	1.162 Mgm^{-3}
Absorption coefficient	0.421 mm^{-1}
$F(000)$	1308
Crystal size	0.90 × 0.70 × 0.70 mm^3
θ range for data collection	3.54 - 24.94°
Index ranges	-15 ≤ h ≤ 15, -10 ≤ k ≤ 17, -18 ≤ l ≤ 22
Reflections collected	3231
Independent reflections	3028 ($R(\text{int}) = 0.0717$)
Refinement method	Full-matrix least-squares on F^2
Data / restraints / parameters	3028 / 0 / 174
Goodness-of-fit on F^2	1.015
Final R indices [$I > 2\sigma(I)$]	$R1 = 0.0595$, $wR2 = 0.1597$
R (all data)	$R1 = 0.0670$, $wR2 = 0.1701$
Largest diff. peak and hole	0.762 and -0.834 $\text{e} \cdot \text{\AA}^{-3}$

Compound	7
Empirical formula	C ₃₇ H ₆₁ Cl ₂ LiMnN ₂ O ₂
Formula weight	698.66
Temperature	153(2) K
Wavelength	0.71073 Å
Crystal system	monoclinic
Space group	<i>P</i> 2 ₁ / <i>n</i>
Unit cell dimensions	$a = 12.053(2)$ Å $b = 21.327(4)$ Å $\beta = 100.11(3)^\circ$ $c = 15.706(3)$ Å
Volume	3974.3(14) Å ³
Z	4
Density (calculated)	1.168 Mgm ⁻³
Absorption coefficient	0.498 mm ⁻¹
<i>F</i> (000)	1500
Crystal size	0.90 × 0.60 × 0.30 mm ³
θ range for data collection	3.57 - 25.05°
Index ranges	-14 ≤ <i>h</i> ≤ 14, -8 ≤ <i>k</i> ≤ 25, -18 ≤ <i>l</i> ≤ 18
Reflections collected	10312
Independent reflections	6998 (<i>R</i> (int) = 0.0574)
Refinement method	Full-matrix least-squares on <i>F</i> ²
Data / restraints / parameters	6998 / 0 / 420
Goodness-of-fit on <i>F</i> ²	1.026
Final <i>R</i> indices [<i>I</i> > 2σ(<i>I</i>)]	<i>R</i> 1 = 0.0505, <i>wR</i> 2 = 0.1213
<i>R</i> (all data)	<i>R</i> 1 = 0.0636, <i>wR</i> 2 = 0.1322
Largest diff. peak and hole	0.562 and -0.634 e·Å ⁻³

Compound	8
Empirical formula	C ₅₈ H ₈₂ Cl ₂ Mn ₂ N ₄
Formula weight	1006.06
Temperature	200(2) K
Wavelength	0.71073 Å
Crystal system	monoclinic
Space group	C2/c
Unit cell dimensions	$a = 22.921(5)$ Å $b = 14.8779(15)$ Å $\beta = 90.884(12)^\circ$ $c = 16.291(2)$ Å
Volume	5555.1(15) Å ³
Z	4
Density (calculated)	1.215 Mgm ⁻³
Absorption coefficient	0.590 mm ⁻¹
<i>F</i> (000)	2168
Crystal size	0.60 × 0.40 × 0.40 mm ³
θ range for data collection	3.51 - 24.98°
Index ranges	-27 ≤ <i>h</i> ≤ 27, -17 ≤ <i>k</i> ≤ 17, -6 ≤ <i>l</i> ≤ 19
Reflections collected	7144
Independent reflections	4872 (<i>R</i> (int) = 0.0307)
Refinement method	Full-matrix least-squares on <i>F</i> ²
Data / restraints / parameters	4872 / 0 / 308
Goodness-of-fit on <i>F</i> ²	1.024
Final <i>R</i> indices [<i>I</i> > 2σ(<i>I</i>)]	<i>R</i> 1 = 0.0626, <i>wR</i> 2 = 0.1648
<i>R</i> (all data)	<i>R</i> 1 = 0.0821, <i>wR</i> 2 = 0.1817
Largest diff. peak and hole	0.400 and -1.366 e·Å ⁻³

Compound	9 incl. 4 THF
Empirical formula	C ₈₂ H ₁₃₀ Cl ₄ Mn ₃ N ₄ O ₆
Formula weight	1574.52
Temperature	133(2) K
Wavelength	0.71073 Å
Crystal system	monoclinic
Space group	<i>C2/m</i>
Unit cell dimensions	$a = 17.238(3)$ Å $b = 18.411(3)$ Å $\beta = 113.947(13)^\circ$ $c = 14.729(2)$ Å
Volume	4272.3(12) Å ³
Z	2
Density (calculated)	1.224 Mgm ⁻³
Absorption coefficient	0.612 mm ⁻¹
<i>F</i> (000)	1682
Crystal size	0.30 × 0.20 × 0.20 mm ³
θ range for data collection	1.51 - 24.80°
Index ranges	-20 ≤ <i>h</i> ≤ 20, -21 ≤ <i>k</i> ≤ 21, -17 ≤ <i>l</i> ≤ 17
Reflections collected	22430
Independent reflections	3785 (<i>R</i> (int) = 0.1105)
Refinement method	Full-matrix least-squares on <i>F</i> ²
Data / restraints / parameters	3785 / 0 / 214
Goodness-of-fit on <i>F</i> ²	1.028
Final <i>R</i> indices [<i>I</i> > 2σ(<i>I</i>)]	<i>R</i> 1 = 0.0777, <i>wR</i> 2 = 0.2045
<i>R</i> (all data)	<i>R</i> 1 = 0.1171, <i>wR</i> 2 = 0.2295
Largest diff. peak and hole	1.021 and -0.646 e·Å ⁻³

Compound	10
Empirical formula	C ₄₀ H ₆₂ Cl ₂ MnN ₄
Formula weight	724.78
Temperature	150(2) K
Wavelength	0.71073 Å
Crystal system	orthorhombic
Space group	<i>P</i> 2 ₁ 2 ₁ 2 ₁
Unit cell dimensions	<i>a</i> = 11.218(4) Å <i>b</i> = 12.606(10) Å <i>c</i> = 28.93(2) Å
Volume	4090(1) Å ³
Z	4
Density (calculated)	1.177 Mg m ⁻³
Absorption coefficient	0.484 mm ⁻¹
<i>F</i> (000)	1556
Crystal size	0.60 × 0.60 × 0.50 mm ³
θ range for data collection	3.53 - 22.49°
Index ranges	0 ≤ <i>h</i> ≤ 12, -4 ≤ <i>k</i> ≤ 13, -31 ≤ <i>l</i> ≤ 31
Reflections collected	3116
Independent reflections	2999 (<i>R</i> (int) = 0.0745)
Refinement method	Full-matrix least-squares on <i>F</i> ²
Data / restraints / parameters	2999 / 0 / 449
Goodness-of-fit on <i>F</i> ²	1.089
Final <i>R</i> indices [<i>I</i> > 2σ(<i>I</i>)]	<i>R</i> 1 = 0.0445, <i>wR</i> 2 = 0.1009
<i>R</i> (all data)	<i>R</i> 1 = 0.0653, <i>wR</i> 2 = 0.1136
Largest diff. peak and hole	0.533 and -0.505 e·Å ⁻³

Compound	11
Empirical formula	C ₃₈ H ₅₄ MnN ₂ O
Formula weight	609.77
Temperature	133(2) K
Wavelength	0.71073 Å
Crystal system	orthorhombic
Space group	<i>P</i> 2 ₁ 2 ₁ 2 ₁
Unit cell dimensions	<i>a</i> = 10.007(2) Å <i>b</i> = 16.985(3) Å <i>c</i> = 20.081(4) Å
Volume	3413.3(12) Å ³
Z	4
Density (calculated)	1.187 Mg m ⁻³
Absorption coefficient	0.417 mm ⁻¹
<i>F</i> (000)	1316
Crystal size	0.30 × 0.30 × 0.30 mm ³
θ range for data collection	1.57 - 24.72°
Index ranges	-11 ≤ <i>h</i> ≤ 11, -19 ≤ <i>k</i> ≤ 19, -23 ≤ <i>l</i> ≤ 23
Reflections collected	36246
Independent reflections	5798 (<i>R</i> (int) = 0.0371)
Refinement method	Full-matrix least-squares on <i>F</i> ²
Data / restraints / parameters	5798 / 0 / 389
Goodness-of-fit on <i>F</i> ²	1.064
Final <i>R</i> indices [<i>I</i> > 2σ(<i>I</i>)]	<i>R</i> 1 = 0.0255, <i>wR</i> 2 = 0.0617
<i>R</i> (all data)	<i>R</i> 1 = 0.0280, <i>wR</i> 2 = 0.0626
Largest diff. peak and hole	0.305 and -0.291 e·Å ⁻³

Compound	12
Empirical formula	C ₃₀ H ₄₄ MnN ₂
Formula weight	487.61
Temperature	133(2) K
Wavelength	0.71073 Å
Crystal system	monoclinic
Space group	C2/c
Unit cell dimensions	$a = 22.612(5)$ Å $b = 14.880(3)$ Å $\beta = 90.05(3)^\circ$ $c = 16.481(3)$ Å
Volume	5545.2(19) Å ³
Z	8
Density (calculated)	1.168 Mgm ⁻³
Absorption coefficient	0.495 mm ⁻¹
<i>F</i> (000)	2104
Crystal size	0.30 × 0.20 × 0.10 mm ³
θ range for data collection	1.64 - 24.71°
Index ranges	-26 ≤ <i>h</i> ≤ 26, -17 ≤ <i>k</i> ≤ 17, -19 ≤ <i>l</i> ≤ 19
Reflections collected	20857
Independent reflections	4662 (<i>R</i> (int) = 0.0360)
Refinement method	Full-matrix least-squares on <i>F</i> ²
Data / restraints / parameters	4662 / 0 / 320
Goodness-of-fit on <i>F</i> ²	1.068
Final <i>R</i> indices [<i>I</i> > 2σ(<i>I</i>)]	<i>R</i> 1 = 0.0327, <i>wR</i> 2 = 0.0736
<i>R</i> (all data)	<i>R</i> 1 = 0.0413, <i>wR</i> 2 = 0.0772
Largest diff. peak and hole	0.257 and -0.260 e·Å ⁻³

Compound	13
Empirical formula	C ₃₅ H ₄₆ MnN ₂
Formula weight	549.68
Temperature	133(2) K
Wavelength	0.71073 Å
Crystal system	orthorhombic
Space group	<i>Pnma</i>
Unit cell dimensions	$a = 16.6103(13)$ Å $b = 20.943(2)$ Å $c = 9.2785(13)$ Å
Volume	3227.8(6) Å ³
Z	4
Density (calculated)	1.131 Mgm ⁻³
Absorption coefficient	0.433 mm ⁻¹
<i>F</i> (000)	1180
Crystal size	0.30 × 0.20 × 0.20 mm ³
θ range for data collection	1.94 - 22.99°
Index ranges	-16 ≤ <i>h</i> ≤ 16, -23 ≤ <i>k</i> ≤ 22, -8 ≤ <i>l</i> ≤ 10
Reflections collected	8044
Independent reflections	2191 (<i>R</i> (int) = 0.0751)
Refinement method	Full-matrix least-squares on <i>F</i> ²
Data / restraints / parameters	2191 / 0 / 183
Goodness-of-fit on <i>F</i> ²	1.029
Final <i>R</i> indices [<i>I</i> > 2σ(<i>I</i>)]	<i>R</i> 1 = 0.0514, <i>wR</i> 2 = 0.1188
<i>R</i> (all data)	<i>R</i> 1 = 0.0758, <i>wR</i> 2 = 0.1296
Largest diff. peak and hole	0.199 and -0.408 e·Å ⁻³

Compound	14
Empirical formula	C ₃₆ H ₅₄ MnN ₂ O
Formula weight	585.75
Temperature	133(2) K
Wavelength	0.71073 Å
Crystal system	triclinic
Space group	<i>P</i> -1
Unit cell dimensions	$a = 9.034(2) \text{ \AA}$ $\alpha = 87.22(2)^\circ$ $b = 12.177(4) \text{ \AA}$ $\beta = 77.909(16)^\circ$ $c = 15.952(3) \text{ \AA}$ $\gamma = 89.24(2)^\circ$
Volume	1713.9(7) Å ³
Z	2
Density (calculated)	1.135 Mg m ⁻³
Absorption coefficient	0.413 mm ⁻¹
<i>F</i> (000)	634
Crystal size	0.30 × 0.30 × 0.30 mm ³
θ range for data collection	1.67 - 24.72°
Index ranges	-10 ≤ <i>h</i> ≤ 10, -13 ≤ <i>k</i> ≤ 14, -18 ≤ <i>l</i> ≤ 18
Reflections collected	18432
Independent reflections	5810 (<i>R</i> (int) = 0.0417)
Refinement method	Full-matrix least-squares on <i>F</i> ²
Data / restraints / parameters	5810 / 0 / 379
Goodness-of-fit on <i>F</i> ²	1.036
Final <i>R</i> indices [<i>I</i> > 2σ(<i>I</i>)]	<i>R</i> 1 = 0.0341, <i>wR</i> 2 = 0.0772
<i>R</i> (all data)	<i>R</i> 1 = 0.0487, <i>wR</i> 2 = 0.0814
Largest diff. peak and hole	0.380 and -0.220 e·Å ⁻³

Compound	15
Empirical formula	C ₇₄ H ₉₂ Mn ₂ N ₄
Formula weight	1147.40
Temperature	100(2) K
Wavelength	1.54178 Å
Crystal system	monoclinic
Space group	<i>P2(1)/n</i>
Unit cell dimensions	$a = 14.010(1) \text{ \AA}$ $b = 13.257(1) \text{ \AA}$ $\beta = 98.59(1)^\circ$ $c = 17.697(1) \text{ \AA}$
Volume	3250(1) Å ³
Z	2
Density (calculated)	1.172 Mgm ⁻³
Absorption coefficient	3.483 mm ⁻¹
<i>F</i> (000)	1228
Crystal size	0.30 × 0.20 × 0.10 mm ³
θ range for data collection	3.76 - 59.46°
Index ranges	-15 ≤ <i>h</i> ≤ 15, -13 ≤ <i>k</i> ≤ 14, -19 ≤ <i>l</i> ≤ 19
Reflections collected	15989
Independent reflections	4637 (<i>R</i> (int) = 0.0458)
Refinement method	Full-matrix least-squares on <i>F</i> ²
Data / restraints / parameters	4637 / 0 / 375
Goodness-of-fit on <i>F</i> ²	1.049
Final <i>R</i> indices [<i>I</i> > 2σ(<i>I</i>)]	<i>R</i> 1 = 0.0356, <i>wR</i> 2 = 0.0803
<i>R</i> (all data)	<i>R</i> 1 = 0.0503, <i>wR</i> 2 = 0.0860
Largest diff. peak and hole	0.441 and -0.251 e·Å ⁻³

Compound	16
Empirical formula	C ₆₂ H ₈₈ Mn ₂ N ₄ O ₄
Formula weight	1063.24
Temperature	203(2) K
Wavelength	0.71073 Å
Crystal system	monoclinic
Space group	<i>P</i> 2 ₁ / <i>c</i>
Unit cell dimensions	<i>a</i> = 17.32(3) Å <i>b</i> = 15.210(17) Å <i>β</i> = 101.94(6)° <i>c</i> = 23.30(3) Å
Volume	6010(2) Å ³
Z	4
Density (calculated)	1.176 Mgm ⁻³
Absorption coefficient	0.467 mm ⁻¹
<i>F</i> (000)	2280
Crystal size	0.70 × 0.40 × 0.30 mm ³
<i>θ</i> range for data collection	3.53 - 22.50°
Index ranges	-18 ≤ <i>h</i> ≤ 14, 0 ≤ <i>k</i> ≤ 16, 0 ≤ <i>l</i> ≤ 25
Reflections collected	7382
Independent reflections	7382 (<i>R</i> (int) = 0.0000)
Refinement method	Full-matrix least-squares on <i>F</i> ²
Data / restraints / parameters	7382 / 0 / 671
Goodness-of-fit on <i>F</i> ²	1.013
Final <i>R</i> indices [<i>I</i> > 2σ(<i>I</i>)]	<i>R</i> 1 = 0.0815, <i>wR</i> 2 = 0.1843
<i>R</i> (all data)	<i>R</i> 1 = 0.1403, <i>wR</i> 2 = 0.2315
Largest diff. peak and hole	0.579 and -0.721 e·Å ⁻³

Compound	17
Empirical formula	C ₃₃ H ₄₉ IMnN ₂ O
Formula weight	671.58
Temperature	203(2) K
Wavelength	0.71073 Å
Crystal system	monoclinic
Space group	<i>P2(1)/c</i>
Unit cell dimensions	$a = 16.752(2)$ Å $b = 20.290(6)$ Å $\beta = 91.317(14)^\circ$ $c = 19.620(3)$ Å
Volume	6670(1) Å ³
Z	8
Density (calculated)	1.336 Mgm ⁻³
Absorption coefficient	1.348 mm ⁻¹
<i>F</i> (000)	2776
Crystal size	0.70 × 0.50 × 0.30 mm ³
θ range for data collection	3.52 - 25.03°
Index ranges	-19 ≤ <i>h</i> ≤ 19, -4 ≤ <i>k</i> ≤ 24, -23 ≤ <i>l</i> ≤ 23
Reflections collected	14274
Independent reflections	11722 (<i>R</i> (int) = 0.0616)
Refinement method	Full-matrix least-squares on <i>F</i> ²
Data / restraints / parameters	11722 / 0 / 705
Goodness-of-fit on <i>F</i> ²	1.053
Final <i>R</i> indices [<i>I</i> > 2σ(<i>I</i>)]	<i>R</i> 1 = 0.0534, <i>wR</i> 2 = 0.1296
<i>R</i> (all data)	<i>R</i> 1 = 0.0714, <i>wR</i> 2 = 0.1457
Largest diff. peak and hole	0.971 and -1.279 e·Å ⁻³

Compound	18 incl. toluene
Empirical formula	C ₆₅ H ₉₀ I ₂ Mn ₂ N ₄
Formula weight	1291.22
Temperature	203(2) K
Wavelength	0.71073 Å
Crystal system	monoclinic
Space group	C2/m
Unit cell dimensions	$a = 19.188(3)$ Å $b = 21.000(4)$ Å $\beta = 100.053(8)^\circ$ $c = 16.5839(13)$ Å
Volume	6580.0(16) Å ³
Z	4
Density (calculated)	1.396 Mgm ⁻³
Absorption coefficient	1.366 mm ⁻¹
<i>F</i> (000)	2856
Crystal size	0.50 × 0.50 × 0.40 mm ³
θ range for data collection	3.57 - 25.00°
Index ranges	-22 ≤ <i>h</i> ≤ 22, -5 ≤ <i>k</i> ≤ 24, -19 ≤ <i>l</i> ≤ 19
Reflections collected	7832
Independent reflections	5952 (<i>R</i> (int) = 0.0425)
Refinement method	Full-matrix least-squares on <i>F</i> ²
Data / restraints / parameters	5952 / 0 / 374
Goodness-of-fit on <i>F</i> ²	1.018
Final <i>R</i> indices [<i>I</i> > 2σ(<i>I</i>)]	<i>R</i> 1 = 0.0349, <i>wR</i> 2 = 0.0900
<i>R</i> (all data)	<i>R</i> 1 = 0.0388, <i>wR</i> 2 = 0.0936
Largest diff. peak and hole	0.977 and -0.788 e·Å ⁻³

Compound	20
Empirical formula	C ₅₂ H ₇₉ MnN ₅
Formula weight	829.14
Temperature	133(2) K
Wavelength	0.71073 Å
Crystal system	monoclinic
Space group	<i>P</i> 2(1)/ <i>c</i>
Unit cell dimensions	<i>a</i> = 11.694(2) Å <i>b</i> = 19.388(4) Å <i>β</i> = 102.59(3)° <i>c</i> = 22.168(4) Å
Volume	4905.3(17) Å ³
Z	4
Density (calculated)	1.123 Mgm ⁻³
Absorption coefficient	0.307 mm ⁻¹
<i>F</i> (000)	1804
Crystal size	unmeasured
<i>θ</i> range for data collection	1.78 - 24.72°
Index ranges	-13 ≤ <i>h</i> ≤ 13, -22 ≤ <i>k</i> ≤ 22, -24 ≤ <i>l</i> ≤ 26
Reflections collected	34511
Independent reflections	8269 (<i>R</i> (int) = 0.0717)
Refinement method	Full-matrix least-squares on <i>F</i> ²
Data / restraints / parameters	8269 / 0 / 543
Goodness-of-fit on <i>F</i> ²	0.932
Final <i>R</i> indices [<i>I</i> > 2σ(<i>I</i>)]	<i>R</i> 1 = 0.0422, <i>wR</i> 2 = 0.0983
<i>R</i> (all data)	<i>R</i> 1 = 0.0616, <i>wR</i> 2 = 0.1044
Largest diff. peak and hole	0.431 and -0.469 e·Å ⁻³

Compound	21
Empirical formula	C ₅₈ H ₈₂ Mn ₂ N ₄
Formula weight	945.16
Temperature	133(2) K
Wavelength	0.71073 Å
Crystal system	monoclinic
Space group	<i>P</i> 2(1)/ <i>c</i>
Unit cell dimensions	<i>a</i> = 14.4602(9) Å <i>b</i> = 14.2263(6) Å <i>β</i> = 94.999(6)° <i>c</i> = 26.795(2) Å
Volume	5491.1(6) Å ³
Z	4
Density (calculated)	1.143 Mgm ⁻³
Absorption coefficient	0.498 mm ⁻¹
<i>F</i> (000)	2032
Crystal size	unmeasured
<i>θ</i> range for data collection	1.62 - 24.81°
Index ranges	-17 ≤ <i>h</i> ≤ 16, -16 ≤ <i>k</i> ≤ 16, -30 ≤ <i>l</i> ≤ 31
Reflections collected	38085
Independent reflections	9401 (<i>R</i> (int) = 0.1276)
Refinement method	Full-matrix least-squares on <i>F</i> ²
Data / restraints / parameters	9401 / 0 / 597
Goodness-of-fit on <i>F</i> ²	0.953
Final <i>R</i> indices [<i>I</i> > 2σ(<i>I</i>)]	<i>R</i> 1 = 0.0414, <i>wR</i> 2 = 0.0781
<i>R</i> (all data)	<i>R</i> 1 = 0.0716, <i>wR</i> 2 = 0.0825
Largest diff. peak and hole	0.496 and -0.567 e·Å ⁻³

Compound	22
Empirical formula	C ₅₈ H ₈₂ Mn ₂ N ₄ O ₂
Formula weight	977.16
Temperature	133(2) K
Wavelength	0.71073 Å
Crystal system	monoclinic
Space group	C2/c
Unit cell dimensions	$a = 15.4921(12)$ Å $b = 16.3958(9)$ Å $\beta = 90.802(6)^\circ$ $c = 21.3688(17)$ Å
Volume	5427.3(7) Å ³
Z	4
Density (calculated)	1.196 Mgm ⁻³
Absorption coefficient	0.509 mm ⁻¹
<i>F</i> (000)	2096
Crystal size	unmeasured
θ range for data collection	1.81 - 24.77°
Index ranges	-18 ≤ <i>h</i> ≤ 16, -19 ≤ <i>k</i> ≤ 19, -25 ≤ <i>l</i> ≤ 25
Reflections collected	18243
Independent reflections	4641 (<i>R</i> (int) = 0.0637)
Refinement method	Full-matrix least-squares on <i>F</i> ²
Data / restraints / parameters	4641 / 0 / 308
Goodness-of-fit on <i>F</i> ²	1.024
Final <i>R</i> indices [<i>I</i> > 2σ(<i>I</i>)]	<i>R</i> 1 = 0.0421, <i>wR</i> 2 = 0.0873
<i>R</i> (all data)	<i>R</i> 1 = 0.0664, <i>wR</i> 2 = 0.0962
Largest diff. peak and hole	0.325 and -0.257 e·Å ⁻³

Compound	23
Empirical formula	C ₃₅ H ₆₀ Li ₂ N ₂ O ₂
Formula weight	554.73
Temperature	200(2) K
Wavelength	0.71073 Å
Crystal system	monoclinic
Space group	<i>P2(1)/n</i>
Unit cell dimensions	$a = 11.224(2)$ Å $b = 9.6466(19)$ Å $\beta = 92.19(3)^\circ$ $c = 32.070(6)$ Å
Volume	3469.7(12) Å ³
Z	4
Density (calculated)	1.062 Mgm ⁻³
Absorption coefficient	0.063 mm ⁻¹
<i>F</i> (000)	1224
Crystal size	1.00 × 0.70 × 0.60 mm ³
θ range for data collection	3.60 - 22.53°
Index ranges	-12 ≤ <i>h</i> ≤ 12, -10 ≤ <i>k</i> ≤ 10, -34 ≤ <i>l</i> ≤ 34
Reflections collected	7629
Independent reflections	4515 (<i>R</i> (int) = 0.0710)
Refinement method	Full-matrix least-squares on <i>F</i> ²
Data / restraints / parameters	4515 / 0 / 393
Goodness-of-fit on <i>F</i> ²	1.115
Final <i>R</i> indices [<i>I</i> > 2σ(<i>I</i>)]	<i>R</i> 1 = 0.0979, <i>wR</i> 2 = 0.2922
<i>R</i> (all data)	<i>R</i> 1 = 0.1357, <i>wR</i> 2 = 0.3219
Largest diff. peak and hole	0.527 and -0.427 e·Å ⁻³

Compound	24
Empirical formula	C ₅₄ H ₈₀ Mn ₂ N ₄
Formula weight	895.10
Temperature	203(2) K
Wavelength	0.71073 Å
Crystal system	triclinic
Space group	<i>P</i> -1
Unit cell dimensions	$a = 11.545(9)$ Å $b = 13.642(10)$ Å $\beta = 94.01(3)^\circ$ $c = 18.014(15)$ Å
Volume	2490(1) Å ³
Z	2
Density (calculated)	1.192 Mgm ⁻³
Absorption coefficient	0.545 mm ⁻¹
<i>F</i> (000)	964
Crystal size	1.00 × 0.50 × 0.30 mm ³
θ range for data collection	3.54 - 25.04°
Index ranges	-13 ≤ <i>h</i> ≤ 13, -16 ≤ <i>k</i> ≤ 15, -19 ≤ <i>l</i> ≤ 21
Reflections collected	11007
Independent reflections	8774 (<i>R</i> (int) = 0.0616)
Refinement method	Full-matrix least-squares on <i>F</i> ²
Data / restraints / parameters	8774 / 0 / 557
Goodness-of-fit on <i>F</i> ²	1.023
Final <i>R</i> indices [<i>I</i> > 2σ(<i>I</i>)]	<i>R</i> 1 = 0.0461, <i>wR</i> 2 = 0.1150
<i>R</i> (all data)	<i>R</i> 1 = 0.601, <i>wR</i> 2 = 0.1258
Largest diff. peak and hole	0.533 and -0.638 e·Å ⁻³

7. References

1. (a) P. M. Treichel, in *Comprehensive Organometallic Chemistry*, Eds: G. Wilkinson, F. G. A. Stone, E. W. Abel; Elsevier: Oxford, UK, **1982**; Vol. 4, Chapter 29. (b) S. G. Davies, *Organotransition Metal Chemistry: Application to Organic Synthesis*; Pergamon Press: Elmsford, New York, **1982**. (c) G. Cahiez, A. Martin, T. Delacroix, *Tetrahedron Lett.* **1999**, 40, 6407. (d) C. Boucley, G. Cahiez, S. Carini, V. Cerè, M. Comes-Franchini, P. Knochel, S. Pollicino, A. Ricci, *J. Organomet. Chem.* **2001**, 624, 223.
2. D. C. Weatherburn, S. Mandal, S. Mukhopadhyay, S. Bhaduri, L. F. Lindoy, in *Comprehensive Coordination Chemistry II*, Eds: E. C. Constable, J. R. Dilworth, Elsevier: Oxford, UK, **2004**; Vol. 5.
3. W. Adam, J. Jekö, A. Lévai, Z. Majer, C. Nemes, T. Patonay, L. Párkányi, P. Sebök *Tetrahedron: Asymmetry* **1996**, 7, 2437.
4. (a) D. Bourissou, O. Guerret, F. P. Gabbaï, G. Bertrand, *Chem. Rev.* **2000**, 100, 39. (b) L. Jafarpour, S. P. Nolan, *Adv. Organomet. Chem.* **2000**, 46, 181. (c) W. A. Herrmann, T. Weskamp, V. P. W. Böhm, *Adv. Organomet. Chem.* **2002**, 48, 1.
5. A. J. Arduengo, III, R. L. Harlow, M. Kline, *J. Am. Chem. Soc.* **1991**, 113, 361.
6. A. J. Arduengo, III, H. V. R. Dias, F. Davidson, R. L. Harlow, *J. Organomet. Chem.* **1993**, 462, 13.
7. M. Albrecht, J. R. Miecznikowski, A. Samuel, J. W. Faller, R. H. Crabtree, *Organometallics* **2002**, 21, 3596.
8. V. César, S. Bellemin-Laponnaz, L. H. Gade, *Organometallics* **2002**, 21, 5204.
9. J. Louie, R. H. Grubbs, *J. Chem. Soc., Chem. Commun.* **2000**, 1479.
10. (a) K. H. Dötz, H. Fischer, P. Hoffmann, F. R. Kreissl, U. Schubert, K. Weiss, *Transition Metal Carbene Complexes* VCH: Weinheim, **1983**. (b) N. M. Kostić, R. F. Fenske, *J. Am. Chem. Soc.* **1982**, 104, 3879. (c) N. Lugan, C. Kelley, M. R. Terry, G. L. Geoffroy, A. L. Rheingold, *J. Am. Chem. Soc.* **1990**, 112, 3220. (d) T. R. Hoye, G. M. Rehberg, *Organometallics* **1990**, 9, 3014.
11. M. F. Lappert, P. L. Pye, *J. Chem. Soc., Dalton Trans.* **1977**, 2172.
12. A. Wacker, H. Pritzkow, W. Siebert, *Eur. J. Inorg. Chem.* **1998**, 843.
13. R. A. Bartlett, M. M. Olmstead, P. P. Power, S. C. Shoner, *Organometallics* **1988**, 7, 1801.

14. J. G. Donkervoort, J. L. Vicario, J. T. B. H. Jastrzebski, R. A. Gossage, G. Chiez, G. Van Koten, *J. Organomet. Chem.* **1998**, 558, 61.
15. Selected samples: (a) G. Cahiez, A. Masuda, D. Bernard, J. F. Normant, *Tetrahedron Lett.* **1976**, 17, 3155. (b) G. Cahiez, B. Figadere, *Tetrahedron Lett.* **1986**, 27, 4445. (c) G. Cahiez, M. Alami, *Tetrahedron* **1989**, 45, 4163.
16. (a) U. Riese, B. Neumüller, N. Faza, W. Massa, K. Dehnicke, *Z. Anorg. Allg. Chem.* **1997**, 623, 351. (b) H.-J. Mai, B. Neumüller, K. Dehnicke, *Z. Naturforsch.* **1996**, 51b, 433.
17. D. M. Roundhill, *Photochemistry and Photophysics of Metal Complexes*, Plenum Press, New York, **1994**.
18. R. Bianchi, G. Gervasio, D. Marabello, *Inorg. Chem.* **2000**, 39, 2360.
19. (a) P. L. Holland, T. R. Cundari, L. L. Perez, N. A. Eckert, R. J. Lachicotte, *J. Am. Chem. Soc.* **2002**, 124, 14416. (b) J. M. Smith, R. J. Lachicotte, K. A. Pittard, T. R. Cundari, G. Lukat-Rodgers, K. R. Rodger, P. L. Holland, *J. Am. Chem. Soc.* **2001**, 123, 9222.
20. (a) A. Panda, M. Stender, R. J. Wright, M. M. Olmstead, P. Klavins, P. P. Power, *Inorg. Chem.* **2002**, 41, 3909. (b) J. Chai, H. Zhu, H. Fan, H. W. Roesky, J. Magull, *Organometallics* **2004**, 23, 1177. (c) J. J. Ellison, P. P. Power, S. C. Shoner, *J. Am. Chem. Soc.* **1989**, 111, 8044.
21. (a) C. W. Hoganson, G. T. Babcock, *Science* **1997**, 277, 1953. (b) H. Sakiyama, A. Sugawara, M. Sakamoto, K. Unoura, K. Inoue, M. Yamasaki, *Inorg. Chim. Acta* **2000**, 310, 163. (c) J. Stubbe, W. A. van der Donk, *Chem. Rev.* **1998**, 98, 705.
22. G. C. Dismukes, *Chem. Rev.* **1996**, 96, 2909.
23. H. Sakiyama, A. Sugawara, M. Sakamoto, K. Unoura, K. Inoue, M. Yamasaki, *Inorg. Chim. Acta* **2000**, 310, 163.
24. I. Romero, L. Dubois, M.-N. Collomb, A. Deronzier, J.-M. Latour, J. Pécaut, *Inorg. Chem.* **2002**, 41, 1795.
25. W. A. Herrmann, K. Öfele, M. Elison, F. E. Kühn, P. W. Roesky, *J. Organomet. Chem.* **1994**, 480, C7.
26. N. Hebdanz, F. H. Köhler, G. Müller, *Inorg. Chem.* **1984**, 23, 3043.
27. B. Beagley, J. C. Briggs, A. Hosseiny, W. E. Hill, T. J. King, C. A. McAuliffe, K. Minten, *J. Chem. Soc., Chem. Commun.* **1984**, 305.
28. W. A. Herrmann, F. C. Munck, G. R. J. Artus, O. Runte, R. Anwender, *Organometallics*, **1997**, 16, 682.

29. B. Albela, M. Corbella, J. Ribas, I. Castro, J. Sletten, H. Stoeckli-Evans, *Inorg. Chem.* **1998**, *37*, 788.
30. L. Dubois, D.-F. Xiang, X.-S. Tan, J. Pécaut, P. Jones, S. Baudron, L. Le Pape, J.-M. Latour, C. Baffert, S. Chardon-Noblat, M.-N. Collomb, A. Deronzier, *Inorg. Chem.* **2003**, *42*, 750 and references cited therein.
31. W. K. Dean, G. L. Simon, P. M. Treichel, L. F. Dahl, *J. Organomet. Chem.* **1973**, *50*, 193.
32. R. M. Wood, D. M. Stucker, L. M. Jones, W. B. Lynch, S. K. Misra, J. H. Freed, *Inorg. Chem.* **1999**, *38*, 5384 and references cited therein.
33. R. D. Dowsing, J. F. Gibson, D. M. L. Goodgame, M. Goodgame, P. J. Hayward, *J. Chem. Soc., Dalton Trans.* **1969**, 1242.
34. R. D. Dowsing, J. F. Gibson, M. Goodgame, P. J. Hayward, *J. Chem. Soc., Dalton Trans.* **1970**, 1133.
35. L. Bourget-Merle, M. F. Lappert, J. R. Severn, *Chem. Rev.* **2002**, *102*, 3031.
36. C. Cui, H. W. Roesky, H.-G. Schmidt, M. Noltemeyer, H. Hao, F. Cimpoesu, *Angew. Chem.* **2000**, *112*, 4444; *Angew. Chem. Int. Ed.* **2000**, *39*, 4274.
37. (a) G. Bai, Y. Peng, H. W. Roesky, J. Li, H.-G. Schmidt, M. Noltemeyer, *Angew. Chem.* **2003**, *115*, 1164; *Angew. Chem. Int. Ed.* **2003**, *42*, 1132. (b) G. Bai, H. W. Roesky, J. Li, M. Noltemeyer, H.-G. Schmidt, *Angew. Chem.* **2003**, *115*, 5660; *Angew. Chem. Int. Ed.* **2003**, *42*, 5502.
38. Y. Ding, H. W. Roesky, M. Noltemeyer, H.-G. Schmidt, P. P. Power, *Organometallics* **2001**, *20*, 1190.
39. W. Clegg, E. K. Cope, A. J. Edwards, F. S. Mair, *Inorg. Chem.* **1998**, *37*, 2317.
40. (a) J. Prust, K. Most, I. Müller, A. Stasch, H. W. Roesky, I. Usón, *Eur. J. Inorg. Chem.* **2001**, 1613. (b) J. M. Smith, R. J. Lachicotte, P. L. Holland, *J. Chem. Soc., Chem. Commun.* **2001**, 1542.
41. J. Chai, H. Zhu, K. Most, H. W. Roesky, D. Vidovic, H.-G. Schmidt, M. Noltemeyer, *Eur. J. Inorg. Chem.* **2003**, 4332.
42. S. Filippini, J. N. Jones, J. A. Johnson, A. H. Cowley, F. Grepioni, D. Braga, *Chem. Commun.* **2003**, 2716.
43. F. H. Köhler, N. Hebandanz, G. Müller, U. Thewalt, B. Kanellakopulos, R. Klenze, *Organometallics* **1987**, *6*, 115.
44. M. Tamura, J. Kochi, *J. Organomet. Chem.* **1971**, *29*, 111.

-
45. J. Heck, W. Massa, P. Wenig, *Angew. Chem.* **1984**, *96*, 699; *Angew. Chem. Int. Ed. Engl.* **1984**, *23*, 722.
46. R. A. Andersen, E. Carmona-Guzman, J. F. Gibson, G. Wilkinson, *J. Chem. Soc., Dalton Trans.* **1976**, 2204.
47. L. E. Manzer, L. J. Guggenberger, *J. Organomet. Chem.* **1977**, *139*, C34.
48. J. I. Davies, C. G. Howard, A. C. Skapski, G. Wilkinson, *J. Chem. Soc., Chem. Commun.* **1982**, 1077.
49. R. J. Morris, G. S. Girolami, *Organometallics* **1989**, *8*, 1478.
50. S. Gambarotta, C. Floriani, A. Chiesi-Villa, C. Guastini, *J. Chem. Soc., Chem. Commun.* **1983**, 1128.
51. (a) N. H. Buttrus, C. Eaborn, P. B. Hitchcock, J. D. Smith, A. C. Sullivan, *J. Chem. Soc., Chem. Commun.* **1985**, 1380. (b) R. A. Andersen, A. Haaland, K. Rypdal, H. V. Volden, *J. Chem. Soc., Chem. Commun.* **1985**, 1807.
52. R. Ahlrichs, M. Bär, H.-P. Baron, R. Bauernschmitt, S. Böcker, P. Deglmann, M. Ehrig, K. Eichkorn, S. Elliott, F. Furche, F. Haase, M. Häser, H. Horn, C. Hättig, C. Huber, U. Huniar, M. Kattannek, A. Köhn, C. Kölmel, M. Kollwitz, K. May, C. Ochsenfeld, H. Öhm, A. Schäfer, U. Schneider, M. Sierka, O. Treutler, B. Unterreiner, M. von Arnim, F. Weigend, P. Weis, H. Weiss, *TURBOMOLE 5.5*, Universität Karlsruhe, FRG, **2002**.
53. M. J. Frisch, G. W. Trucks, H. B. Schlegel, G. E. Scuseria, M. A. Robb, J. R. Cheeseman, V. G. Zakrzewski, J. A. Montgomery, J. R. E. Stratmann, J. C. Burant, S. Dapprich, J. M. Millam, A. D. Daniels, K. N. Kudin, M. C. Strain, O. Farkas, J. Tomasi, V. Barone, M. Cossi, R. Cammi, B. Mennucci, C. Pomelli, C. Adamo, S. Clifford, J. Ochterski, G. A. Petersson, P. Y. Ayala, Q. Cui, K. Morokuma, D. K. Malick, A. D. Rabuck, K. Raghavachari, J. B. Foresman, J. Cioslowski, J. V. Ortiz, A. G. Baboul, B. B. Stefanov, G. Liu, A. Liashenko, P. Piskorz, I. Komaromi, R. Gomperts, R. L. Martin, D. J. Fox, T. Keith, M. A. Al-Laham, C. Y. Peng, A. Nanayakkara, M. Hallacombé, P. M. W. Gill, B. Johnson, W. Chen, M. W. Wong, J. L. Andres, C. Gonzalez, M. Head-Gordon, E. S. Replogle, J. A. Pople, *Gaussian 98*, Revision A.9; Gaussian, Inc.: Pittsburgh, Pa, **1998**.
54. S. Tsuzuki, K. Honda, T. Uchimaru, M. Mikami, K. Tanabe, *J. Am. Chem. Soc.* **2002**, *124*, 104.
55. (a) S. F. Boys, *Rev. Mod. Phys.* **1960**, *32*, 296. (b) G. Schaftenaar, *MOLDEN 3.8*, CAOS/CAMM Center Nijmegen, NL, **2003**.
56. J. Manna, K. D. John, M. D. Hopkins, *Adv. Organometal. Chem.* **1995**, *38*, 79.

57. (a) G. Liehr, H.-J. Seibold, H. Behrens, *J. Organomet. Chem.* **1983**, *248*, 351. (b) P. G. Lenhert, C. M. Lukehart, K. Srinivasan, *J. Am. Chem. Soc.* **1984**, *106*, 124. (c) B. J. Brisdon, D. A. Edwards, J. W. White, M. G. B. Drew, *J. Chem. Soc., Dalton Trans.* **1980**, 2129.
58. B. Morosin, J. Howatson, *J. Organomet. Chem.* **1970**, *29*, 7.
59. (a) X. Solans, J. Solans, C. Miravittles, D. Miguel, V. Riera, J. M. Rubio-Gonzalez, *Acta Crystallogr. C* **1986**, *42*, 975. (b) G. A. Carriedo, D. Miguel, V. Riera, X. Solans, M. Font-Altaba, M. Coll, *J. Organomet. Chem.* **1986**, *299*, C43.
60. X.-M. Chen, Y.-X. Tong, Z.-T. Xu, T. C. W. Mark, *J. Chem. Soc., Dalton Trans.* **1995**, 4001 and references cited therein.
61. G. B. Nikiforov, H. W. Roesky, T. Labahn, D. Vidovic, D. Neculai, *Eur. J. Inorg. Chem.* **2003**, 433.
62. D. Walther, P. Gebhardt, R. Fischer, U. Kreher, H. Görls, *Inorg. Chim. Acta* **1998**, *281*, 181.
63. D. Reardon, G. Aharonian, S. Gambarotta, G. P. A. Yap, *Organometallics* **2002**, *21*, 786 and references cited therein.
64. C. Eaborn, P. B. Hitchcock, J. D. Smith, S. Zhang, W. Clegg, K. Izod, P. O'Shaughnessy, *Organometallics* **2000**, *19*, 1190 and references cited therein.
65. P. Friedrich, G. Besl, E. O. Fischer, G. Huttner, *J. Organomet. Chem.* **1977**, *139*, C68.
66. W. A. Herrmann, J. L. Hubbard, I. Bernal, J. D. Korp, B. L. Haymore, G. L. Hillhouse, *Inorg. Chem.* **1984**, *23*, 2978.
67. E. O. Fischer, W. Kleine, W. Schambeck, U. Schubert, *Z. Naturforsch.* **1981**, *36b*, 1575.
68. U. Schubert, *Organometallics* **1982**, *1*, 1085.
69. D. S. McGuinness, B. F. Yates, K. J. Cavell, *Organometallics* **2002**, *21*, 5408 and references cited therein.
70. B. L. Balzer, M. Cazanoue, M. Sabat, M. G. Finn, *Organometallics* **1992**, *11*, 1759.
71. H. Chen, R. A. Bartlett, H. V. R. Dias, M. M. Olmstead, P. P. Power, *Inorg. Chem.* **1991**, *30*, 2487 and references cited therein.
72. R. D. Adams, O.-S. Kwon, M. D. Smith, *Inorg. Chem.* **2002**, *41*, 5525.
73. (a) N. Kitajima, U. P. Singh, H. Amagai, M. Osawa, Y. Morooka, *J. Am. Chem. Soc.* **1991**, *113*, 7757. (b) P. A. Goodson, A. R. Oki, J. Glerup, D. J. Hodgson, *J. Am. Chem. Soc.* **1990**, *112*, 6248. (c) P. A. Goodson, D. J. Hodgson, *Inorg. Chem.* **1989**, *28*, 3606.

-
74. (a) J. D. Scollard, D. H. McConville, N. C. Payne, J. J. Vittal, *Macromolecules* **1996**, *29*, 5241. (b) J. D. Scollard, D. H. McConville, *J. Am. Chem. Soc.* **1996**, *118*, 10008. (c) J. D. Scollard, D. H. McConville, J. J. Vittal, *Organometallics* **1997**, *16*, 4415.
75. (a) F. G. N. Cloke, B. R. Elvidge, P. B. Hitchcock, V. M. E. Lamarche, *J. Chem. Soc., Dalton Trans.* **2002**, 2413. (b) P. W. Roesky, *Organometallics* **2002**, *21*, 4756.
76. H. Zhu, J. Chai, H. W. Roesky, M. Noltemeyer, H.-G. Schmidt, D. Vidovic, J. Magull, *Eur. J. Inorg. Chem.* **2003**, 3113.
77. (a) D. C. Bradley, M. B. Hursthouse, K. M. A. Malik, R. Mösele, *Transition Met. Chem.* **1978**, *3*, 253. (b) B. D. Murray, P. P. Power, *Inorg. Chem.* **1984**, *23*, 4584.
78. H. Chen, R. A. Bartlett, H. V. R. Dias, M. M. Olmstead, P. P. Power, *J. Am. Chem. Soc.* **1989**, *111*, 4338.
79. M. M. Olmstead, P. P. Power, S. C. Shoner, *Inorg. Chem.* **1991**, *30*, 2547.
80. D. F. Shriver, M. A. Drezdson, *The Manipulation of Air-Sensitive Compounds*, 2nd Edn., Wiley-Interscience, New York, **1986**.
81. G. M. Sheldrick, *Acta Crystallogr. A* **1997**, *46*, 467.
82. G. M. Sheldrick, SHELXS-97, Universität Göttingen, FRG, **1997**.
83. N. Kuhn, T. Kratz, *Synthesis* **1993**, 561.
84. J. Feldman, S. J. McLain, A. Parthasarathy, W. J. Marshall, J. C. Calabrese, S. D. Arthur, *Organometallics* **1997**, *16*, 1514.
85. R. J. Kern, *J. Inorg. Nucl. Chem.* **1962**, *24*, 1105.
86. B. Horvath, R. Mösele, E. G. Horvath, *Z. Anorg. Allg. Chem.* **1979**, *450*, 165.
87. B. Hübler-Blank, M. Witt, H. W. Roesky, *J. Chem. Educ.* **1993**, *70*, 408.
88. H. W. Roesky, *Inorg. Chem.* **2001**, *40*, 6855.

Lebenslauf

Jianfang Chai, geboren am 30. Aug. 1976 in Anyang, Henan, China

Staatsangehörigkeit Chinesisch

Familienstand verheiratet

Schulausbildung

Aug. 1983 – Jul. 1988 Dongzhuangying Grundschule, Anyang, China

Aug. 1988 – Jul. 1991 Liuguzhen No.1 Junior Middle School, Anyang, China

Aug. 1991 – Jul. 1994 Huaxian No. 1 Senior Middle School, Anyang, China

Hochschulausbildung

Sep. 1994 – Jul. 1998 Studium Chemie am Fachbereich Chemie der *Xinyang Normal College*, Xinyang, China

Sep. 1998 – Jul. 2001 Studium Chemie am Fachbereich Chemie der *Nankai University*, Tianjin, China

Sep. 2001 – Oct. 2001 Äquivalenzprüfung zum Diplomexamen - Fach Chemie

Nov. 2001 – Oct. 2004 Anfertigung der Dissertation unter Anleitung von Prof. Dr. Dr. h. c. mult. H. W. Roesky am *Institut für Anorganische Chemie der Universität Göttingen*